MIGRATORY INSERTION OF CARBENE COMPLEXES OF RUTHENIUM: PREPARATION OF RUTHENABENZENE

By

JING YANG

A DISSERTATION PRESENTED TO THE GRADUATE SCHOOL
OF THE UNIVERSITY OF FLORIDA IN PARTIAL FULFILLMENT
OF THE REQUIREMENTS FOR THE DEGREE OF
DOCTOR OF PHILOSOPHY

UNIVERSITY OF FLORIDA

1995

To my husband, Bill Dolbier

ACKNOWLEDGEMENTS

It is with much gratitude that I acknowledge the excellent guidance of my research advisor, Dr. William M. Jones., for having made the fulfillment of this dream possible. His enthusiasm for chemistry and his understanding nature have been an inspiration to me throughout the course of my graduate studies.

I would like to give my special thanks to my committee members, especially, Dr. Merle Battiste and Dr. James Boncella for taking the time to discuss my projects and providing valuable insight.

It is a pleasure to thank the many friends and colleagues whom I have met and worked with at the University of Florida, including Dr. Yin-sheng Wang, Dr. Conrad Burkholder, Michael Bartberger, Xiao-xin Rong, Dr. Ronda Trace, Dr. Tatjana Omrcen, Dr. Lu Zheng, and Jerzy Klosen for their helpful discussions and comraderie over the years. The friendship and guidance of Dr. Jian-guo Yin was especially appreciated. The assistance of Mr. Rudy Strosheim in constructing numerous glassware, including my special low temperature apparatus, was very much appreciated, as were the essential contributions of Dr. Roy King and Dr. Khalil Abboud to my research. Thanks also goes to Dr. Neil Allison and Ms. J. Dixon for providing some of the starting materials.

I must also express gratitude to my parents who imbued in me those important values in life which I will carry with me always.

Finally, I would like to thank Dr. Bill Dolbier, my best friend and my husband, for his understanding and his loving support.

TABLE OF CONTENTS

Page

ACKNOWEDGEMENTS.....iii

ABSTRACT.....v

CHAPTER

1 INTRODUCTION.....1

2 SYNTHESIS AND STUDY OF THE MIGRATORY INSERTION OF A NON-HETEROATOM-SUBSTITUTED RUTHENIUM CARBENE COMPLEX.....15

3 SYNTHESIS AND STUDY OF THE MIGRATORY INSERTION OF ACYCLIC RUTHENIUM CARBENE COMPLEXES.....32

4 SYNTHESIS AND STUDY OF NOVEL TRANSITION METALLAAROMATIC RUTHENAPHENANTHRENES AND RUTHENABENZENE.....54

5 CONCLUSIONS.....84

6 EXPERIMENTAL.....86

APPENDIX

TABLES OF CRYSTALLOGRAPHIC DATA.....104

REFERENCES.....117

BIOGRAPHICAL SKETCH.....120

Abstract of Dissertation Presented to the Graduate School
of the University of Florida in Partial Fulfillment of the
Requirements for the Degree of Doctor of Philosophy

MIGRATORY INSERTION OF CARBENE COMPLEXES OF RUTHENIUM :
PREPARATION OF RUTHENABENZENE

By

Jing Yang

May, 1995

Chairman: William M. Jones
Major Department: Chemistry

Research was carried out with the overall purpose of better understanding migratory insertion processes of ruthenium carbene complexes.

A methoxy-stabilized metallaindene complex of ruthenium (**2.04**) was prepared. Reaction of this complex with phenyllithium or *p*-tolylithium followed by treatment with trimethylsilyl triflate afforded the first stable aryl substituted Fischer carbene complexes of ruthenium (**2.03a** and **2.03b**) which do not bear a heteroatom stabilizing substitutent on the carbene carbon. In solution, these complexes underwent a novel thermal rearrangement to form ruthenacene derivatives **2.11a** and **2.11b**. A possible mechanism for this rearrangement which involves a ruthenanaphthalene intermediate is proposed.

Attempts to isolate and study the kinetics of the migratory insertion of acyclic ruthenium carbene complexes, $CH_3(CO)Ru=C(OR)C_6H_5$ (R = $SiMe_3$ & C_2H_5), were unsuccessful. Neverthless, insight regarding their reactivity was obtained, including the fact that apparently such complexes rearrange rapidly at temperatures as low as -78 °C.

Introduction of potential aromaticity into such carbene complexes by synthesis of a ruthenaphenanthrene (**4.01**) was not sufficient to slow migratory insertion to the point that the carbene complex could be observed. The rapid rearrangement of **4.01** at -50 °C was observed.

On the other hand, introduction of a greater degree of aromaticity into a ruthenium carbene complex through the synthesis of a diphenyl substituted ruthenabenzene (**4.16**) was sufficient to permit its detection at -50 °C. **4.16** is the first second row, late transition metallabenzene which has been reported.

CHAPTER 1
INTRODUCTION

A carbene migratory insertion is defined as the 1, 2-rearrangement of a hydrogen, alkyl or aryl group from a transition metal of a carbene complex, such as **1.01**, to a carbene carbon to give an unsaturated species **1.02**.

1.01

18-electron metal

R = H, Alkyl, Aryl

1.02

16-electron metal

Scheme 1-1

The recognition that carbene migratory insertions are fundamentally important, discrete steps in organometallic reactions dates back twenty five years ago.[1] However, during the last few years the postulation of migratory insertions in discussions of mechanisms of organometallic reactions has become especially common.[2-13]

Mechanistic studies by Bercaw[14] on carbene migratory insertions of the early transition metal tantalum, such as shown in Scheme 1-2, were instrumental in the development of a general understanding of such processes.

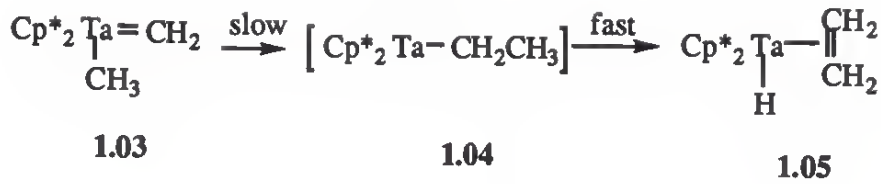

1.03 **1.04** **1.05**

Scheme 1-2

Complex **1.03** cleanly rearranges to π-complex **1.05** *via* methyl migration from Ta to methylidene ($\Delta G^{\ddagger}$ = 30.3 kcal/mol at 140 °C), followed by rapid β-H elimination from the ethyl complex **1.04**.

Theory predicts that migratory insertion rearrangements should be reversable, the reverse step to form a carbene complex being known as *alpha* elimination (right to left in Scheme 1-1). However, other than for rearrangements of hydrogen, such *alpha* eliminations have only been rarely observed. In fact, the example of Grubbs and his coworkers,[15] shown in Scheme 1-3, was the only case in which strong evidence had been provided for such a rearrangement until Jones' work in 1986.

Scheme 1-3

Theoreticians have rationalized the lack of observation of rearrangements of alkyl or aryl groups from saturated carbon to metals on the basis of thermodynamics. First Hoffmann[16], but more recently Ziegler[17], and Goddard[13] have predicted migratory insertions to be exothermic. Goddard's results, which dealt with hydride shifts within

ruthenium carbene complex **1.06** (in Scheme 1-4), predicted a strong kinetic and thermodynamic preference for rearrangement from the metal center (i.e, migratory insertion), while Ziegler's calculations for manganese complex **1.07** (shown in Scheme 1-5) predicted a smaller preference for methyl migration than for hydride migration.

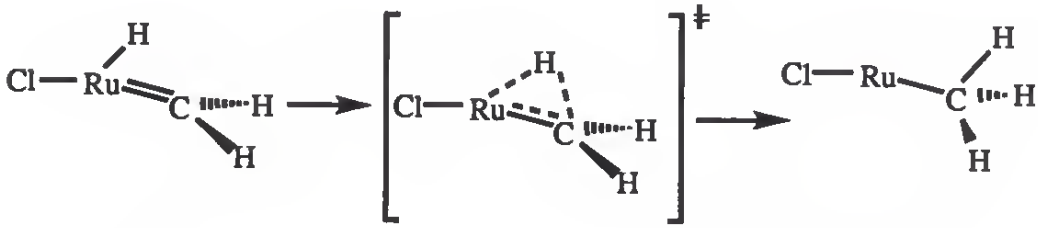

1.06

Ea=10.9 +1.7 kcal/mol

ΔH=-10.5 +1.0 kcal/mol

Scheme 1-4

1.07

R=H Δ H = - 31.74 kcal/mol

R=CH_3 ΔH = - 16.94 kcal/mol

Scheme 1-5

Recent research within the Jones group has been directed towards gaining insight into those structural factors which control such equilibria. One aspect of this research has sought to design systems which would favor *alpha* elimination, while the purpose of

another has been to study the migratory insertion process. Moreover, the Jones' group has centered its attention upon the chemistry of the first and second row late transition metals, such as manganese, iron and ruthenium etc., because there have been little data reported on *alpha* elimination or migratory insertion processes of those carbene complexes.

As a matter of fact, before Jones' work, only the two stabilized iron carbene complexes, **1.08** and **1.09** of Rosenblum[18] had been reported with alkyl groups on iron, presumably because of the strong propensity of lesser stabilized species to undergo migratory insertion.

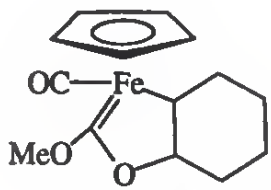

1.08

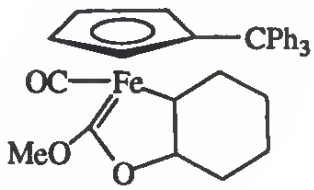

1.09

In contrast, a number of stable third-row, late-transition-metal complexes have been reported[3, 19] lately. Two examples are shown in Scheme 1-6.

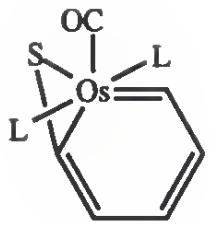

L = PPh_3

1.10

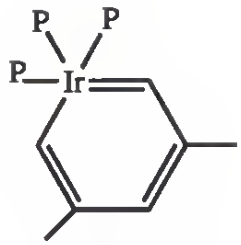

P = PEt_3

1.11

Scheme 1-6

The observed greater stablization of such third row, late-transiton metal carbene complexes probably derives from their stronger carbon-metal double bond that compensates for the strength of the carbon-carbon bond which would be formed as a result of migratory insertion.

Recently, Jones and his coworkers[4-7,10,20] developed a novel strategy for isolation of alkyl- and aryl-substituted carbene complexes of iron, ruthenium and manganese (Scheme 1-7).

Jones' Strategy

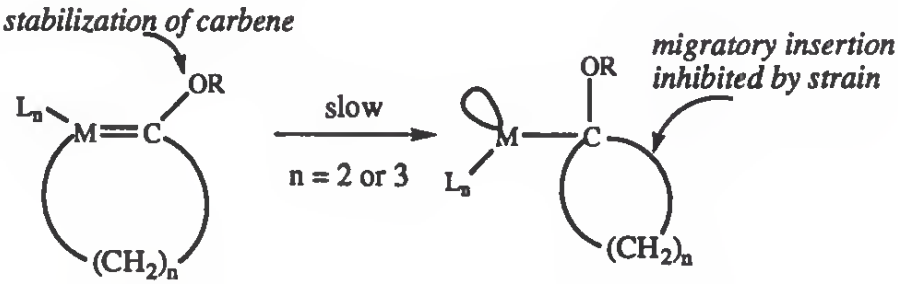

1.12 **1.13**

Scheme 1-7

They concluded that by introducing ring strain into the migratory insertion product **1.13**, it should be possible to shift the thermodynamic equilibrium in favor of carbene complexes such as **1.12**, and thus inhibit their migratory insertion.

Moreover, they concluded that they should be able to use relief of ring strain during the reverse, α-elimination process to provide a general synthetic method for such carbene complexes.

General Method

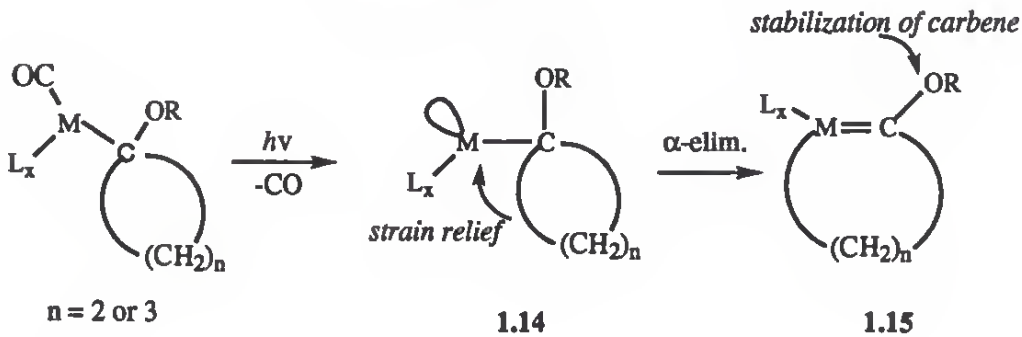

n = 2 or 3 **1.14** **1.15**

Scheme 1-8

Indeed, Jones and his coworkers have been able to design a number of systems, generally described by Scheme 1-8, in which unsaturated small ring σ-complexes of iron and manganese, such as **1.14** formed by photoelimination of CO, undergo α-eliminative ring expansions to produce examples of isolable carbene complexes such as **1.15**.

An early and significant example of such a rearrangement of an alkyl group from saturated carbon to metal to give a carbene complex is outlined in Scheme 1-9.[5] The significance of this example derives from the fact that there was evidence of facile α-elimination at room temperature and because the carbene complex, **1.19**, was actually able to be isolated.

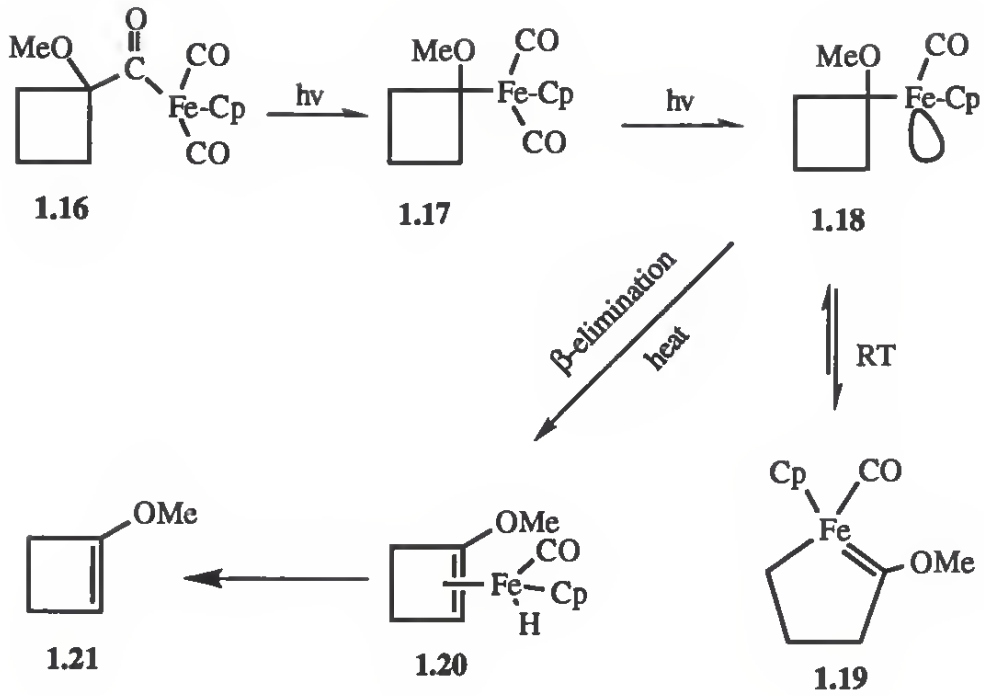

Scheme 1-9

Compound **1.17** was prepared in situ by the photolytic decarbonylation of its acyl complex **1.16**, and apparently loses another mole of CO to generate the sixteen electron intermediate **1.18**. This electron-deficient intermediate then rearranges to give the carbene complex **1.19**.

Jones rationalized that one of the important factors in favor of formation of the carbene complex is the 20-25 kcal/mole relief of strain energy[21] which occurs upon rearrangement of **1.18** to **1.19**. Another important factor is the electronic character of the substituent on the carbene carbon, where it is known that an electron-donating substituent such as OCH_3 provides stablilization to the Fischer-type carbene system.

Jones and Trace[22] demonstrated that relief of cyclobutane strain without sufficient carbene stabilization is apparently not enough to induce this rearrangement, since the phenyl-substituted substrate failed to rearrange (Scheme 1-10).

Scheme 1-10

Resonance stablization of the carbene complex, such as shown in Scheme 1-11 provides a reasonable explanation for the need of an ether or amine substituent at the α-carbon.

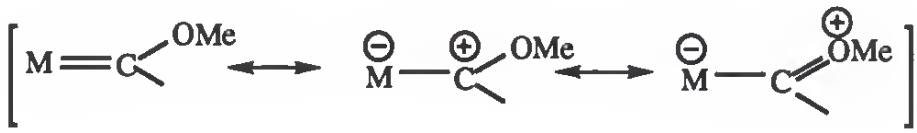

Scheme 1-11

As can be seen from the conversion of **1.18** to **1.21** in Scheme 1-9, side reactions can occur in competition with the desired *alpha*-elimination process. In a study of an analogous manganese system, Jones and Crowther[23] confirmed that the dominant side reaction was β-hydride elimination (as shown in Scheme 1-12).

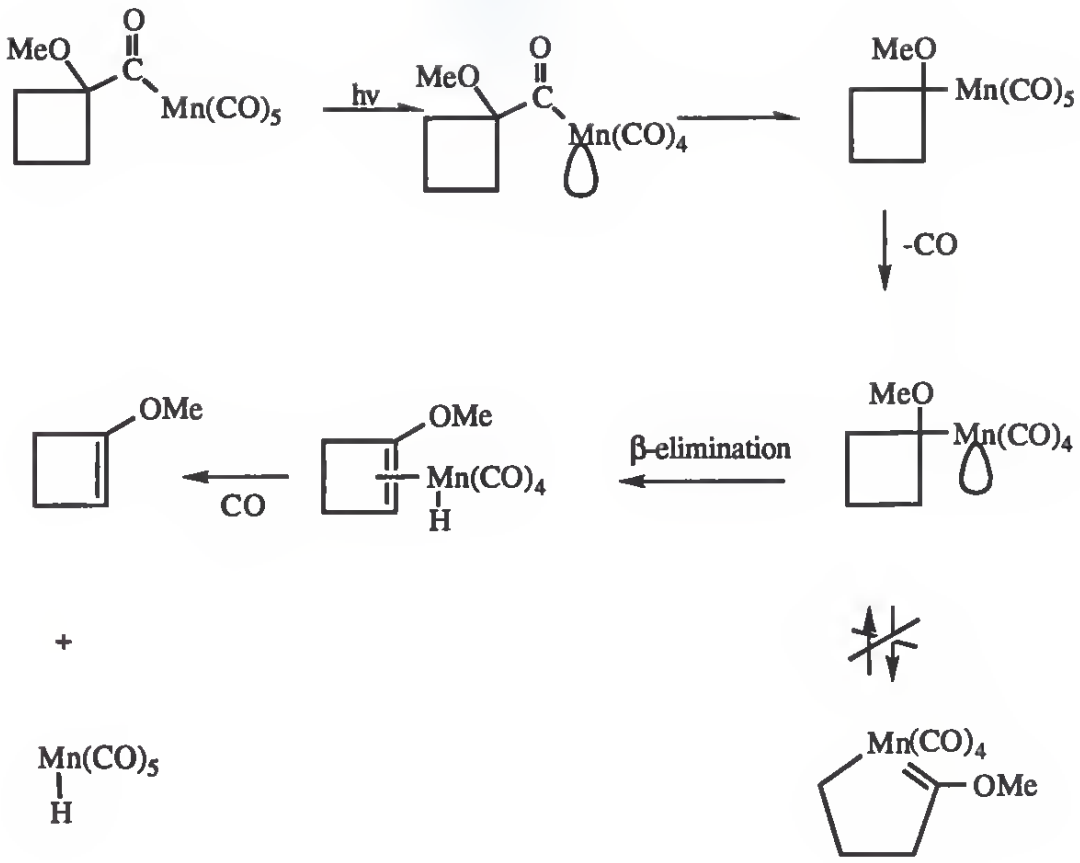

Scheme 1-12

In order to diminish the β-hydride elimination side reaction, Stenstron[6] and Crowther[10] investigated the benzocyclobutene system **1.23** (in Scheme 1-13) in which they predicted that β-hydride elimination should be minimized because of the unlikelihood of forming antiaromatic product **1.25**

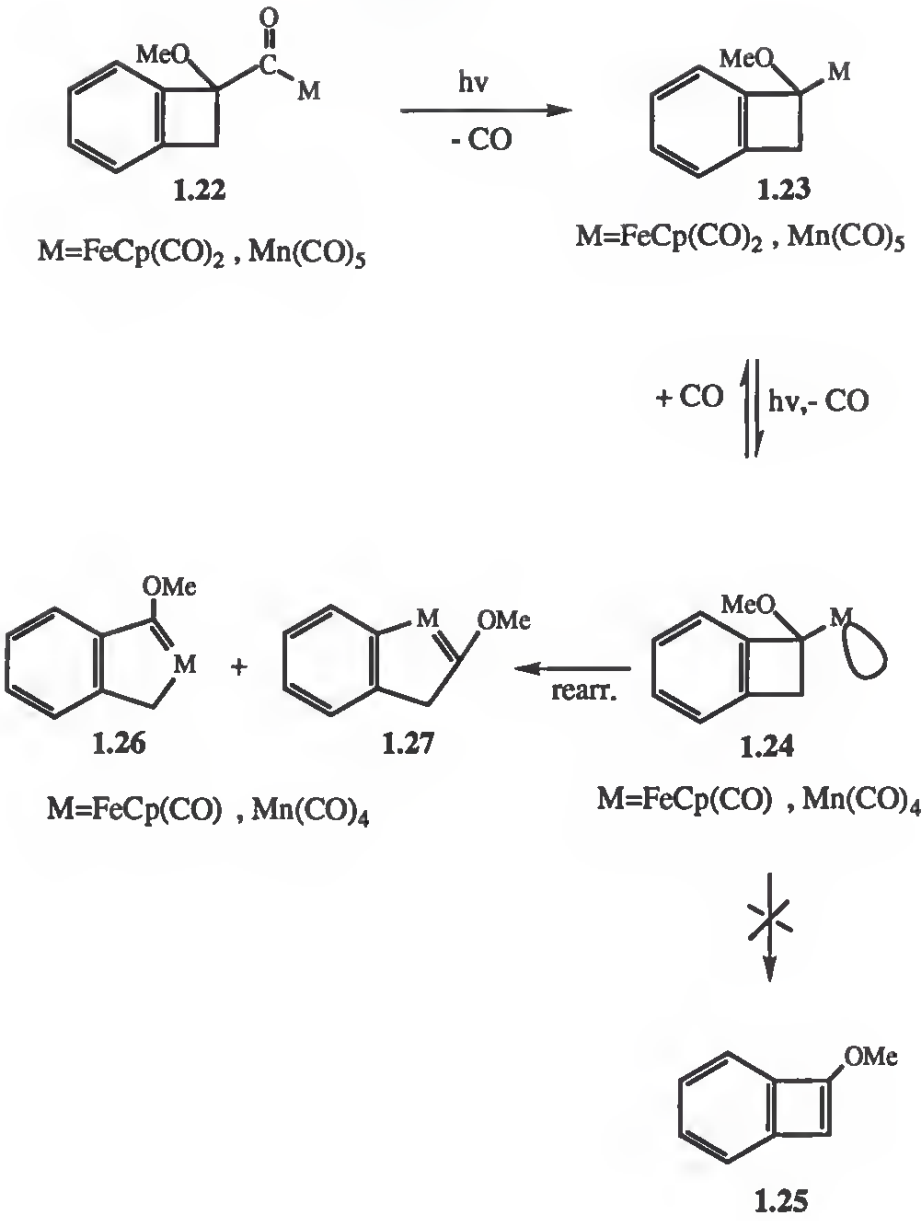

Scheme 1-13

As expected, no **1.25** was observed, and exclusive rearrangement to the carbene complexes, **1.26** and **1.27**, was observed.

Since these early studies, the Jones group has centered its attention on comparing the carbene migratory insertion reactions of complexes of the first and second row, late transition metals ruthenium and iron because both are catalytically active in the Fisher-Tropsch reaction, a reaction in which this rearrangement is presumably a key step.[13]

Unfortunately, the photodecarbonylation α-elimination process which had worked so well for iron and selected manganese alkly- and aryl-substituted carbene complexes failed completely for the related ruthenium carbene complexes, **1.28** and **1.29** (Scheme 1-14).

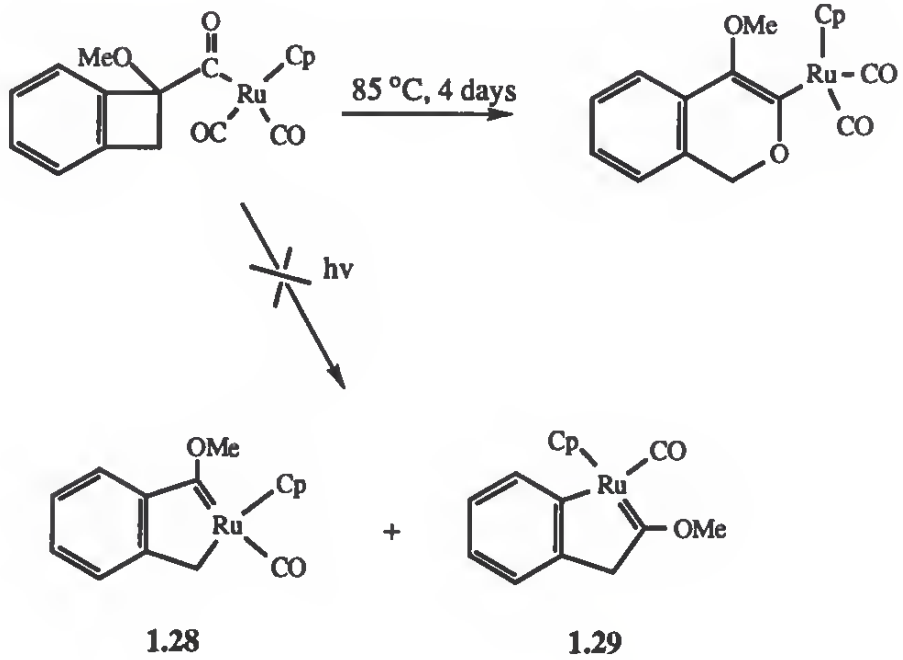

1.28 **1.29**

Scheme 1-14

With the ultimate goal of comparing migratory insertions, Jones and Trace[22], therefore, developed a new method to prepare the ruthenium analogue, **1.30**, of the iron complex **1.19** (Scheme 1-15).

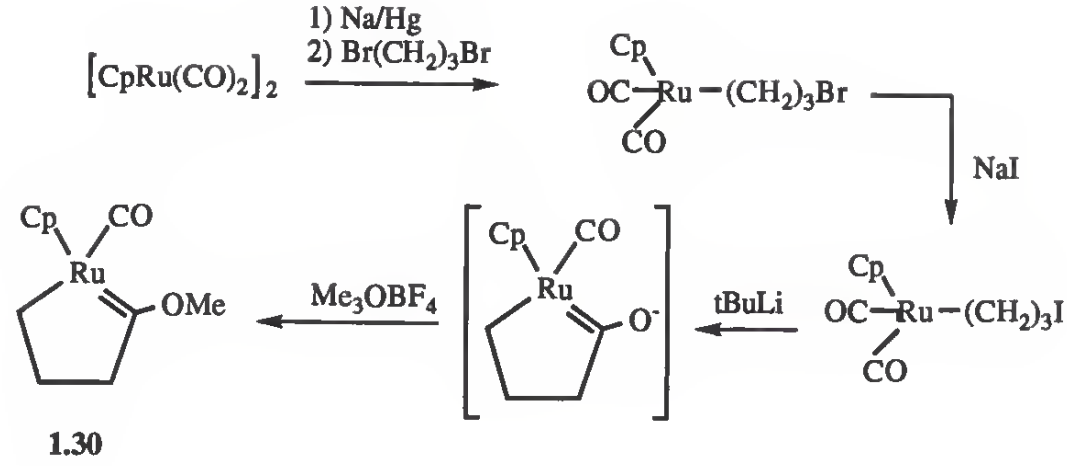

1.30

Scheme 1-15

In Stenstrom and Jones' earlier study,[6] deuterium-labeled iron carbene complex **1.19-d_2** had been used to demonstrate its reversible migratory insertion at room temperature. (Scheme 1-16).

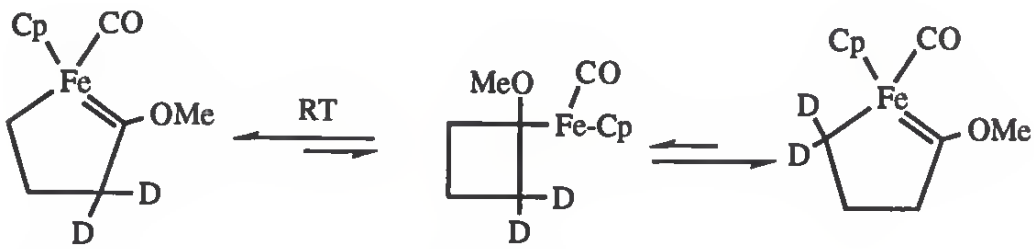

1.19-d_2

26 Kcal / mol Strain

Scheme 1-16

Unfortunately, the analogous ruthenium carbene complex, **1.30-d_2**, proved to be stable to rearrangement at temperatures up to 100 °C (Scheme 1-17), and one could only estimate a minimum rate difference of 10^7-10^8 for the rates of migratory insertion of the two complexes.

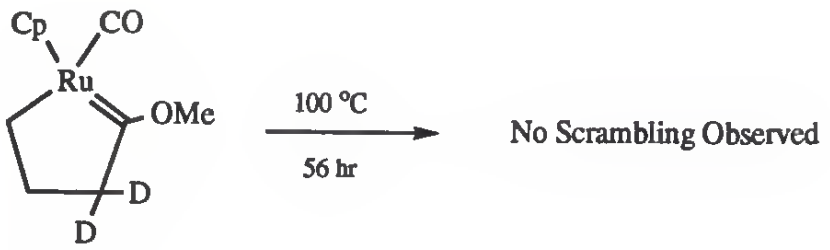

1.30-d_2

Scheme 1-17

Jones[20] rationalized the difference in rate of Fe and Ru complexes on the basis of the difference in strength of the carbon-metal double bonds in the two species. It is a generally accepted presumption that carbon-metal bonds of second row transition metals such as ruthenium are stronger than those of first row transition metals such as iron.

The relative reluctance of the ruthenium complex **1.30** to rearrange suggested two interesting possible projects for further research. First, by using a combination of ring strain and the inherent stability of alkyl substituted ruthenium carbene complexes to retard rearrangement, it might be posssible to prepare non-heteroatom-substituted (i.e. H, alkyl and aryl substituted) carbene complexes, such as **1.31**, which should be less stable and thus more reactive. Such complexes not only would be structurally unique (that is, the first stable alkyl or aryl substituted carbene complexes of ruthenium not stabilized by alkoxy), but also would be more prone to migratory insertion than their alkoxy analogues.

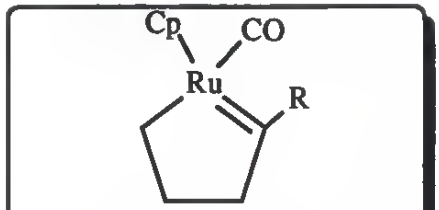

R = H, Alkyl, Aryl

1.31

Secondly, it might be possible to prepare an acyclic Ru carbene complex, such as **1.32**, where strain is not a factor either in the starting material or the rearrangement product, under conditions where it would be observable, and perhaps even isolable. Then, it might be possible to study the migratory insertion process of this complex.

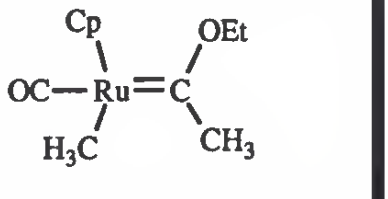

1.32

These ideas led to our two individual research projects which were (1) the synthesis and study of hydrogen-, alkyl-, and phenyl-substituted ruthenium complexes **1.31** which might be stable enough for isolation and further study; and (2) the preparation and study of the migratory insertion of an acyclic alkoxy-stabilized Ru carbene complex **1.32.**

CHAPTER 2
SYNTHESIS AND STUDY OF THE MIGRATORY INSERTION OF A NON-HETEROATOM-SUBSTITUTED RUTHENIUM CARBENE COMPLEX

In order to study the migratory insertion process of the ruthenium carbene complexes, it was decided to prepare a non-heteroatom substituted Ru-carbene complex (**1.31**) since the carbene complex **1.30** which is stablized by a OCH_3 group is so stable that it does not undergo rearrangement. The hope would be that the ground states of such hydrogen-, alkyl-, or aryl-substituted carbene complexes would be raised sufficiently to make the transition states more accessible, with the desired result being that the migratory insertion process would be observable.

Since the carbene complex can be readily synthesized, it was hoped that **1.30** would undergo facile substitution of the methoxy group by nucleophiles as is outlined in Scheme 2-1 for the reaction with phenyllithium.

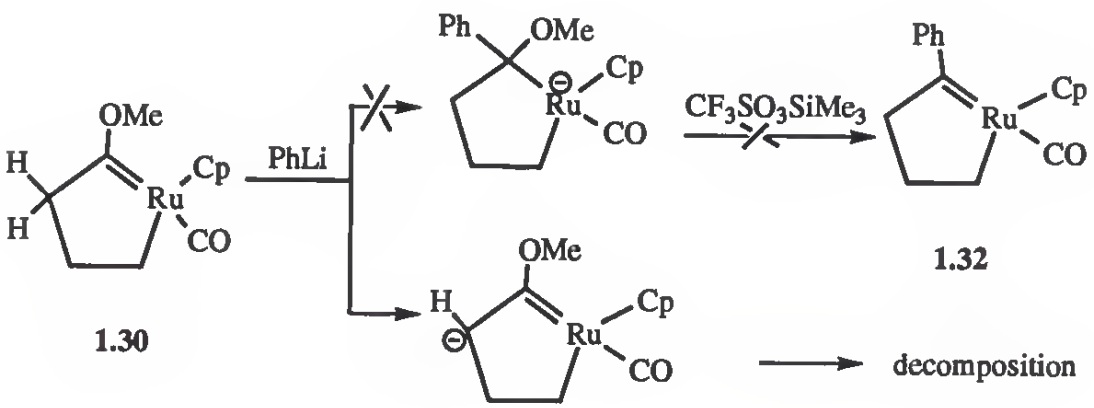

Scheme 2-1

However, it was realized after a failed attempt that the synthetic methodology indicated in the Scheme 2-1 would not work because, instead of the nucleophile attacking the carbene carbon followed by expulsion of the methoxy group, the β-hydrogen would be preferentially deprotonated due to its acidity .

Therefore, we decided to work with a benzannelated system **2.01** (M=Ru) in which there was no such β-hydrogen present in the molecule. This system has the added advantage that, based on MMX calculation, a benzocyclobutene species such as **2.02** should be substantially more strained than cyclobutane (49 vs 31 kcal/mole). Consistent with this, the barrier to rearrangement of **2.01** to **2.02** (M=Fe) has been found to be at least 13 kcal/mol higher than that of its non-benzannelated analogue.[24] The corresponding Mn complex (**2.01**, M=Mn) was also found to be stable.

2.01 **2.02**

Thus, a straightforward synthetic approach to the benzannelated Ru-carbene complex **2.04** was designed as outlined in Scheme 2-2.

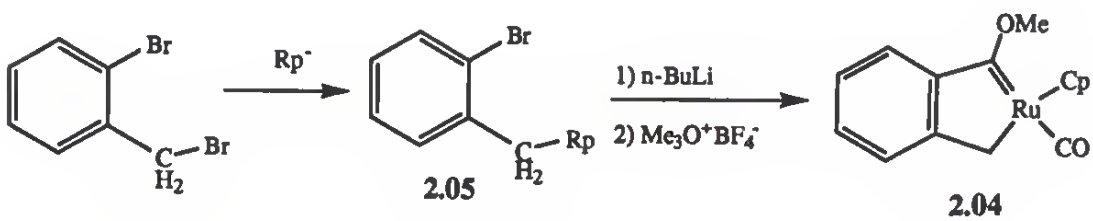

2.05 **2.04**

Scheme 2-2

2-Bromobenzyl ruthenium complex **2.05** was readily prepared in 66% yield as an off-white crystalline solid by reaction of $[CpRu(CO)_2]^-$ (or Rp^-) with 2-bromobenzyl bromide. Addition of 1.2 equivalents of n-BuLi to a solution of compound **2.05** in THF at -100 °C, followed by warming to room temperature overnight and treatment with Me_3OBF_4 gave crystals of **2.04** in moderate yield.

Complex **2.04** was characterized by ^1H and ^{13}C NMR, IR, and elemental analyses. To our knowledge, complex **2.04** is the first example of a benzannelated metallacyclic ruthenium carbene complex. As with its iron and manganese analogues,[7,10] complex **2.04** is exceedingly stable. It showed no evidence of undergoing carbene migratory insertion, which could have been readily detected by observation of its rearrangement to isomeric metallindene **2.06** or by trapping intermedate **2.07** with PMe_3. Neither **2.06** (heating at 80 °C for 5 days) nor **2.08** (photolysis in the presence of PMe_3 for 6 hours) was observed; **2.04** eventually decomposed under such conditions.

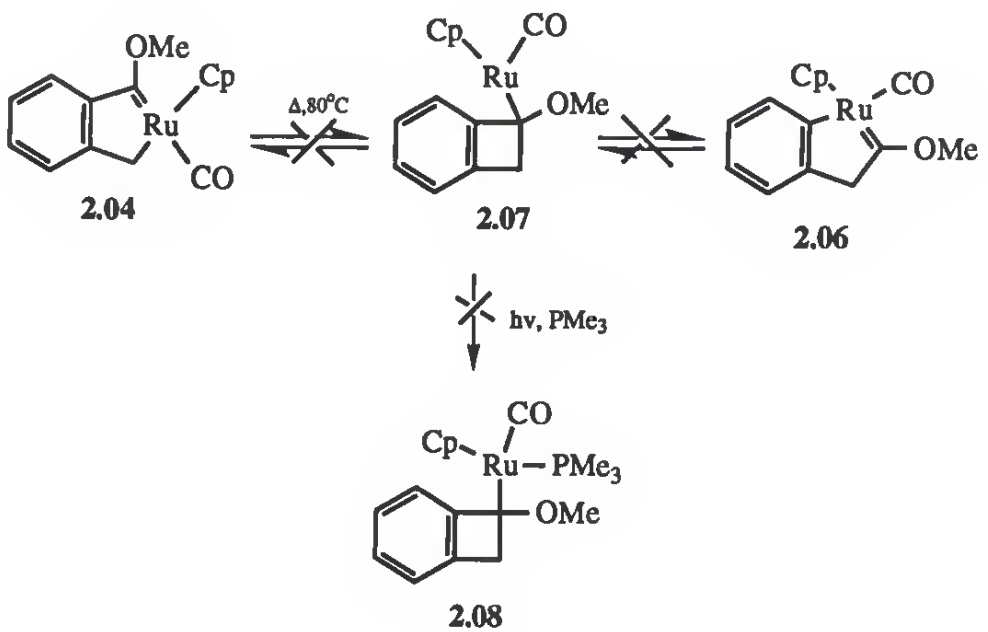

2.04 **2.07** **2.06**

2.08

This stable carbene complex, **2.04**, appeared to be an excellent precursor for our desired synthetic target, **2.03**, and other, non-heteroatom-substituted carbene complexes.*

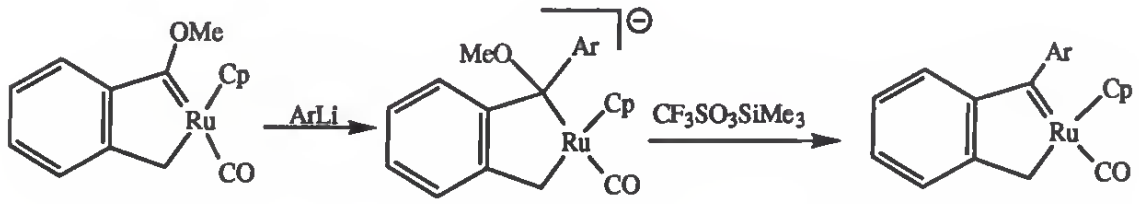

2.04 **2.09** **2.03a**, Ar = Ph
2.03b, Ar = *p*-Tolyl

Scheme 2-3

Reaction of **2.04** with phenyllithium or *p*-tolyllithium in THF at -78 °C, followed by addition of 1.5 equivalents of $Me_3SiOSO_2CF_3$, gave the Ru-carbene complex **2.03a** and **2.03b** in moderate yield, as air-sensitive, black crystals. This nucleophilic substitution reaction is believed to proceed by a stepwise mechanism that involves the anionic intermediate **2.09**.

The Ru complexes **2.03a** and **2.03b** are, to our knowledge, the first examples of stable, aryl substituted, Fischer carbene complexes of ruthenium which do not have a heteroatom stabilizing substituent on the carbene carbon. In the IR spectra of the complexes **2.03a** and **2.03b**, terminal CO absorptions at 1968 and 1966 cm^{-1} were observed, respectively, and their characteristic carbene carbon resonances in the ^{13}C

---

* It is interesting that we found that carbene complex **2.04** undergoes facile substitution of the methoxy group by nucleophiles while its analogues of Mo and W carbeen complexes [25] failed to undergo such a nucleophilic substitution reaction.

NMR were detected at δ 309.5 and 309.2 ppm respectively. Comparing these shifts with those of the carbene resonance of **2.04** (294.2 ppm), it can been seen that the carbene resonances of **2.03a** and **2.03b** are shifed to a relatively lower field, which is in accord with a somewhat reduced electron density on the carbene carbon of the aryl substituted molecules. This is not only because the phenyl is an inherently poorer electron donor than methoxy but also, at least in the crystal, because the phenyl is out of conjugation with the carbon-metal double bond.

The structure of complex **2.03a** was confirmed by x-ray crystallography, the ORTEP representation being shown in Figure 2-1. The compound has a pseudooctahedral geometry with the Cp ring on the top. The bond distance between C6 (carbene carbon) and Ru is 1.949(5)Å a typical bond length for a metal-carbon double bond.[26] Only one phenyl ring (the benzo ring) was found to be conjugated with the Ru-carbene bond. As a result, the C6-C13 bond length of 1.444(7)Å is shorter than C6-C7 [1.470(7)Å] , which is about the length of a normal sp^2-sp^2 single bond (1.48Å).[27] The torsion angle of C18-C13-C6-Ru is 18.4°. The dihedral angle between Ru-C6-C13 and C8-C7-C12 is 46.2°.

A specific purpose for preparation of complexes **2.03a** and **2.03b** was to utilize them in a study of the process of carbene migratory insertion. Thus, an interesting aspect of the chemistry of these molecules was the surprising fact that thermolysis of black compound **2.03a** in benzene at 50 °C failed to give rise to the expected migratory insertion reaction. That is, there was no spectroscopic evidence for formation of the expected carbene migratory insertion product **2.10** as illustrated in Scheme 2-5.

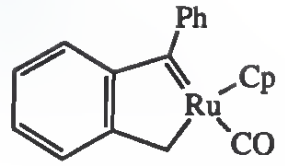

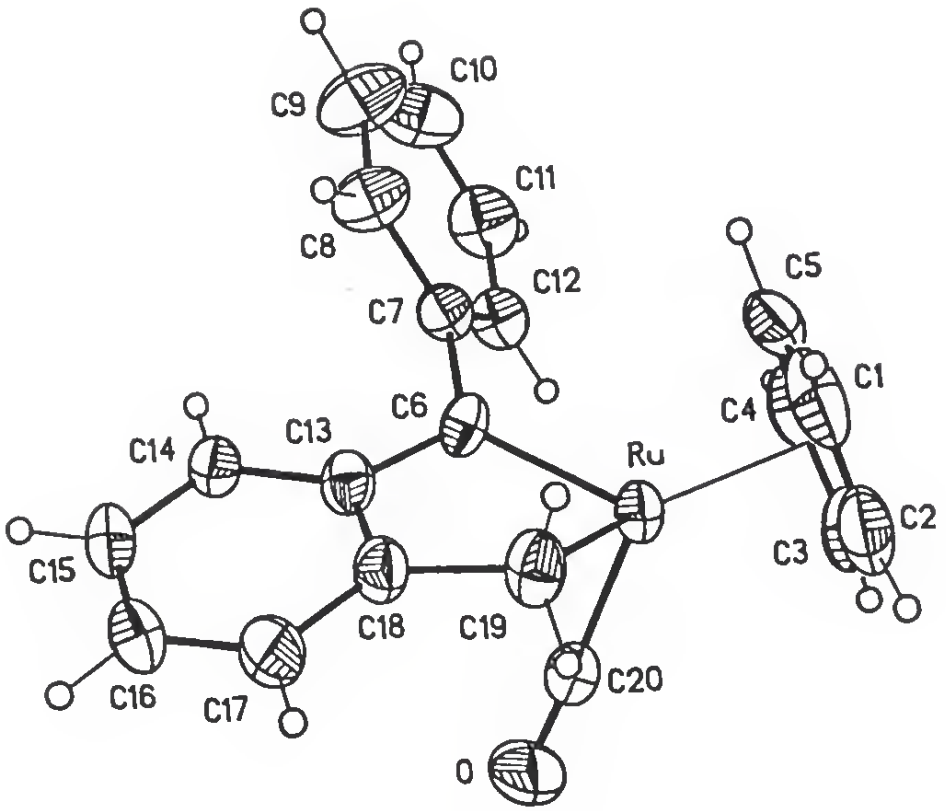

Figure 2-1. Structure and labeling scheme for **2.03a** with 50% probability of thermal ellipsoids.

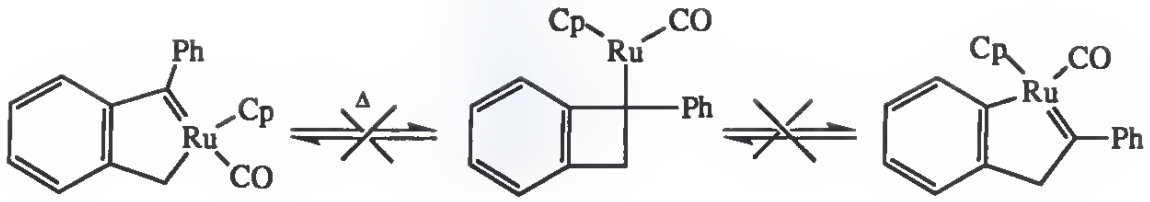

2.03a **2.10**

Scheme 2-5

Instead, exclusively and quantitatively, a clean yellow product which exhibited no characteristeric carbene carbon peak in its ^{13}C NMR spectrum was formed, and in its ^{1}H NMR spectrum the two diastereotopic protons of **2.03a** had disappeared. However, an unusual broad peak at 2.90 ppm and a single peak at 5.19 ppm with an integration ratio of 1:1 were observed in its ^{1}H NMR spectrum. Mixing deuterated water with this unknown product in an NMR tube led to the disappearance of the δ 2.90 peak, a result which implied that this peak was due to the presence of a hydroxyl group in the molecule. Both its mass spectrum and its elemental analysis revealed that the unknown product was an isomer of compound **2.03a**.

Based upon this evidence, a ruthenacene species **2.11a** was proposed for the stucture of this thermolysis product, as shown below.

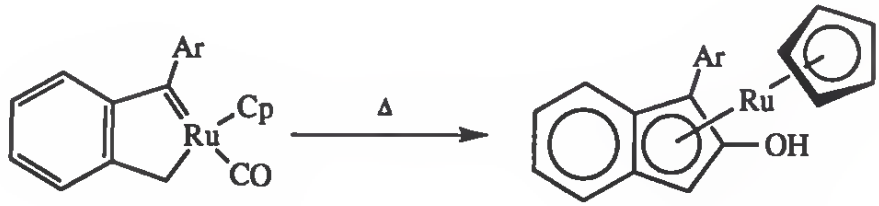

2.03a, Ar = Ph
2.03b, Ar = *p*-Tolyl

2.11a, Ar = Ph
2.11b, Ar = *p*-Tolyl

The identity of the rearranged product **2.11a** was confirmed by a single crystal X-ray diffraction study of the analogous compound **2.11b**.

An ORTEP representation of the structure is given in Figure 2-2. The Cp ring and the indenyl ring are parallel with a dihedral angle of 0.3(3)°. The phenyl ring is not conjugated with the indenyl ring; the dihedral angle between these two rings is 45.6(2)°. The average bond distances of Ru-Cp and Ru-indenyl (five membered ring carbons) are 2.158(4) and 2.203(4)Å, respectively.

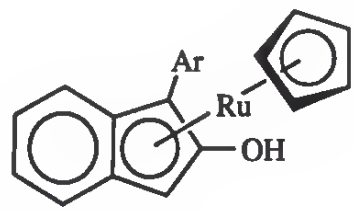

Ar = *p*-Tolyl

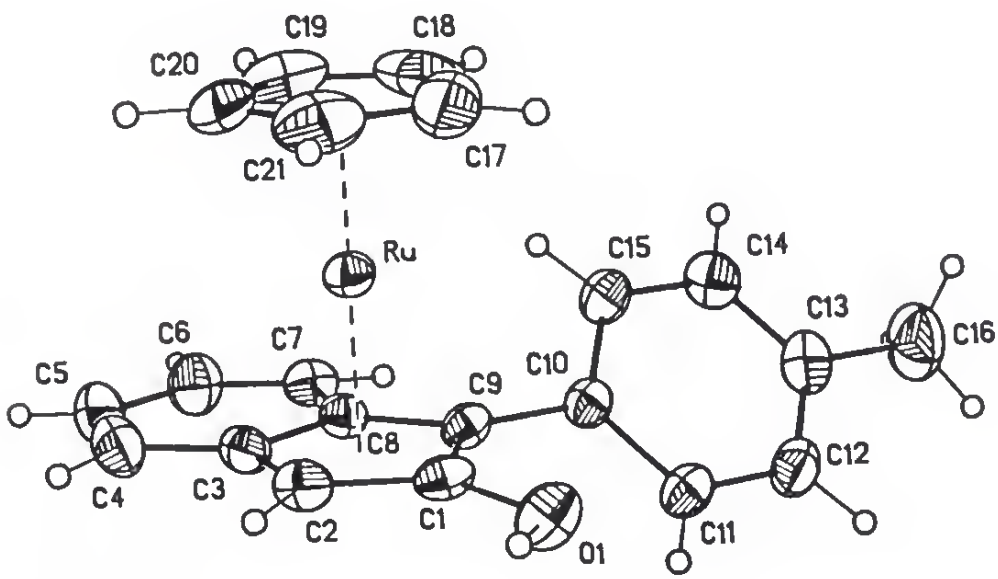

Figure 2-2. Structure and labeling scheme for **2.11b** with 50% probability of thermal ellipsoids.

A proposed reasonable mechanism for the formation of **2.11** from **2.03** is given in Scheme 2-6.

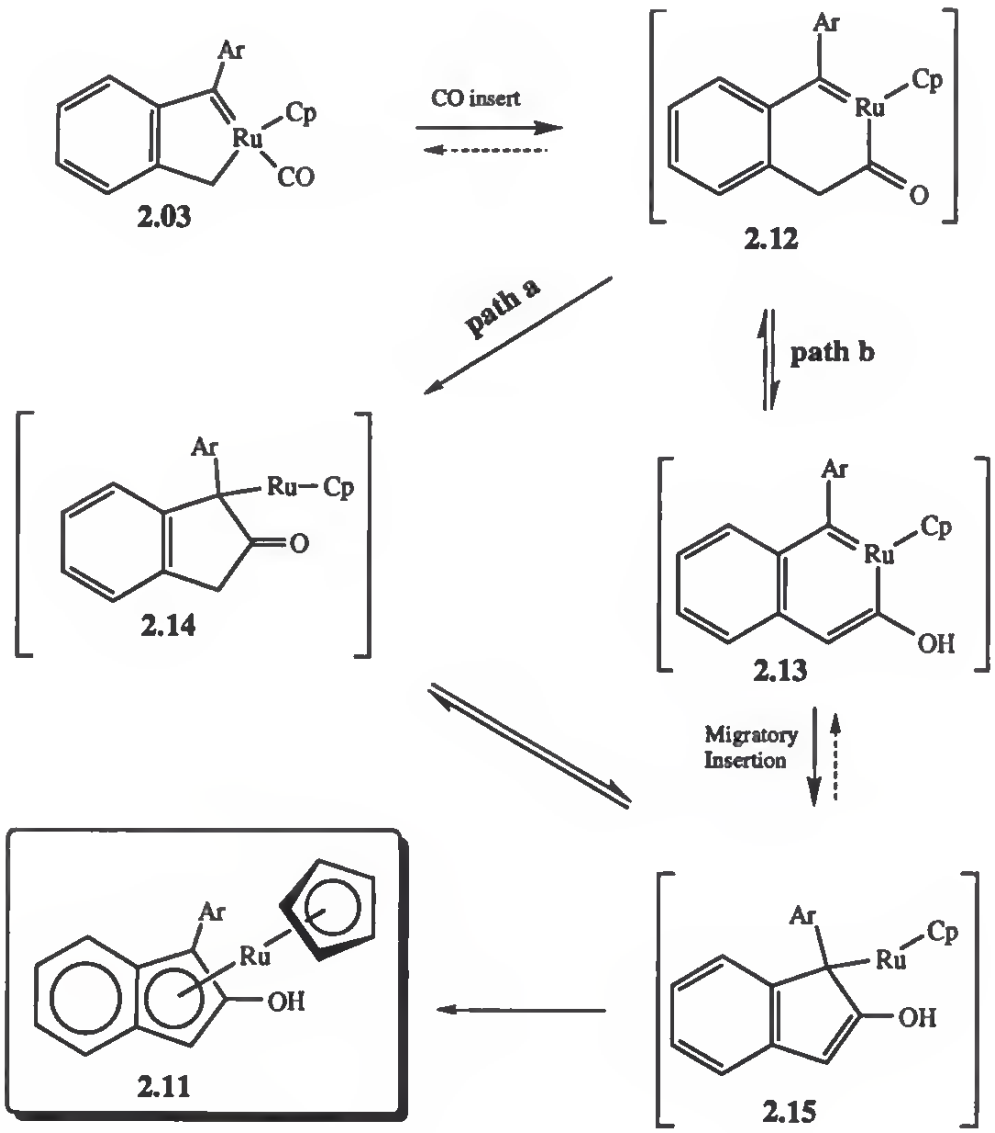

Scheme 2-6

In this mechanism the five membered ring presumably undergoes initial CO insertion to give an intermediate acyl complex **2.12**. This ring expansion step is interesting because it is an example of preferential carbonyl migratory insertion over carbene insertion which is contrary to what appears (from very limited examples) to be usual. For example, Werner[28] found only carbene insertion in **2.17.**

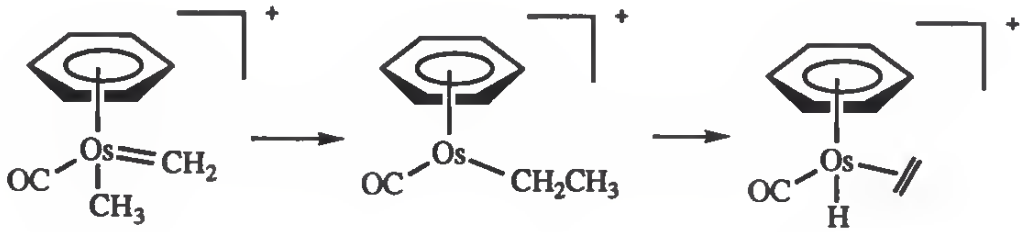

2.17

Jones[5,7] observed a similar result in the cyclic carbene **2.18** which gave only carbene migratory insertion in spite of the attendant cyclobutane strain.

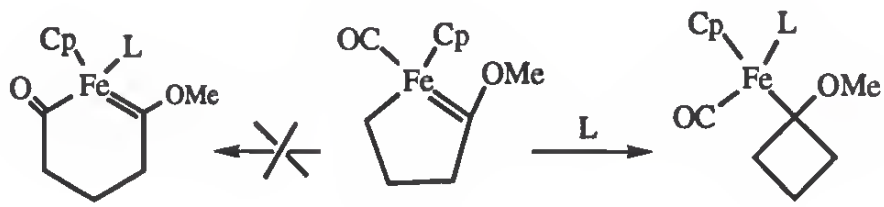

2.18

On the other hand, with enough bias as in **2.19**[8] and , presumably in **2.03** (due to ring strain in benzocyclobutene), carbonyl insertion has also been observed to occur.

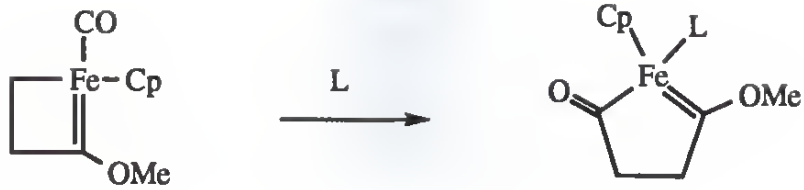

2.19

It is not clear why the thermal labilities of **2.03a** and **2.03b** are so dramatically increased relative to their methoxy substituted precusor **2.04**. One possible explanation is the apparent increased electrophilicity of the terminal carbonyl resulting from replacing the methoxy group with the aryl group. Consistent with this hypothesis is the shift of the carbonyl stretching frequency from 1968.3cm^{-1} for **2.03a** to 1961.3 cm^{-1} for **2.04**.

Interestingly, the conversion of **2.12** to **2.15** could proceed via two different mechanistic pathways. One mechanism (path a) involves an unusual carbene insertion into a metal acyl bond, (for which only one example has been reported.[29]) to give a fourteen electron intermediate **2.14**, followed by tautomerization of **2.14** to give **2.15**. A second mechanism (path b in Scheme 2-6) would involve initial enolization followed by rearrangement of the vinyl group to give **2.15**. Neverthless, by either mechanism, it is apparent that the driving force for the overall reaction is the stability of the metallocenes **2.11**, a kind of product which appears to be characteristic of reactions where metallaaromatic rings may be intermediates.[30-31] Indeed, path b in Scheme 2-6 is particularly intriguing because of its ruthenanaphthalene intermediate **2.13**.

Since intermediates **2.12**, **2.13** and **2.14** are electron-deficient and could be stabilized by complexation with a good ligand, the thermolysis of **2.03** was carried out in the presence of PMe_3.

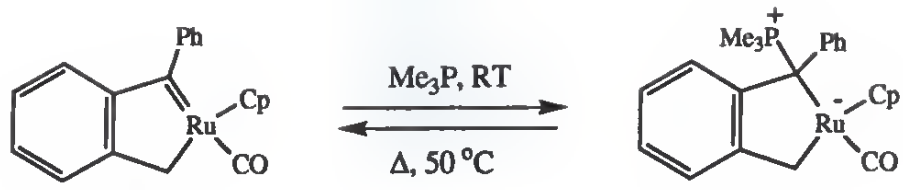

2.03a **2.20**

Unfortunately, it was found that even at room temperature in C_6D_6, PMe_3 simply added rapidly to **2.03a** to give the zwitterion adduct **2.20** in quantitative yield. When **2.20** was heated to 50 °C, it simply dissociated the PMe_3 ligand and regenerated **2.03a** which then rearranged to **2.11** without showing any evidence of a PMe_3 adduct of **2.13** [A small concentration (ca.5%) of **2.03a** could be detected during the conversion of **2.20** to **2.11**].

Complex **2.03b** reacts similarly with PMe_3, undergoing nucleophilic addition to give a zwitterion adduct analogous to **2.20**.

Interestingly, complexes **2.03a** and **2.03b** exhibited different thermal reactivities, with **2.03a** rearranging at 50 °C while **2.03b** rearranged at 70 °C. Such a difference in reactivities is consistent with expectations based upon the better electron donor ability of the tolyl group of **2.03b**, which would tend to stabilize the ground state of the carbene complex and make the carbonyl (CO) of **2.03b** less electrophilic relative to the CO of **2.03a**. Therefore, the CO insertion of **2.03b** should be slowed down in comparasion to that of **2.03a**.

In conclusion, a methoxy stabilized metallaindene complex of ruthenium **2.04** was synthesized. Reaction of this complex with phenyllithium or *p*-tolyllithium followed by treatment with $CF_3SO_2OSiMe_3$ provided the first stable aryl substituted Fischer carbene complexes of ruthenium (**2.03a** and **2.03b**) which do not bear a heteroatom stabilizing substitutent on the carbene carbon. In solution, these complexes underwent a novel thermal rearrangement to form ruthenoence derivatives **2.11a** and

2.11b. A reasonable mechanism for this rearrangement which involves a ruthenanaphthalene intermediate or carbene insertion into an acyl bond is proposed.

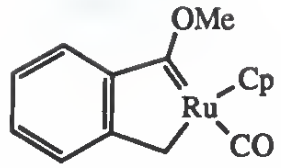

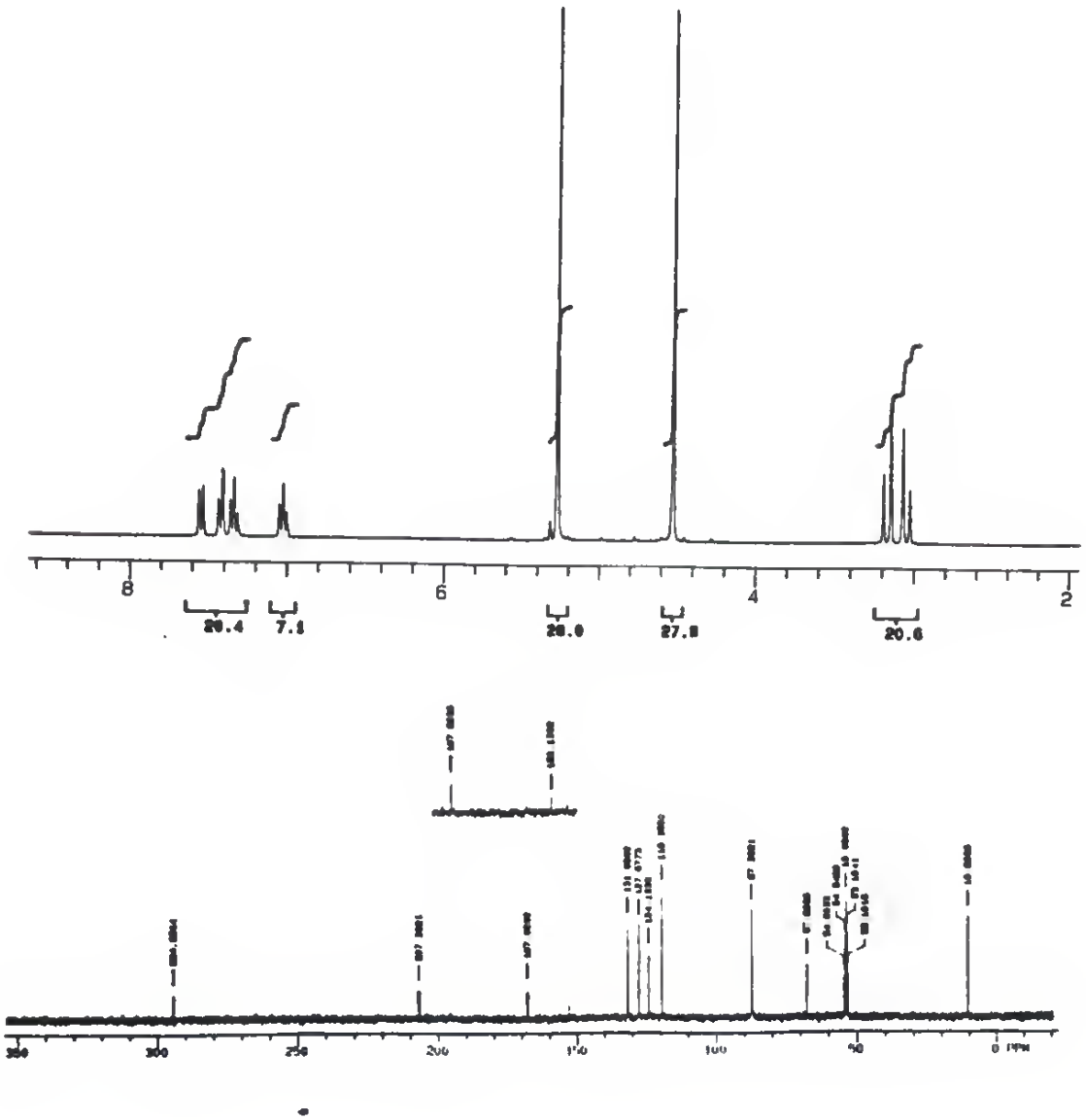

Figure 2-3. ^{1}H and ^{13}C NMR spectra of **2.04**.

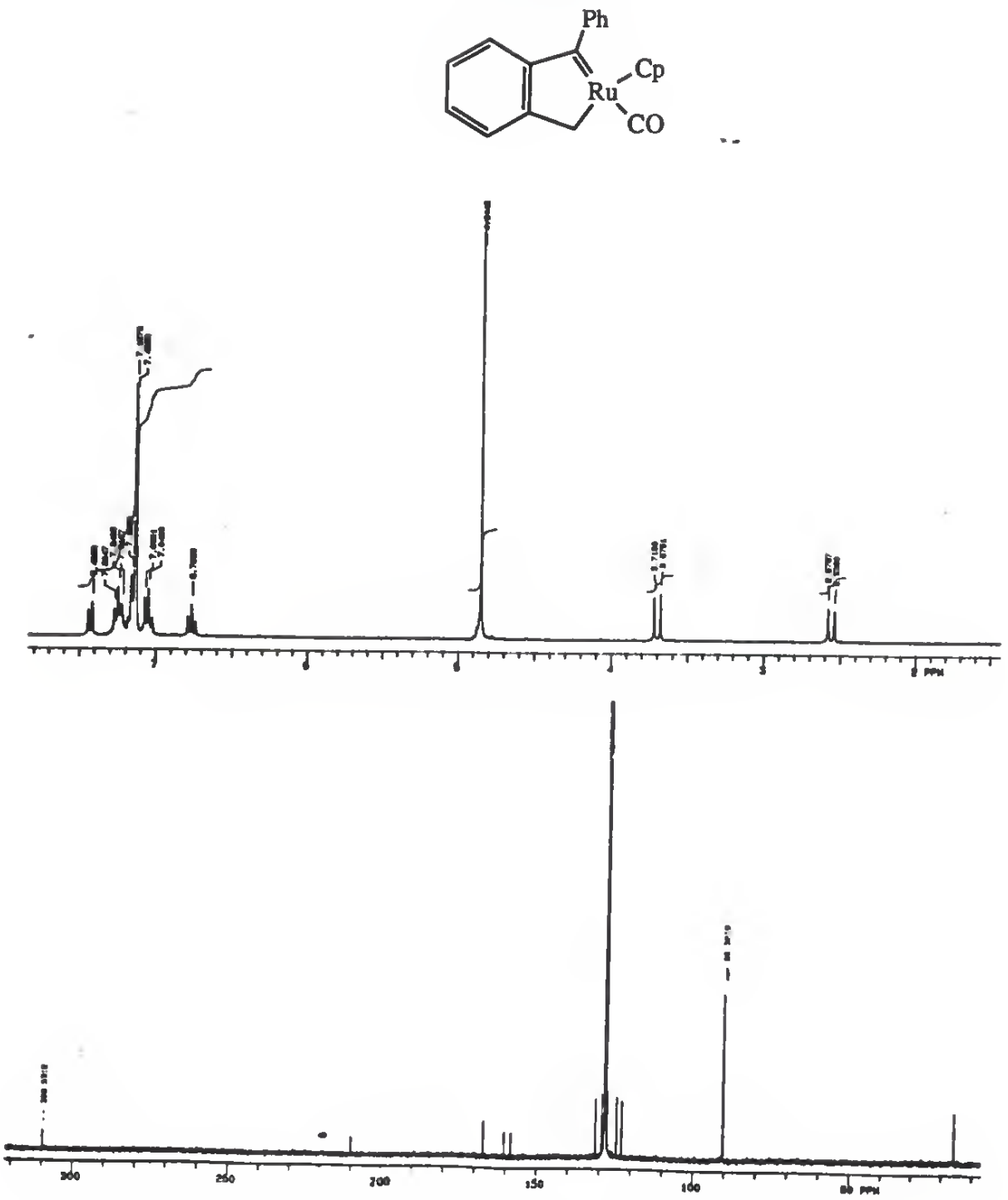

Figure 2-4. ^{1}H and ^{13}C NMR spectra of **2.03a**.

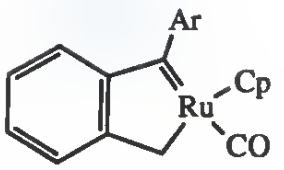

Ar = *p*-Tolyl

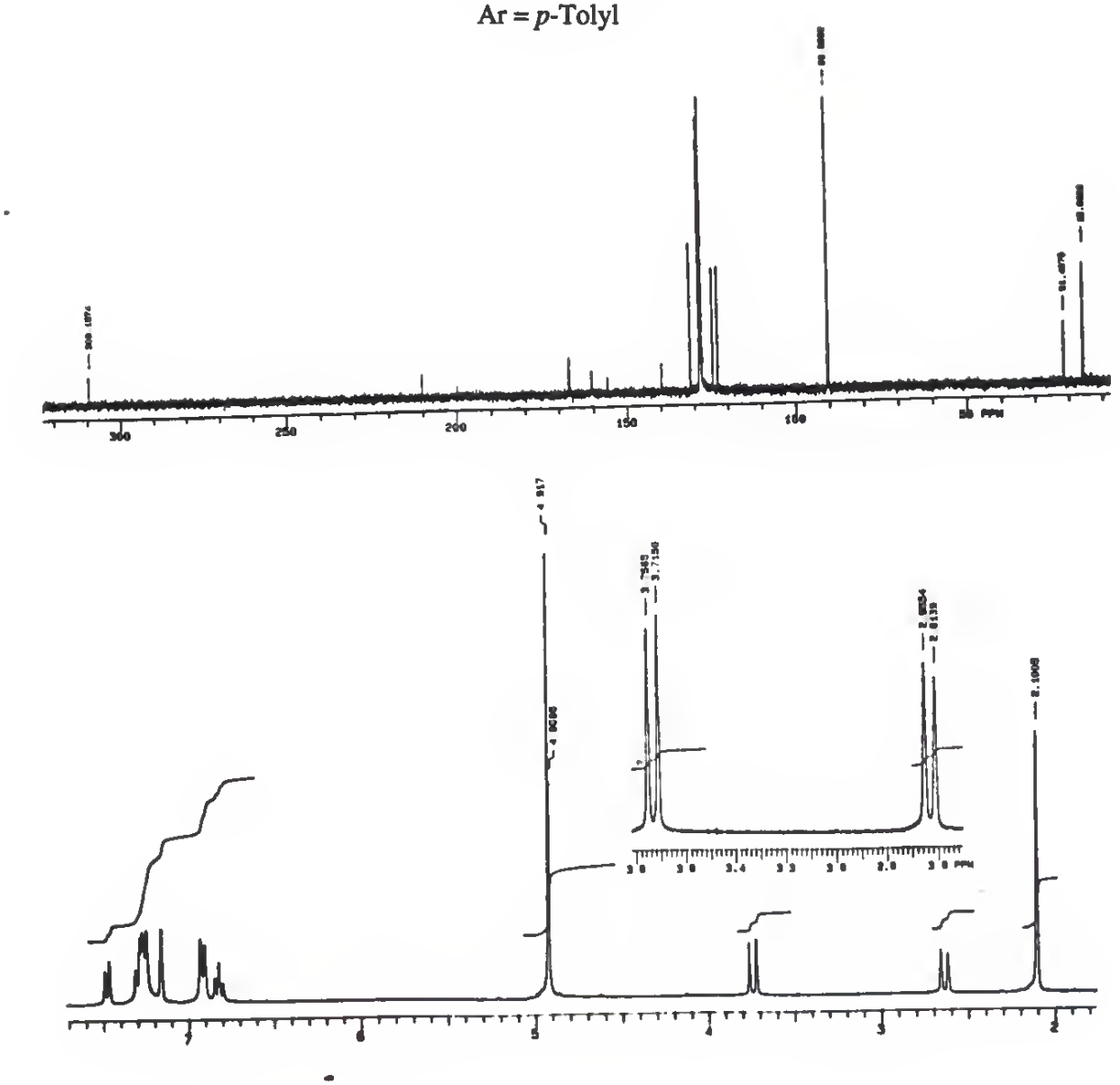

Figure 2-5. ^{1}H and ^{13}C NMR spectra of **2.03b**

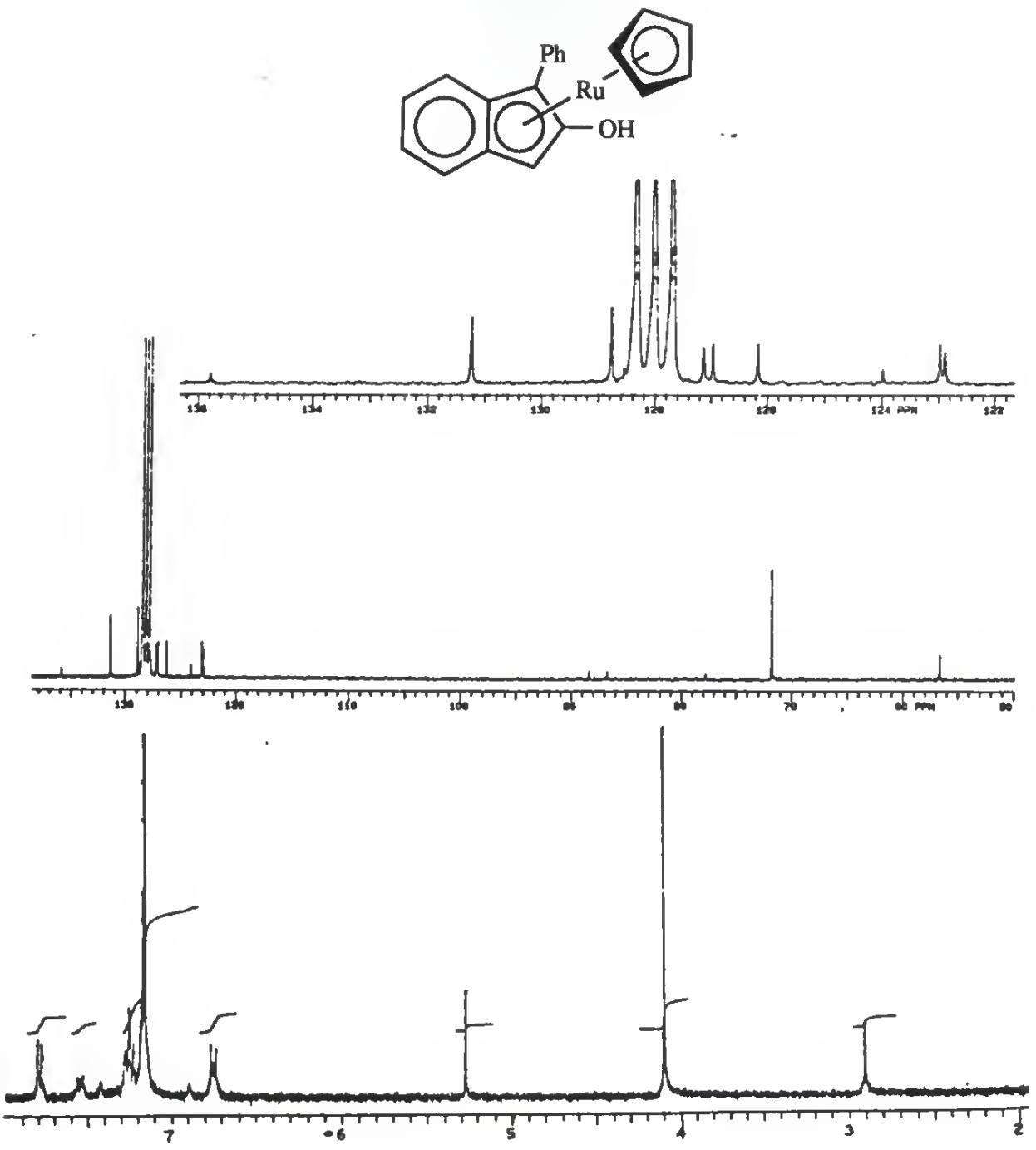

Figure 2-6. ^{1}H and ^{13}C NMR spectra of **2.11a**

CHAPTER 3
SYNTHESIS AND STUDY OF THE MIGRATORY INSERTION OF ACYCLIC RUTHENIUM CARBENE COMPLEXES

Carbene migratory insertion reactions have attracted considerable attention over the years, especially those involving carbene complexes of later transition metals such as iron and ruthenium. This is because such complexes are catalytically active in the Fischer-Tropsch reaction, a reaction in which the carbene migratory insertion step plays a significent role.

However, very few direct studies of the carbene migratory insertion have been published to date.[32] Jones and his co-workers have recently found that the rate of carbene migratory insertion is strongly dependent upon the nature of the metal, and that the rate of rearrangement for iron carbene complex **1.19** is more than 10^7 times faster than that of ruthenium carbene complex **1.30.**

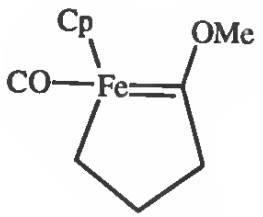

1.19

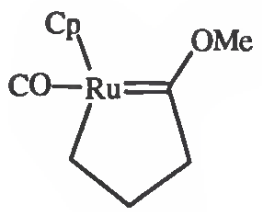

1.30

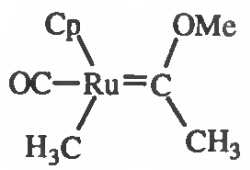

1.32

This observation suggested that it might be possible to synthesize an acyclic ruthenium carbene complex such as **1.32** which would be analogous to the cyclic

ruthenium carbene complex **1.30** except that no strain factors would be present either in the starting material or in the rearrangement product. If such a complex could be made, then its migratory insertion could be directly studied.

However, for initial studies, complex **3.01** was selected with the idea that the thermal stability of an aryl-substituted carbene complex should be greater than its alkyl-substituted carbene complex analogue.[33]

The synthetic strategy for the preparation of acyclic Ru-carbene complex, **3.01** is given in Scheme 3-1.

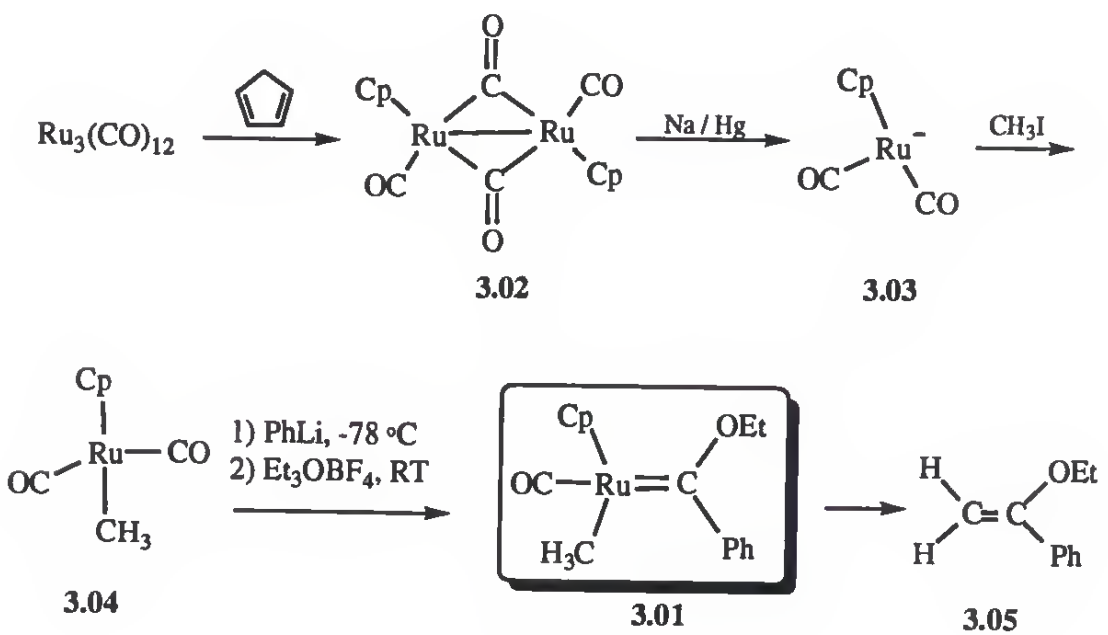

Scheme 3-1

This strategy was satisfactory up to **3.04** (formed air-sensitive Rp-Methyl **3.04** in moderate yield) but when **3.04** was treated with phenyl lithium at - 78° C followed by triethyloxonium fluoroborate (ethoxy was used rather than methoxy because it could be

made in our lab)[48] at room temperature and the reaction mixture worked up, no carbene complex **3.01** was observed; the only detectable product was **3.05** (the structure was confirmed by comparison with an authentic sample).[34] Although it was somewhat disappointing that the carbene complex **3.01** was not observed, formation of **3.05** suggested that the carbene complex **3.01** had been present as a transient intermediate but that migratory insertion as depicted in Scheme 3-2 was too rapid to permit isolation of the carbene complex at ambient temperature.

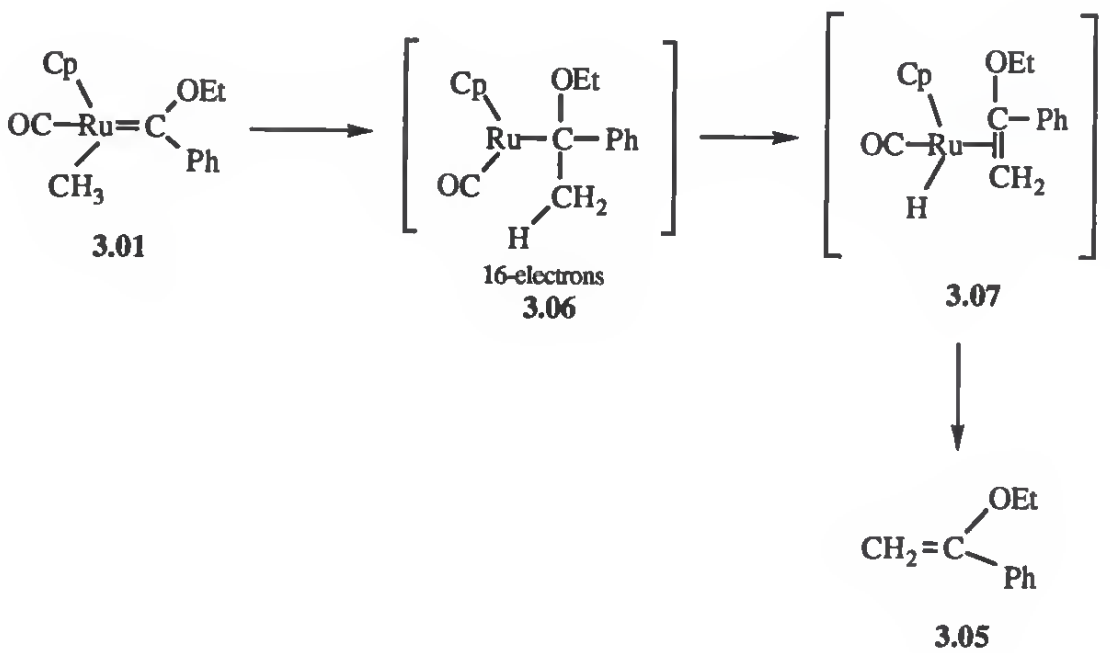

Scheme 3-2

A logical mechanism for formation of enol ether **3.05** from **3.01** involves migratory insertion of **3.01** to form the 16-electron species **3.06** which then undergoes β-elimination to give π-complex **3.07**. Dissociation of **3.07** would yield the enol ether **3.05**.

From these results it became clear that in order to detect and study migratory insertions in acyclic carbene complexes of ruthenium, the reactions would have to be carried out and examined at low temperature. Since isolation under these conditions would be problematic, an apparatus that would permit direct monitoring of the reaction without work-up was required. We therefore constructed and modified a special apparatus which had been designed by Periani and Bergman[35] as shown in Figure 3-1.

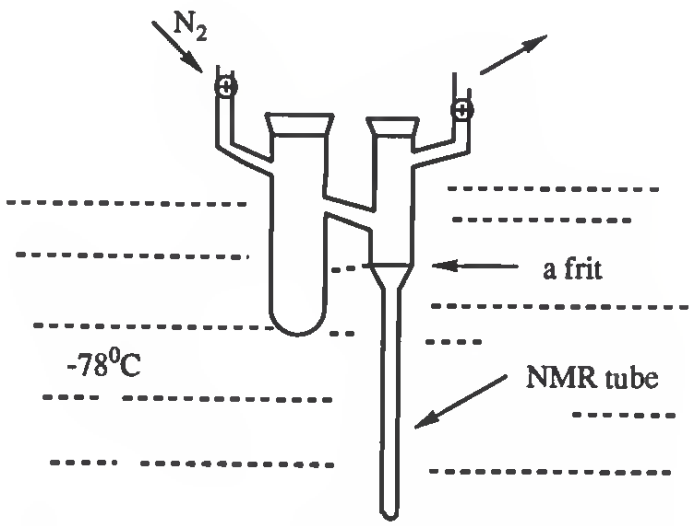

Figure 3-1. Specially-Designed Low Temperature Apparatus

Furthermore, since purification of ethoxy complex **3.01** at such low temperature was not feasible, trimethylsilyl chloride was initially substituted for triethyloxonium fluoroborate because it gave a somewhat cleaner reaction and also because the hyperconjugative stabilizing effect of the O-Si bond should provide additional stability to the carbene complex by retarding the rearrangement and thus increase the chance of observing the carbene complex.

In carrying out these low temperature reactions, the starting material **3.04** in diethyl ether was placed in the specially designed schlenk tube and was allowed to react

with phenyllithium at -78 °C. This was followed by warming the mixture to approximately -30 °C with evaporation of ether solvent at this temperature over a six hour period to gave the yellow ruthenium enolate salt **3.08**. The enolate salt was then treated with one equivalent of trimethylsilylchloride in deuterated methylene chloride at -78 °C, a procedure which we expected would lead to formation of the desired carbene complex **3.09** as shown in Scheme 3-3.

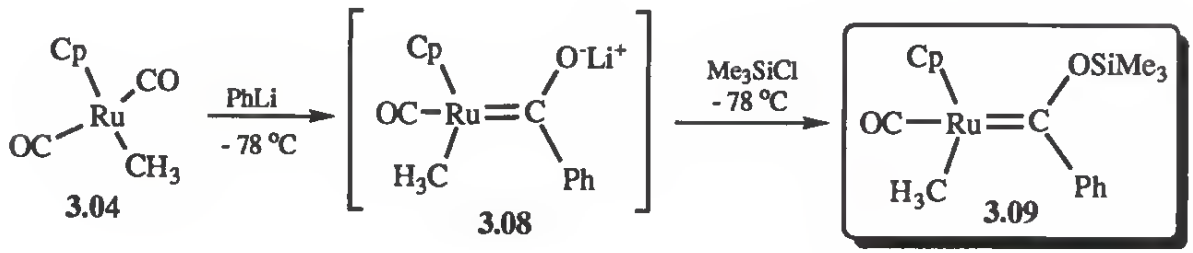

Scheme 3-3

Once the above described procedure was completed, the whole apparatus was immersed in a -78 °C dry-ice/isopropanol bath, and the reaction mixture was then filtered directly through a frit into an nmr tube which was then sealed at liquid nitrogen temperature.

The ^{1}H and ^{13}C NMR spectra of a typical run are shown in Figure 3-2. At -70 °C two Cp signals were observed in the ^{1}H NMR spectrum at 5.064 and 4.964 ppm; the signals coalesced to give a broad peak when the temperature was gradually increased to -40 °C as shown in Figure 3-3. The broadness of the peak clearly indicated that fluxional behavior was being exhibited in the system. The formation of metal hydride (-8.6 ppm) and new Cp signals at 4.86 ppm also began to be observed at -40 °C with loss of the original Cp signal as illustrated in Figure 3-4.

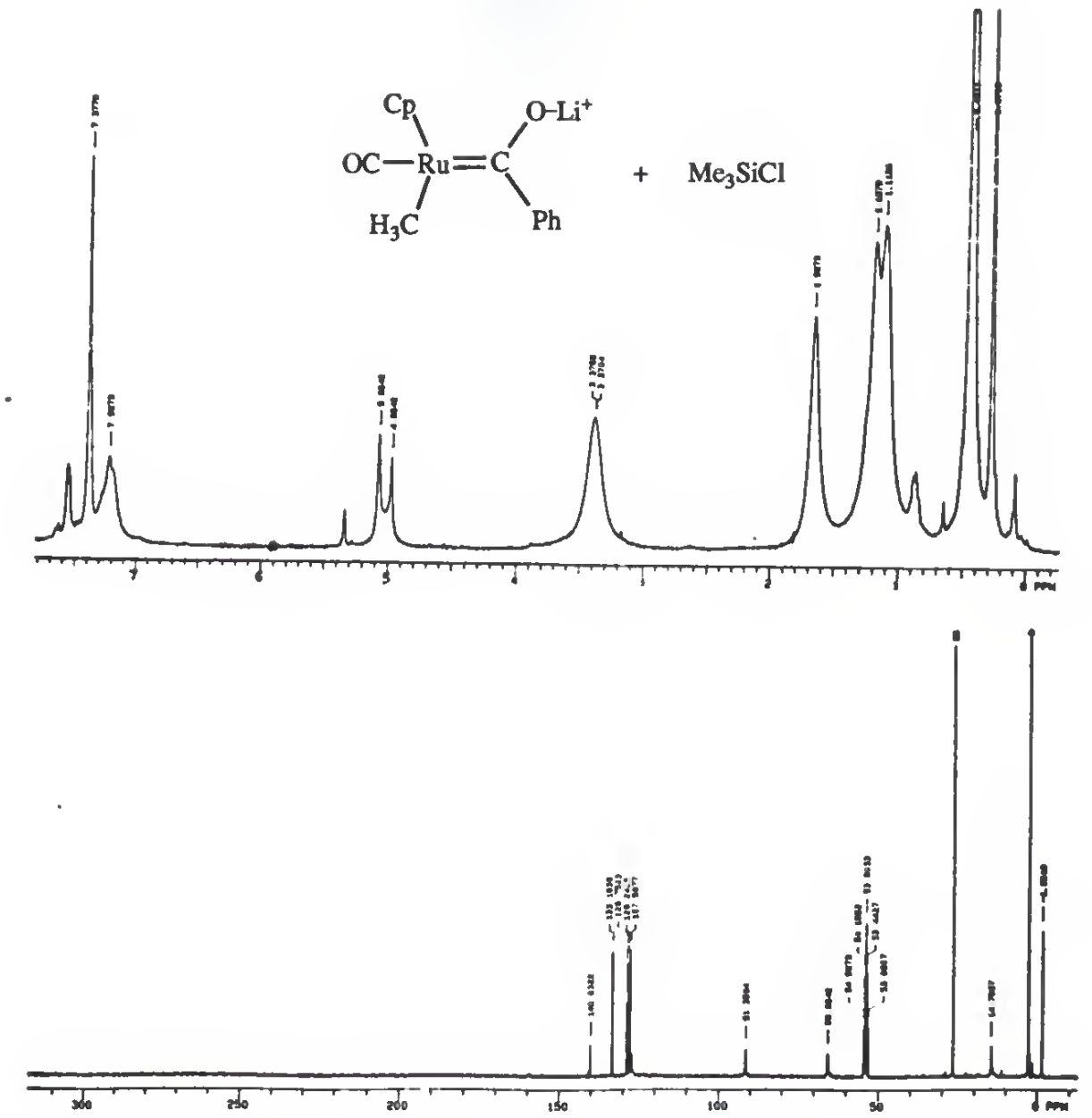

Figure 3-2. ^{1}H and ^{13}C NMR spectra of a typical run at -78 °C attempting to silylate the enolate **3.08**. Two Cp signals (δ 5.064 , 4.964 ppm) were observed. No carbene carbon was observed in its characteristic region.

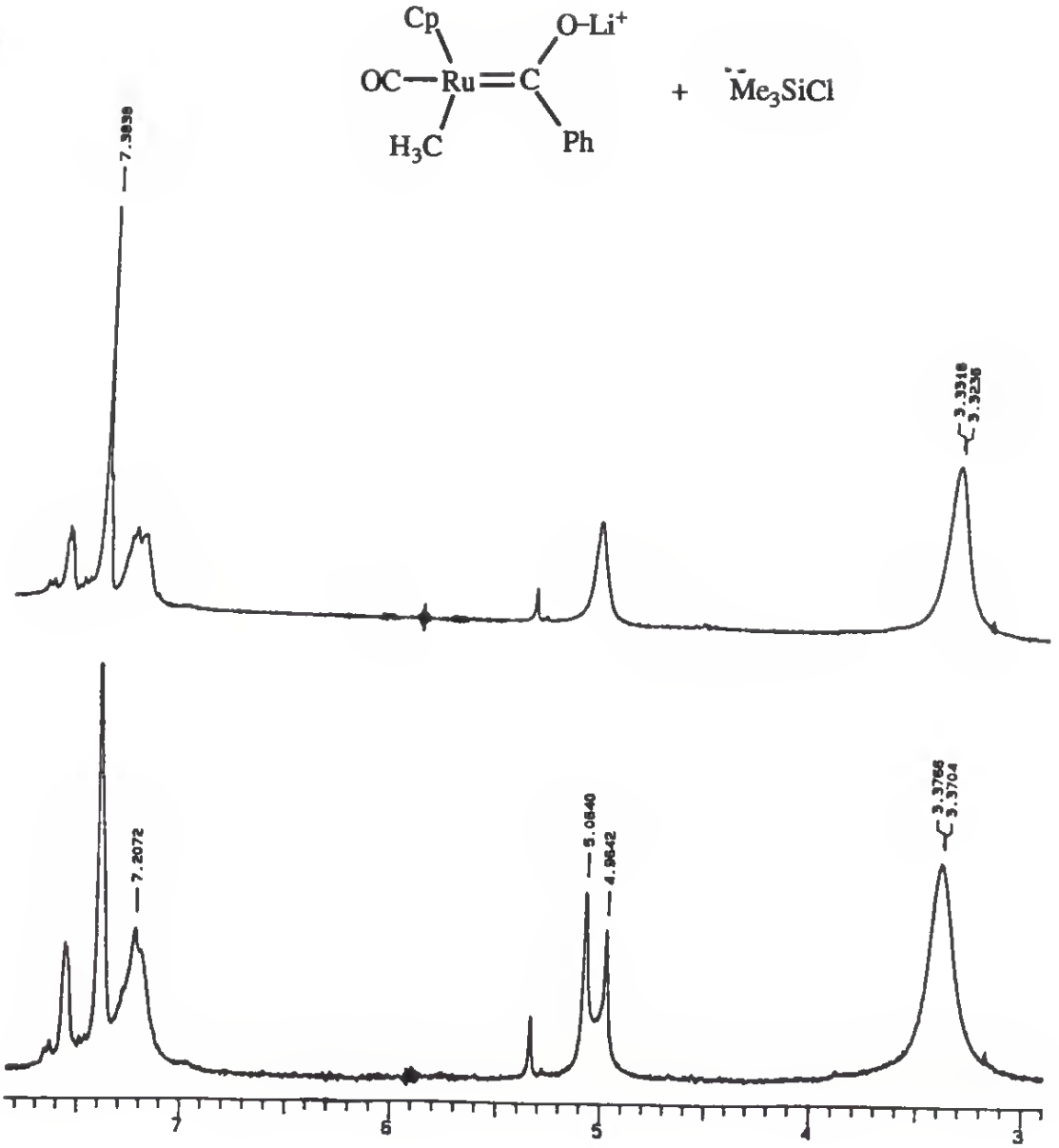

Figure 3-3. ^{1}H NMR spectra of mixture of **3.08** + Me_3SiCl at -40 °C (top) and -70 °C (bottom).

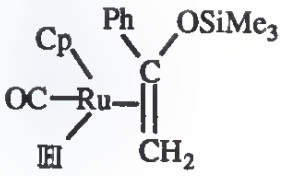

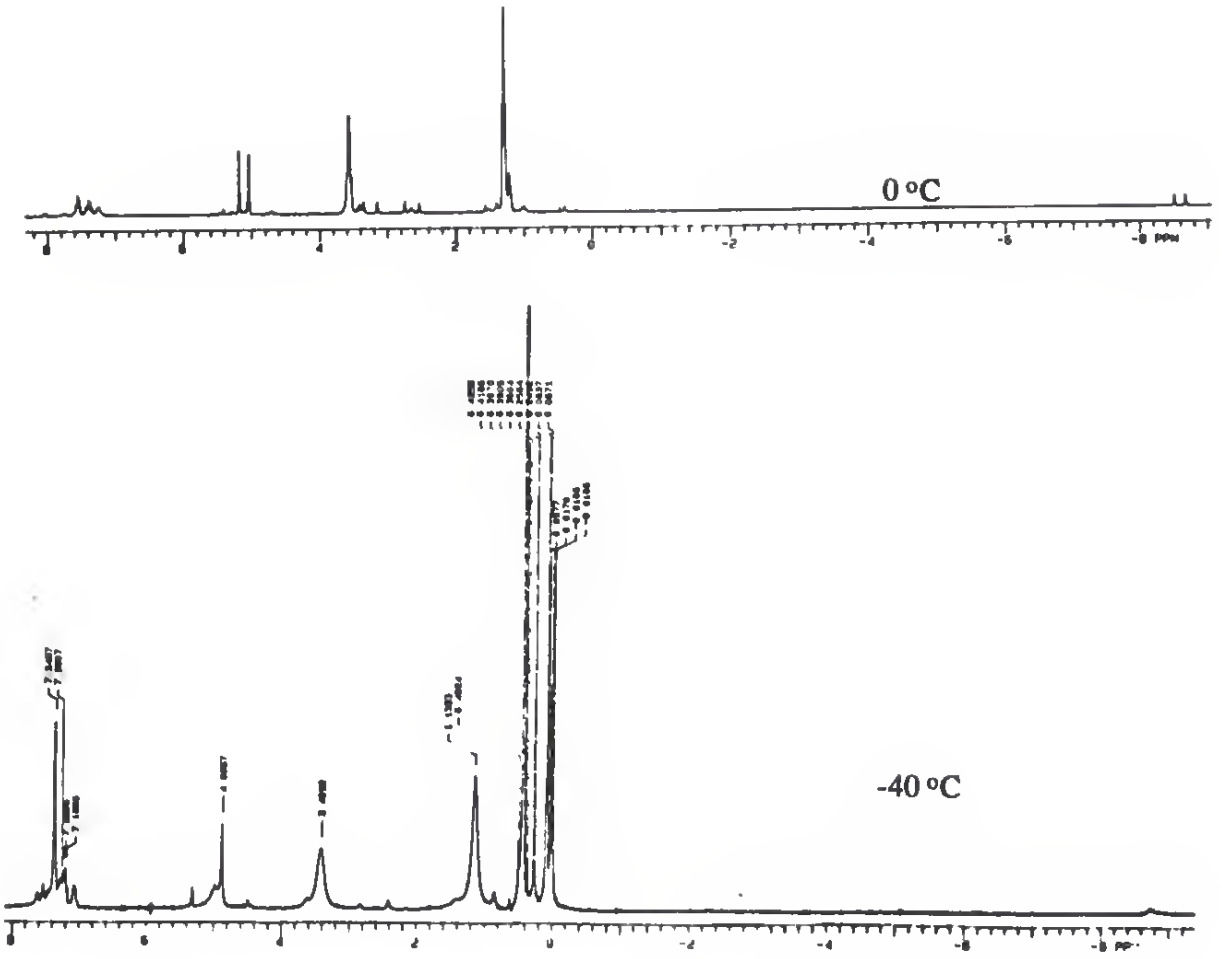

Figure 3-4. ^{1}H NMR spectra showing formation of the π-complex **3.11** (metal hydride δ -8.6 ppm and new Cp signal δ 4.86 ppm) at -40 °C (bottom). Two isomers of **3.11** can be seen at 0 °C (top).

The formation of the free enol ether **3.10** was detected upon further warming of the reaction mixtures. (In order to verify the identity of **3.10**, it was synthesized according to a known literature procedure[36]).

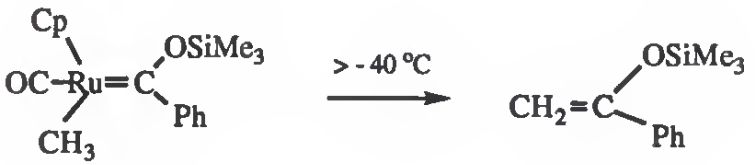

3.09 **3.10**

Formation of the metal hydrides **3.11** and the enol ether **3.10** left little question that the carbene species **3.09** was being formed. Unfortunately, the two resonances that would be expected to be the most characteristic of a carbene complex (a carbene carbon at very low field; i.e. 270 ~ 350 ppm and a methyl carbon at high field; i.e. above TMS) could not be detected in the ^{13}C NMR spectra.

In order to assist us in seeing these peaks, it was decided to enrich both the carbene carbon and the methyl carbon with ^{13}C. The methods used for preparation of these enriched Ru-carbene complexes are shown in Scheme 3-4 .

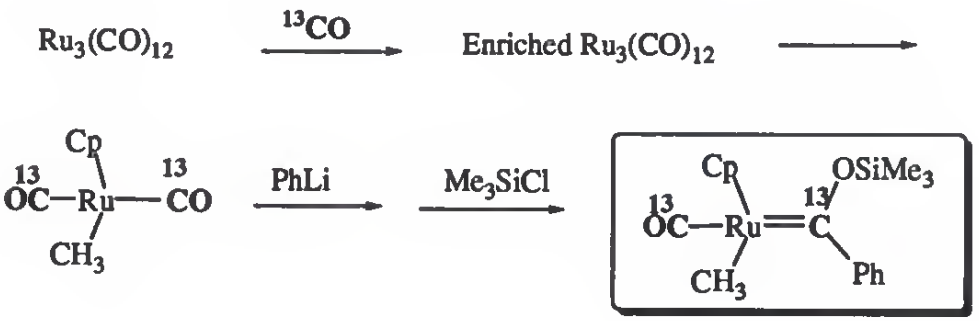

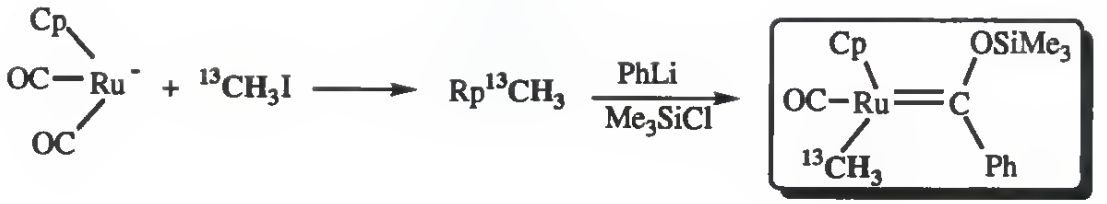

Scheme 3-4

Indeed, when the enriched materials were used, resonances in both the carbene region and the methyl region in the ^{13}C NMR were observed. Since these signals were in the expected regions, it was assumed that the acyclic ruthenium carbene complex **3.09** had been formed at -78 °C. Surprisingly, at -90 °C, multiple resonances in the characteristic carbene carbon region were observed, as well as in the methyl region of the spectrum as shown in Figure 3-5. These resonances coalesced upon warming the reaction mixtures, a result which will be discussed in more detail later.

Upon warming these reaction mixtures, it was found that the decomposition product **3.10** was the same as from those without enriched carbon. The results, thus, seemed consistent with carbene complex formation.

Although the low temperature synthesis of this acyclic ruthenium carbene complex, **3.09**, was technically difficult, the preparation was actually quite clean. It was presumed that, at -40 °C, the migratory insertion process of the ruthenium carbene complex **3.09** was being observed as depicted in Scheme 3-5. In a process similar to that outlined in Scheme 3-2 for the ethoxy complex, trimethylsiloxy complex **3.09** could be expected to give a 16-electron intermediate which would undergo β-elimination to produce π-complexes **3.11**, which were the first products actually to be observed. These π-complexes which exist as isomers, then, could be observed to dissociate to give the free enol ether product **3.10.**

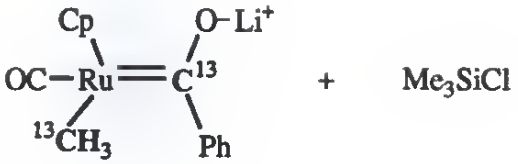

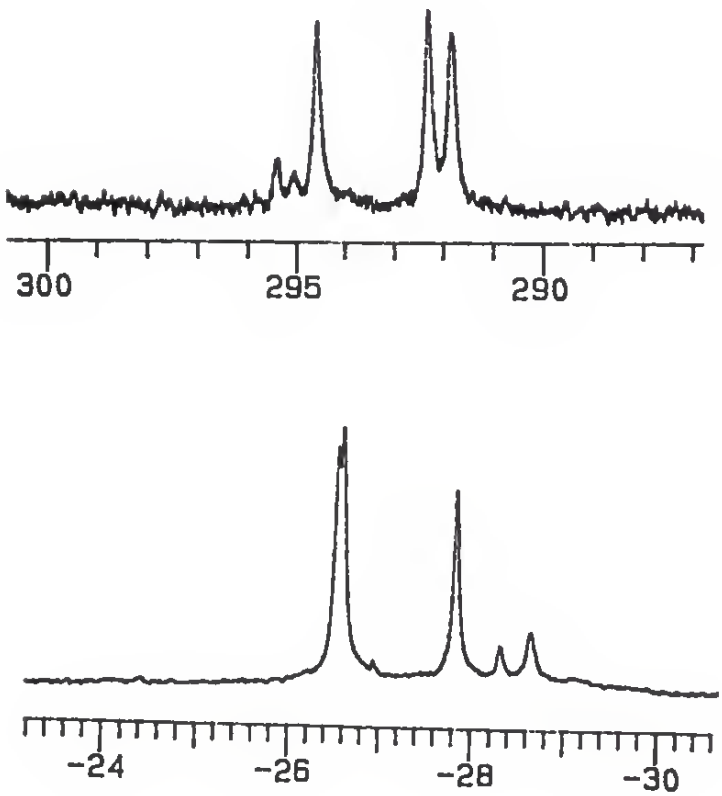

Figure 3-5. ^{13}C NMR spectrum of enriched **3.08** with Me_3SiCl in the expected carbene carbon and methyl regions at -90 °C.

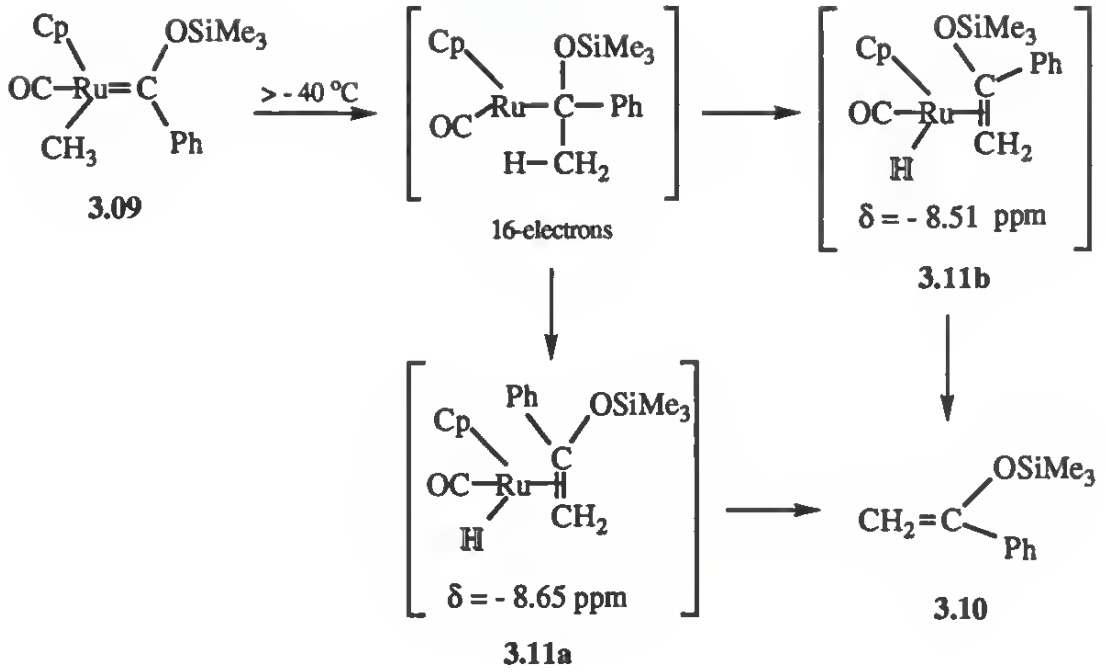

Scheme 3-5

An initial goal of this research was to study the migratory insertion process. Attempts were therefore made to study the kinetics of the reaction that was occurring at -40 °C , Unfortunately, this led to frustrating results. At first, we were quite puzzled by the fact that we could not get reproducable kinetic data, with each attempt to treat the process as first order leading to curved lines, (a result which in the end caused us to suspect that the observed process might not be first order.) Slowly we realized that instead of observing first order decomposition of **3.09**, we might be observing rate-determining reaction of lithium enolate **3.08** with trimethylsilylchloride to form the carbene complex **3.09** which then rearranges rapidly, without detection, to the products of migratory insertion (**3.11** and **3.10**) as illustrated in Scheme 3-6.

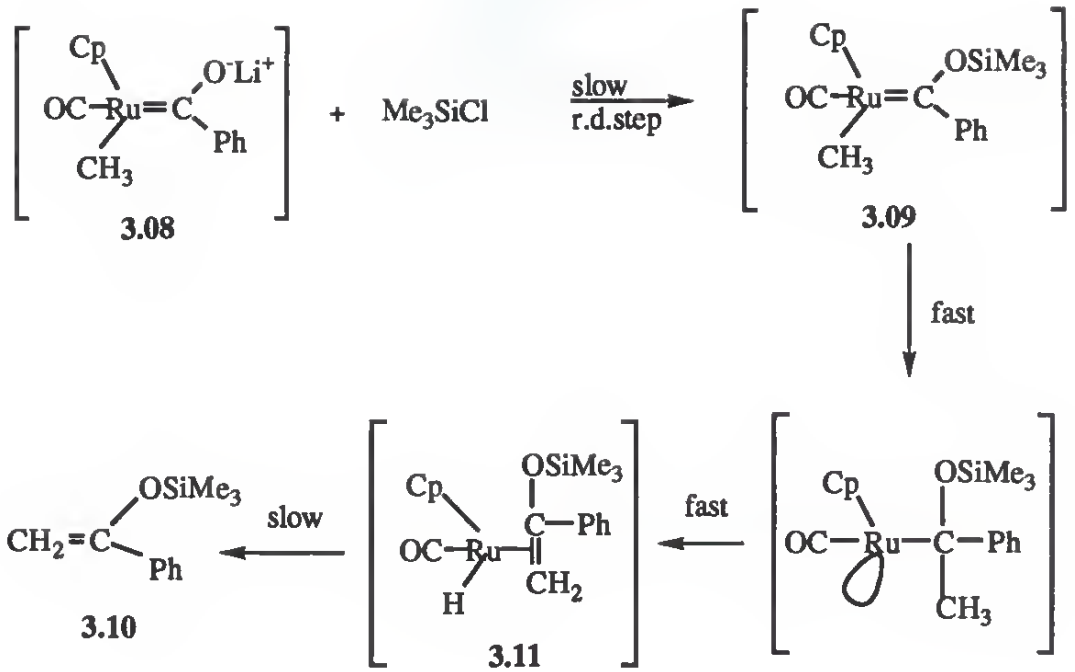

Scheme3-6

To verify this assumption, a control experiment was carried out in the same manner as described in Scheme 3-3 except without addition of trimethylsilylchloride. In other words, the starting material **3.04** was allowed to react with phenyllithium at -78 °C followed by removing solvent at -30 °C to give the lithium enolate **3.08**. This enolate was then dissolved in the deuterated methylene chloride at -78 °C and transferred into an nmr tube for the comparative study.

As a result and to our amazement, it was found that the ^{13}C NMR signals of the lithium enolate **3.08** were virtually identical to those observed for the earlier presumed carbene complex **3.09** at -90 °C as illustrated in Figure 3-6. It would require quite a coincidence if the lithium enolate **3.08** and the carbene complex **3.09** were to have identical chemical shifts in the NMR.

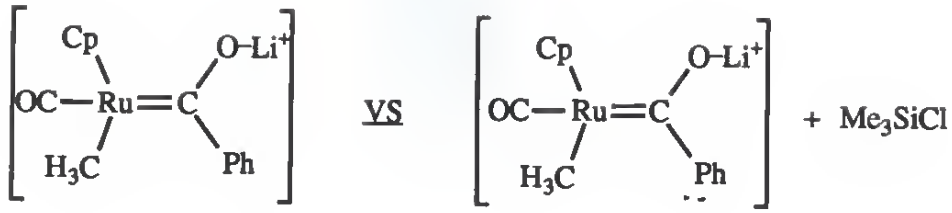

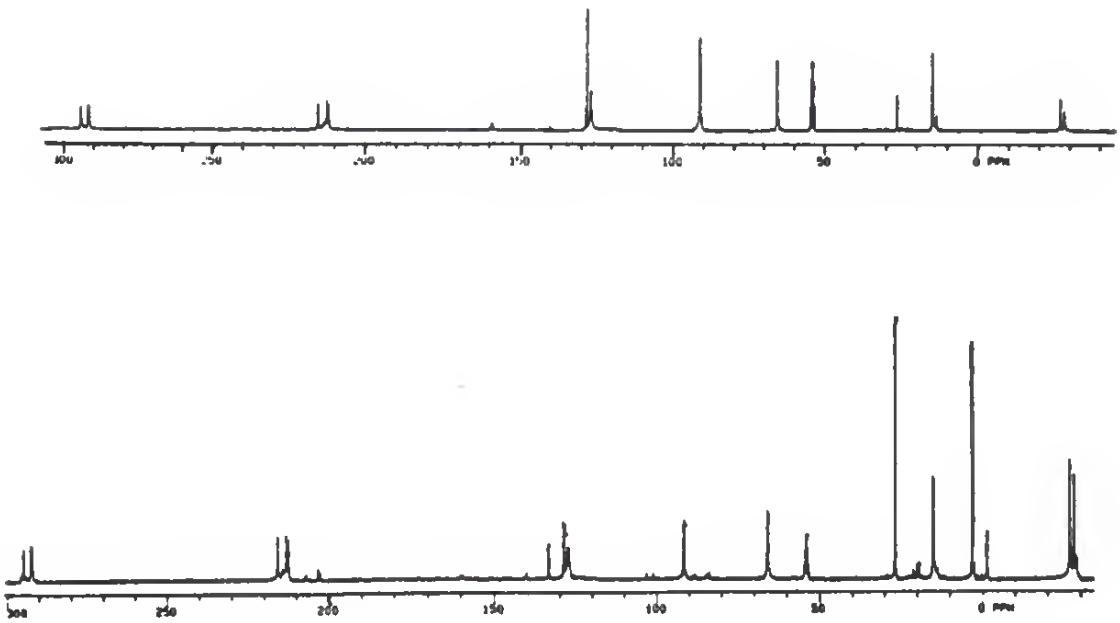

Figure 3-6. ^{13}C NMR spectra of Li-enolate **3.08** (top) and presumed carbene complex **3.09** (bottom) at -90 °C.

This remarkable result induced us to compare the ^{13}C NMR spectra of an authentic ruthenium lithium enolate with its alkylated carbene counterpart (results from chapter 2). For this purpose we chose the isolable ruthenium indene complex **2.04** whose substituents are analogus to those in the acyclic carbene complex **3.09** (alkyl on metal; aryl on carbene carbon) but which is unable to rearrange. This could be prepared from its lithium enolate precusor, **3.12** (Scheme 3-7).

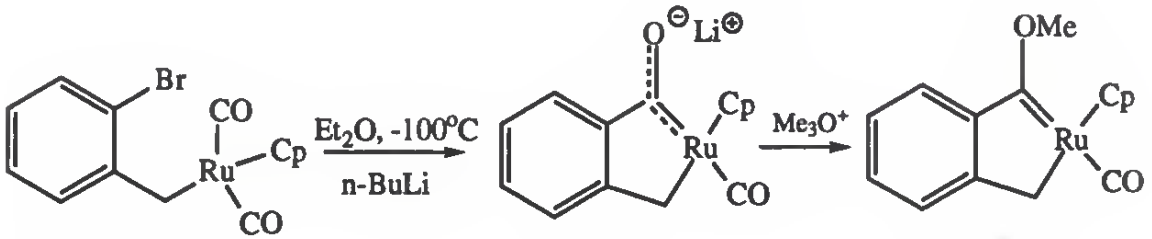

2.05 **3.12** **2.04**

Scheme 3-7

The 2-Bromobenzyl ruthenium complex **2.05** was treated with 1.2 equivalents of *n*-butylithium at -100 °C, followed by warming to room temperature overnight. Evaporation of solvent gave the reddish lithium enolate **3.12**. Methylation of **3.12** was accomplished by treatment of **3.12** with excess Me_3OBF_4 followed by purification and isolation to yield **2.04**. Interestingly, the ^{13}C NMR spectra of **3.12** and **2.04** in deuterated methylene chloride revealed that the chemical shifts of the carbene carbon signals of the lithium enolate **3.12** and those of the methylated indene complex **2.04** are very similar, as shown in Figure 3-7.

This result was somewhat surprising because it was expected that the chemical shifts of a lithium enolate would be quite different from those of an alkylated carbene

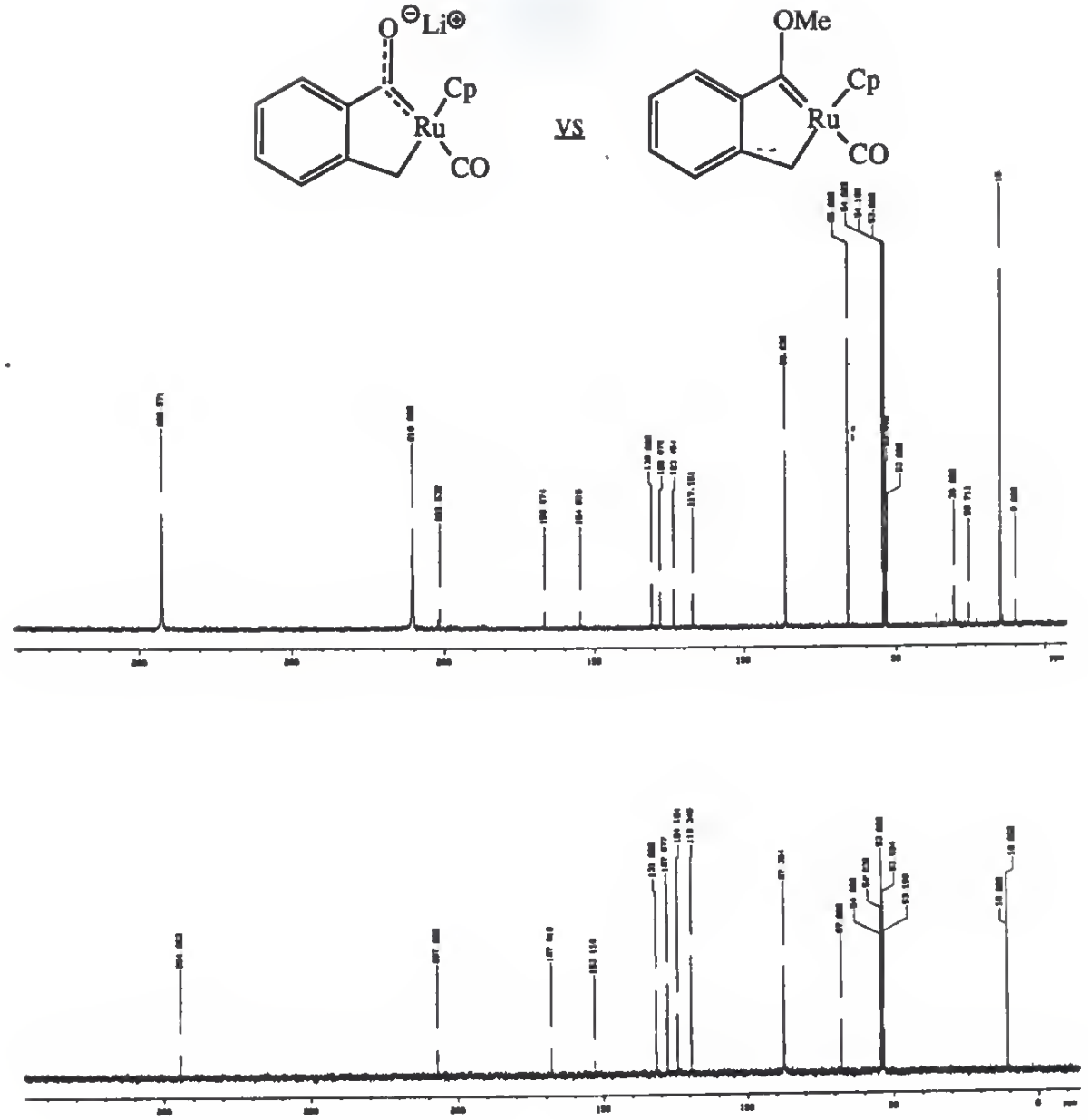

Figure 3-7. ^{13}C NMR spectra of Li-enolate **3.12** (Top) and methylated indene complex **2.04** (bottom).

complex. Normally, acyl carbons of neutral complexes appear at much higher field than carbene carbons (~230 ppm vs ~350 ppm), although examples of anionic acyl complexes[37], such as **3.13**, have now been found which exhibit chemical shifts approaching the value we have observed for **3.08** and **3.12**.

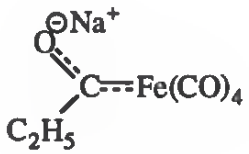

3.13

^{13}C nmr (δ TMS) 279.7 ppm in THF

We, therefore, interpret these nmr results (the comparison of spectra of lithium enolates **3.12** and **3.08** with those of alkylated carbene complex **2.04**) as indicating that the spectra of anionic acyl complexes derive from tightly ion-paired species which are non-acyl-like, but rather structurally more closely resemble their alkylated carbene complexes counterparts.

An additional aspect of the enriched lithium enolate **3.08** proved to be very intriguing. As mentioned earlier, a number of resonances were detected in the characteristic carbene carbon region at -90 °C (Figure 3-5). These signals exhibited a temperature dependence with coalescence being observed upon warming the lithium enolates to -50 °C. The results from this ^{13}C NMR temperature-dependence experiment are illustrated in Figure 3-8.

To be certain that the phenomenon which was being observed at -50 °C was not simply decomposition, the sample was cooled back down to -80 °C, and the original spectrum was seen to return. This indicated that one was observing a dynamic equilibrium process during this experiment. The enriched methyl resonances also exhibited a similar temperature dependence with their coalescence occuring at -40 °C.

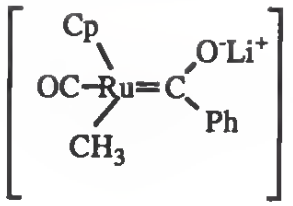

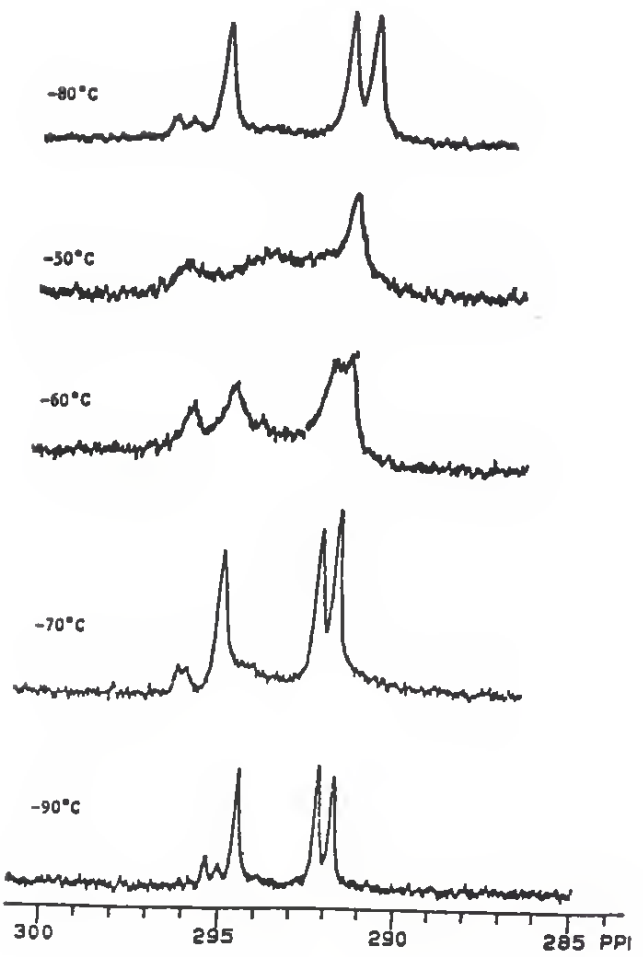

Figure 3-8. ^{13}C NMR Temperature Dependence Experiment of Li-enolate **3.08.**

The origin of these coalescing signals is unknown. In principle, such multiple peaks could originate either from different conformations about the metal carbon bond or from different lithium aggregates. The spectra of the lithium enolate **3.08** were found to be markedly dependent on the nature of the cation and the nature of the solvent. It was found that the multiple peaks in the characteristic carbene carbon region at -90 °C were reduced to two peaks (δ 292 and 282 ppm in CD_2Cl_2) upon addition of ten percent deuterated tetrahydrofuran, a solvent which would be expected to coordinate with lithium (as shown in Figure 3-9, top). In another experiment the multiple peaks were reduced to a single resonance (δ 284 ppm in CD_2Cl_2) when 12-crown-4 ether was added. Such a result could have derived from formation of either the free ion or a very loose contact ion pair [38,39] (as illustrated in Figure 3-9, bottom).

These results are most consistent with aggregates of lithium enolates being the source of the multiple carbene carbon signals. However, conformational equilibra can not be rigorously excluded since relative conformational stabilities might well be affected by change of solvent or presence of additives such as 12-crown-4 ether (e.g. a change in orientation of a phenyl substituent).

It now seems clear that what we have observed in our low-temperature attempt to prepare and isolate acyclic ruthenium complex **3.09** was instead the formation of the lithium enolate **3.08** at -90 °C, which when warmed to -40 °C underwent rate determining silylation to give the desired ruthenium carbene complex **3.09**. Since careful analysis of ^{13}C NMR spectra upon warming to -40 °C did not lead to detection of any transient species [only the gradual growth of peaks deriving from metal hydride species **3.11** could be observed (as shown in Figure 3-4)] it was, therefore, concluded that even at -40 °C the carbene complex **3.09** rearranges too rapidly to the metal hydride species **3.11** to be detected.

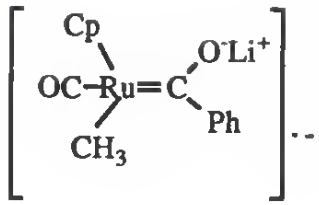

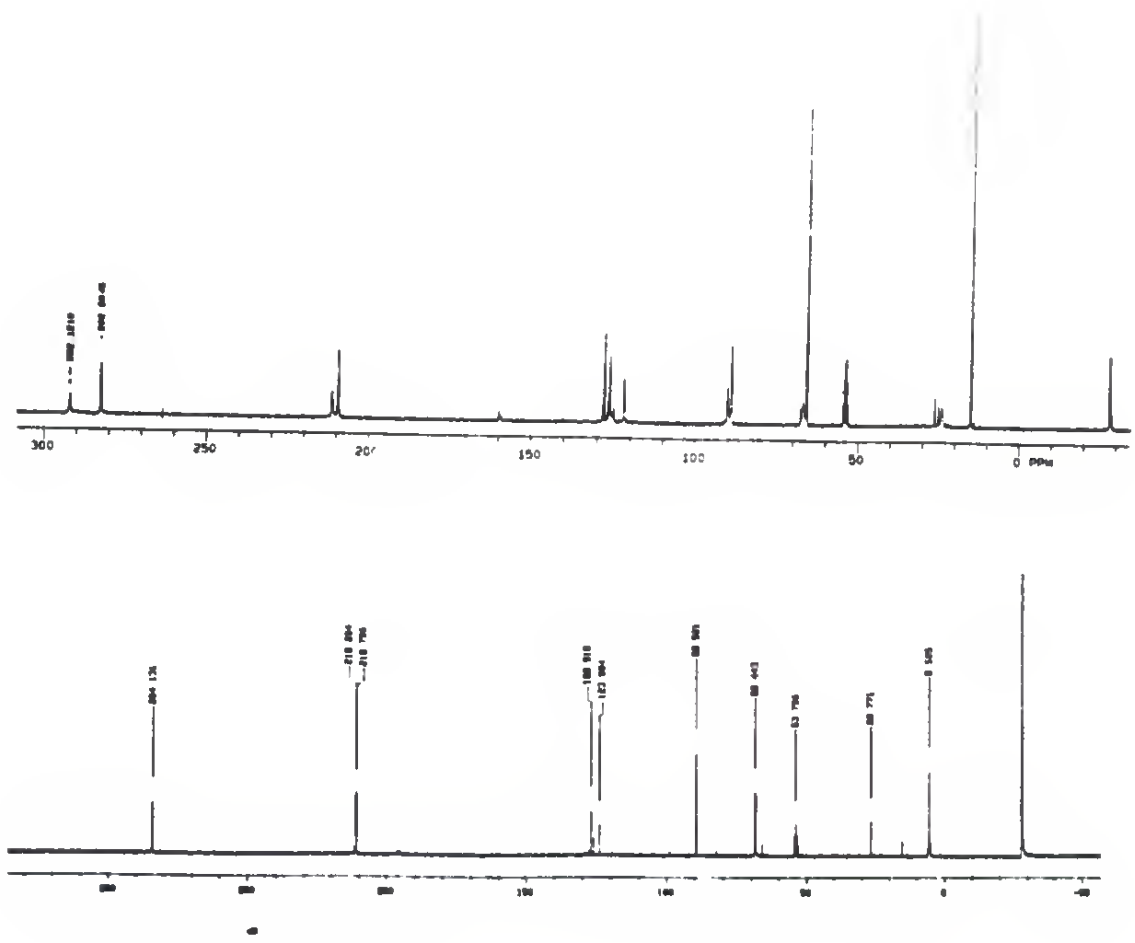

Figure 3-9. ^{13}C NMR spectra of Li-enolate **3.08** at -90 °C in the presence of 10% THF-d_8 (top) and in the presence of 12-crown-4 (bottom).

It should also be mentioned that the lithium enolate species **3.08** (in the absence of silylating agent) was found to be stable at temperatures up to 0 °C. Therefore, **3.08** could not itself be the species which is undergoing the migratory insertion reaction at ca. -40 °C.

This result reinforced our conclusion that acyclic ruthenium carbene complex **3.09** was formed at -40 °C but rearranges and disappears too rapidly to be observed.

Since the rate determining step is silylation of the anionic oxygen, and this apparently occurs at -40 °C in the reaction of the lithium enolate with trimethylsilyl chloride, it is clear that the observation of an alkyl substituted carbene complex and the consequent ability to monitor its migratory insertion would require alkylation at a temperature below -40 °C. Therefore, better silylating or alkylating reagents were sought. Reagents which were tried included trimethylsilyl triflate and triethyloxonium tetrafluoroborate.

Indeed, it was found that when trimethylsilyltriflate was used as the silylating agent the metal hydrides **3.11** were formed even at -78 ° C. The NMR spectra indicated that no significant lithium enolate remained. Therefore, it was concluded that trimethylsilation of the lithium enolate must have occured at -78 °C with this powerful reagent and that the acyclic ruthenium carbene complex **3.09** was not stable even at this temperature.

While attempting to use triethyloxonium tetrafluoroborate as the alkylating agent, it was found that lithium enolate **3.08** remained and thus did not react with this reagent at -78 °C. However, the lithium enolate did react with triethyloxonium tetrafluoroborate and the metal hydrides were detected when the reaction mixture was warmed to -40 °C.

In order to make the acyl anion a better nucleophile by reducing the bonding between the lithium cation and acylate anion, an attempt was made to solvate the lithium ion with 12-crown-4. The experimental results revealed that the reactivity of the lithium enolate was enhanced in the presence of 12-crown-4. Chelation of the lithium ion with 12-crown-4 apparently provided a more nucleophilic enolate oxygen so as to allow reaction with triethyloxonium tetrafluorobroate even at -78 °C. However, the expected acyclic ruthenium carbene complex **3.01** was not observed even under such conditions. Again, the initial products that were observed (-78 °C) were the metal hydrides **3.07**. This result confirmed that ion-pairing phenomena can play a significant role in the chemical reactivity of ruthenium carbonyl anions, but unfortunately our goal of isolating an alkylated or silylated acyclic carbene complex was again thwarted.

Although we have not been successful in isolating and studying the kinetics of the migratory insertion of either silylated or alkylated acyclic ruthenium carbene complexes, we have neverthless obtained insight into their reactivity in that apparently such complexes rearrange rapidly even at temperatures as low as -78 °C.

CHAPTER 4
SYNTHESIS AND STUDY OF NOVEL TRANSITION METALLAAROMATIC RUTHENAPHENANTHRENES AND RUTHENABENZENE

In one of our earlier studies, it was found that incorporation of ring strain into the potential rearrangement product of an alkyl-substituted carbene complex significantly retarded migratory insertion. That is, migratory insertion of the ruthenium carbene complex **2.04** was not observed presumably because of the 49 kcal/mol of ring-strain which would have resulted from such ring contraction.

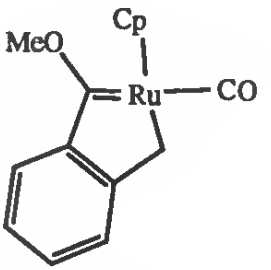

2.04

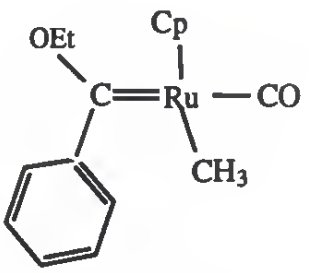

3.09

In contrast , migratory insertion of acyclic analogue **3.09** was so facile that it could not be spectroscopically observed when it was presumably formed at -78 °C.

Thus, the 49 kcal/mol strain which would have been incorporated into the product of migratory insertion of the cyclic carbene complex **2.04** apparently inhibited the rearrangement too much to allow any observation of the process. (It places the

reaction out of sight thermodynamically.) But, when the strain factor was removed entirely in an otherwise completely analogous structure, the migratory insertion process was so rapid that the carbene complex **3.09** could not be observed at -78 °C.

Therefore, it is obvious that something in between these two extremes was needed. In other words, something which would either destabilize the rearrangement product or stabilize the carbene complex but not so much as to totally inhibit migratory insertion.

It occurred to us that by incorporation of a metallacarbene functionality into an aromatic system, there might be enough resultant stabilization of the carbene system to retard such migratory insertion and to allow the observation and kinetic study of the metallacarbene aromatic species.

Indeed, theoretical calculations predict that a selected transition metal can take part in (d-p) π aromatic bonding, if it has a centrally directed d orbital of appropriate energy and overlap to provide an electron pair to the π-system of a carbon framwork that has a low lying vacant MO.[40]

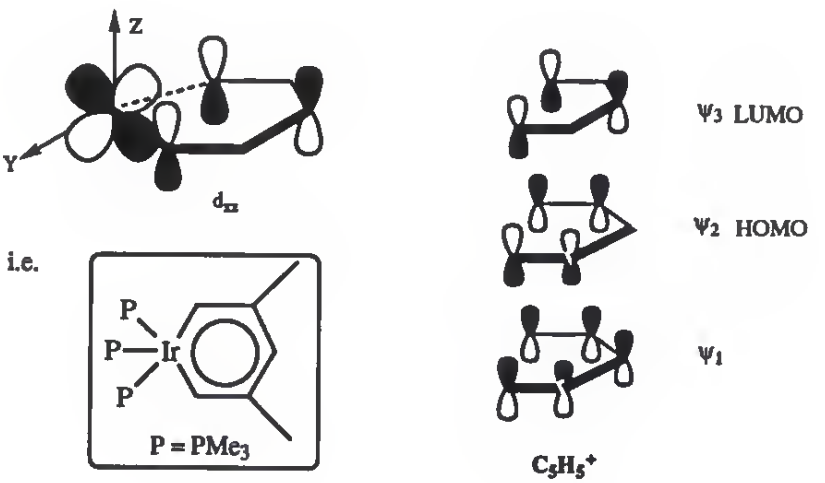

Scheme 4-1

The picture as illustrated in Scheme 4-1 has generally been utilized to depict incorporation of a selected transition metal into a six-membered aromatic ring. As pointed out by Hoffmann,[40] the LUMO of the organic fragment in a metallabenzene is considered to be effectively a pentadienyl cation which can be a π-acceptor of d-electrons to complete an aromatic sextet.

To date, however, successful preparations of transition metal metallabenzenes have been extremely rare. Bleeke[19h] and his co-workers in 1989 reported the best example of a metallabenzene (iridabenzene) **1.11** with all of the usual aromatic properties. In particular, the six-member ring is planar with delocalized bonding around the ring.

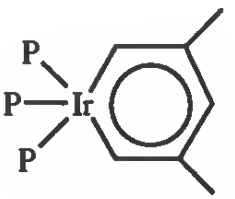

$P = PMe_3$

1.11

As a matter of fact, this metallabenzene complex **1.11** is of a third row transition metal. Related examples of first or second row transition metal metallaaromatic molecules such as metallabenzenes, metallanaphthalenes or metallaphenanthrenes, to our best knowledge, have not yet been reported.

The methodology which was used to prepare acyclic ruthenium carbene complexes (**3.01** and **3.09** from chapter 3) provided the original inspiration for our

synthesis of the second row late transition metal metallaaromatic species, ruthenaphenanthrene **4.01.**

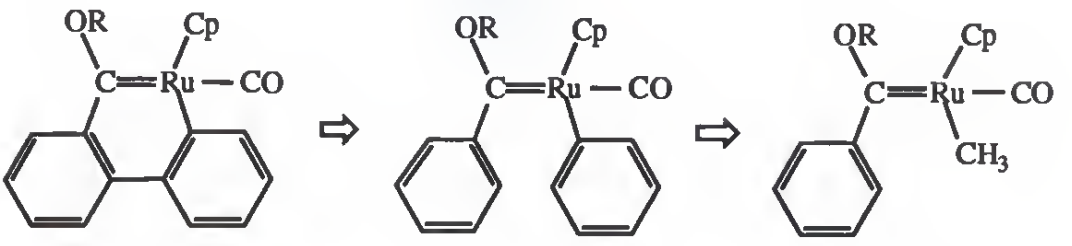

4.01 **4.02** **3.09**

Conceptually, the construction of the ruthenaphenanthrene target required modification of the acyclic carbene complex **3.09** by first replacing the methyl with a phenyl substituent (which would create acyclic carbene complex **4.02**) and secondly joining the two phenyl substituents at the 2,2'-positions by a single bond (which would create the potentially aromatic carbene complex **4.01**).

Thus, we decided to prepare the desired ruthenaphenanthrene **4.01** to see if there is any aromaticity to slow down the migratory insertion enough to observe the carbene complex.

The proposed synthesis of ruthenaphenanthrene **4.01**, is presented in Scheme 4-2.

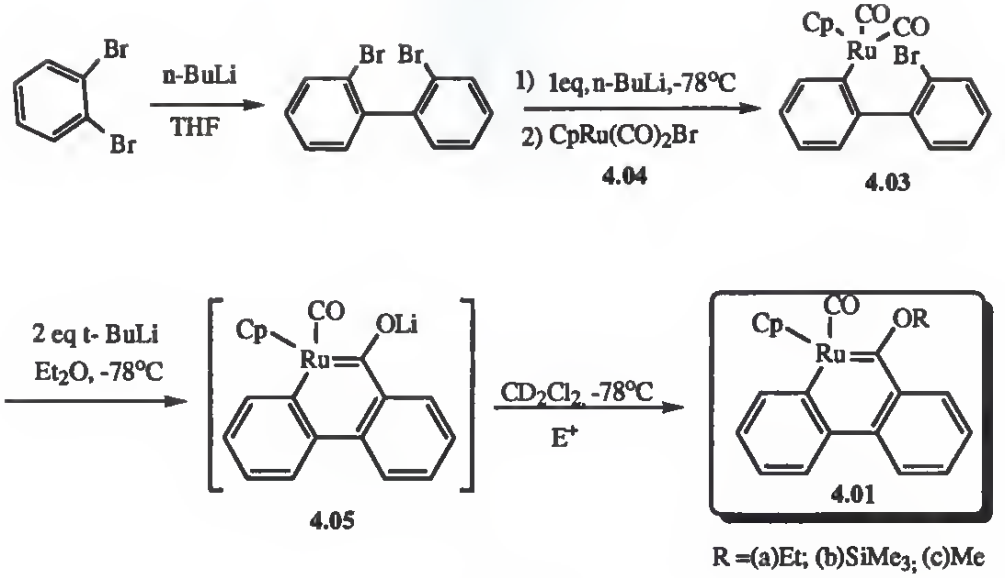

Scheme 4-2

2,2'-Dibromo-biphenyl was prepared according to the literature.[47] The σ-complex **4.03** was generated in moderate yield *via* addition of one equivalent n-butylithium at -78 °C to produce the mono-lithio anion followed by reaction with RpBr (**4.04**). The complex **4.03** was then placed in the special low temperature apparatus described earlier (see chapter 3 page 35), and was allowed to react with t-butyllithium at -78 °C overnight. This reaction mixture was then evaporated to dryness at approximately -30 °C to afford the reddish-yellow lithium enolate **4.05**. Alkylation (or silylation) of this lithium enolate in CD_2Cl_2 at -78 °C would be expected to give the desired product ruthenaphenanthrene **4.01**.

The ^1H NMR spectrum of the alkylated reaction mixture (R=Et) revealed several broad signals in the Cp region at -90 °C and a coalesced broad Cp signal when the temperature was raised to -60 °C (Figure 4-1). From our previous experience, the broadness of the Cp signals

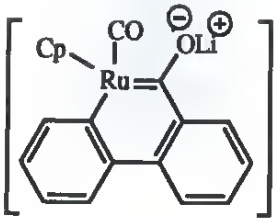

+ Et_3OBF_4

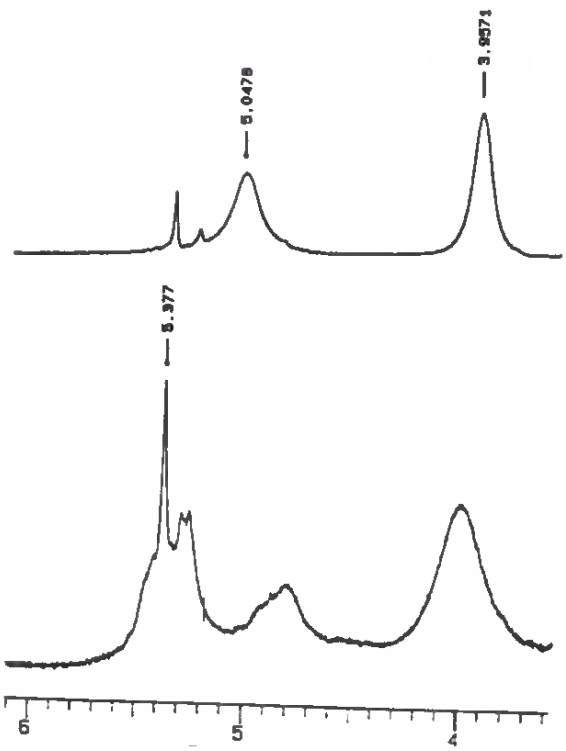

Figure 4-1. ^1H NMR spectra of mixture of enolate **4.05** and Et_3OBF_4 at -90 °C (bottom) and -60 °C (top). (signal at 3.95 ppm is unreacted Et_3O^+).

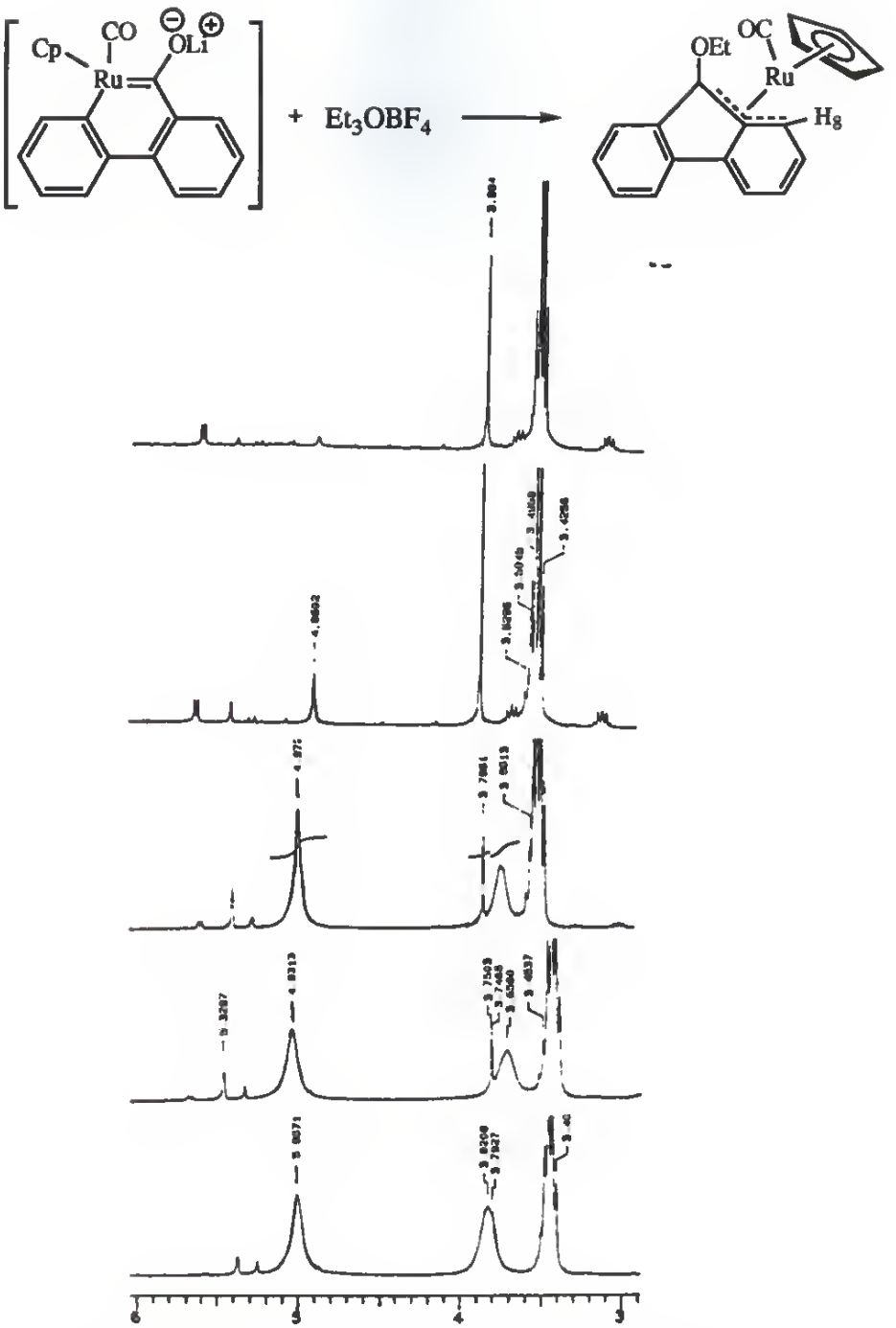

Figure 4-2. ^1H NMR spectra of reacting mixture of enolate + Et_3OBF_4 at -50 °C. The original Cp signal at δ 5.007ppm slowly dissappeared, and a new Cp signal (δ 3.75 ppm) and a doublt at 5.48 ppm (H_8) appeared.

was recognized as an indication of fluxional processes within the molecule. However, at this point the origin of the fluxionality was unknown. Regardless, if the new complex was the ruthenaphenanthrene, it should either be stable enough for characterization or it should undergo rearrangement in a predictable way. Indeed, as a sealed sample of this reaction mixture was gradually warmed to -50 °C, a number of spectral changes were observed. The original Cp signal at δ 5.04 ppm in the ^{1}H NMR spectrum slowly dissappeared, and appeared to convert to a new Cp signal (δ 3.75 ppm) as illustrated in Figure 4-2. Eventually, new and quite clean ^{1}H and ^{13}C nmr spectra were obtained for the product of this reaction (as seen in Figure 4-3). An unusual upfield proton (δ 5.48 ppm) which was coupled with aromatic protons (demostrated via the decoupling experiment depicted in Figure 4-4) eliminated the possibility of the product being 16e intermediate **4.06** because such a 16e intermediate should possess only aromatic protons. Thus, the detected intermediate is probably derived from **4.06**.

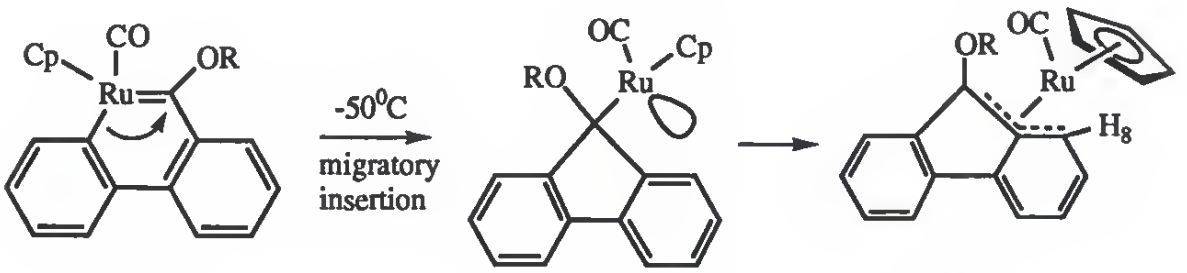

4.01 **4.06** **4.07**

R= (a) Et; (b) $SiMe_3$; (c) Me

The structure of this product is proposed to be the η^3-π-benzyl complex **4.07**. The doublet belongs to H_8, part of the benzylic system, which assignment was made on the basis of comparisons with analogous known compounds[41] and ^{1}H NMR decoupling

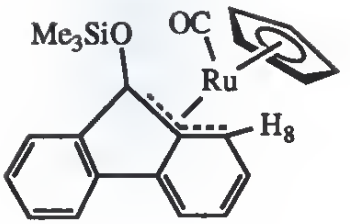

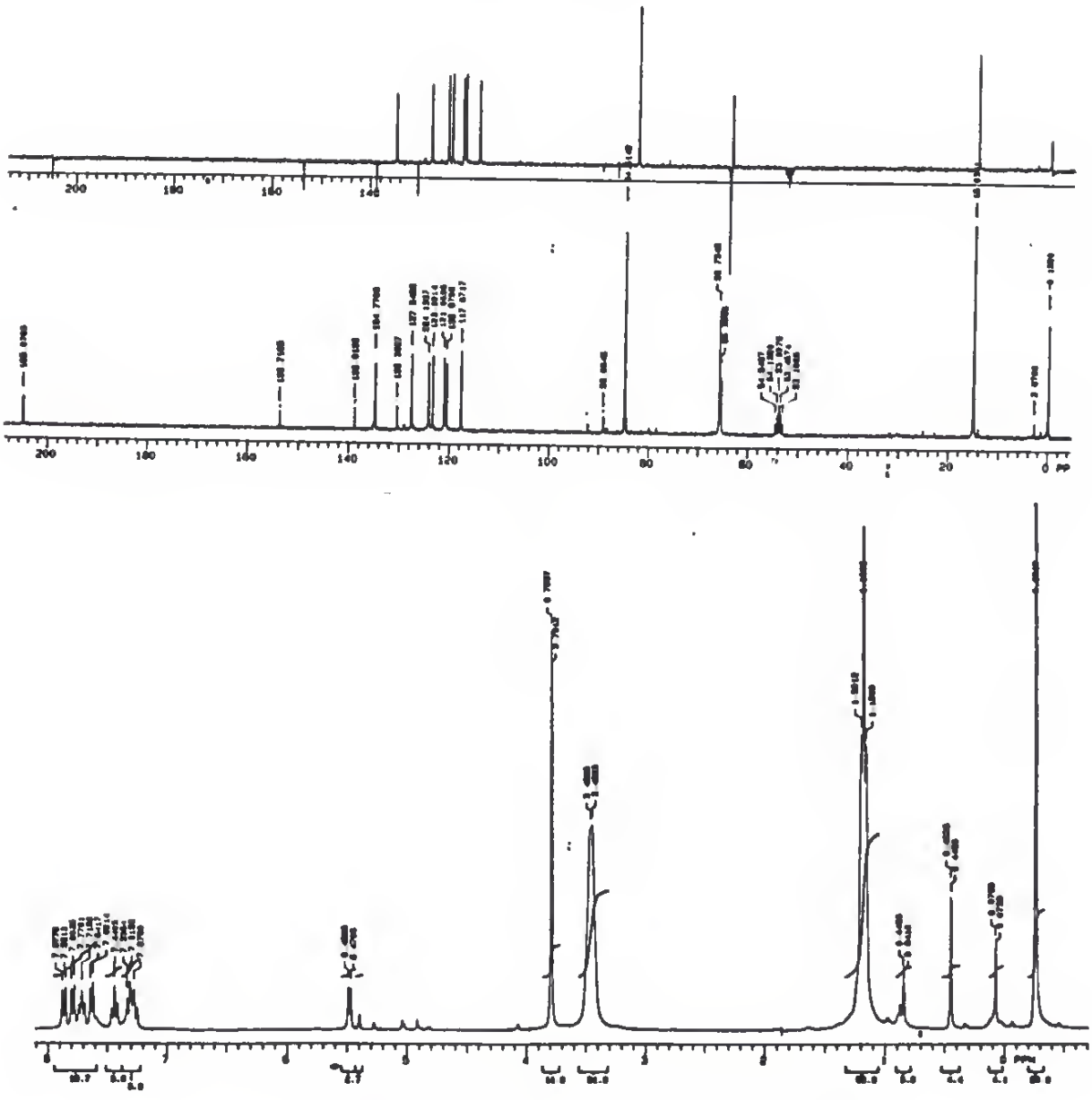

Figure 4-3. ^{1}H and ^{13}C NMR spectra of **4.07b**.

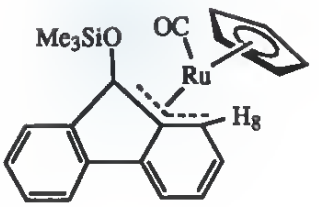

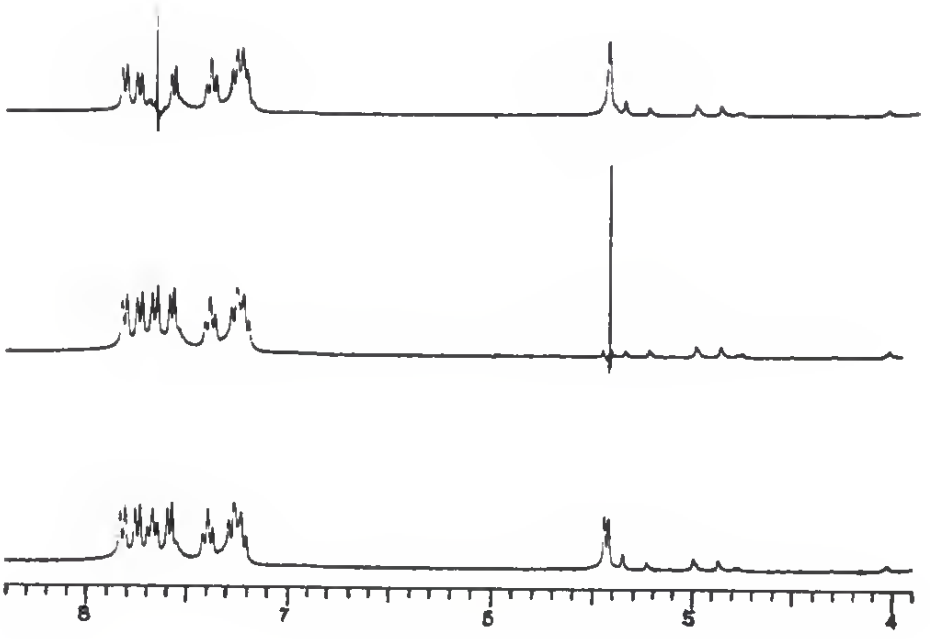

Figure 4-4. ^{1}H NMR spectra of Decoupling Experiment for **4.07b.**

experiments. The one upfield CH carbon and seven CH carbons in the aromatic region instead of eight aromatic CH carbons in the ^{13}C NMR spectra are consistent with this proposed structure (Figure 4-3).

Brookhart[41] published an analogous η^3-benzyl (η^3-$CH_2C_6H_5$) complex $Cp(CO)Fe(\eta^3\text{-}CH(OCH_3)C_6H_5)$ **4.08**, which he and his coworkers characterized by ^1H and ^{13}C NMR spectroscopy. The ortho hydrogens of the phenyl ring H_o and H_o' have very different environments in **4.08** with chemical shifts of 2.45 ppm (H_o) and 7.85 ppm (H_o').

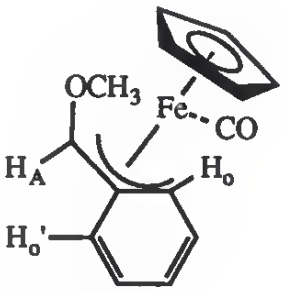

4.08

^1H NMR (Toluene-d_8)

δ 2.45 ppm (H_o; d, J = 6 Hz)
δ 7.85 ppm (H_o'; d, J =6 Hz)

The structure of the η^3-benzyl complex **4.07c** (OR=OMe) was not only confirmed by NMR spectroscopy as shown in Figure 4-5, but it was actually isolated by chromatography at -20 °C as a dark-red crystalline solid when the lithium enolate **4.05** was treated with trimethyloxonium tetrafluoroborate in a relatively large scale experiment. As with **4.07a**, the ^1H NMR chemical shift of the benzylic hydrogen (H_8) of **4.07c** appeared as a distinct doublet (J=6.45 Hz) at 5.57 ppm. In the IR spectrum of the η^3-benzyl complex **4.07c**, a terminal CO absorption at 1967.6 cm^{-1} was observed. The structure of **4.07c** was further verified by elemental analysis.

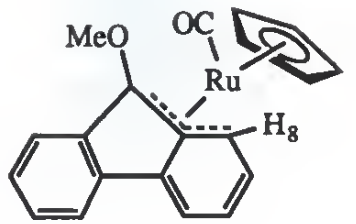

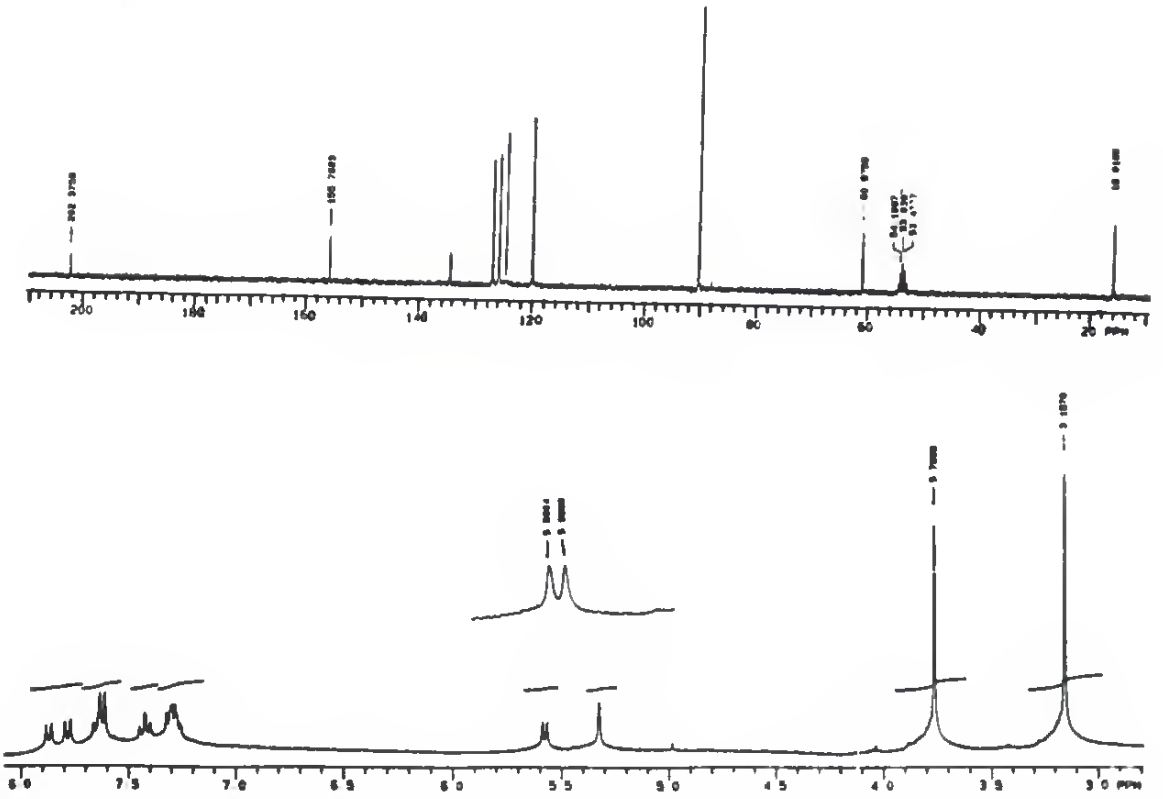

Figure 4-5. ^{1}H and ^{13}C NMR Spectra of **4.07c**

As a further confirmation of the assigned structure, reaction mixtures were allowed to warm up in the presence of carbon monoxide and the expected stable trapping product **4.09** was formed, (isolated at room temperature). This complex was fully characterized by NMR spectroscopy (as illustrated in Figure 4-6), elemental analysis and high resolution mass spectrometry.

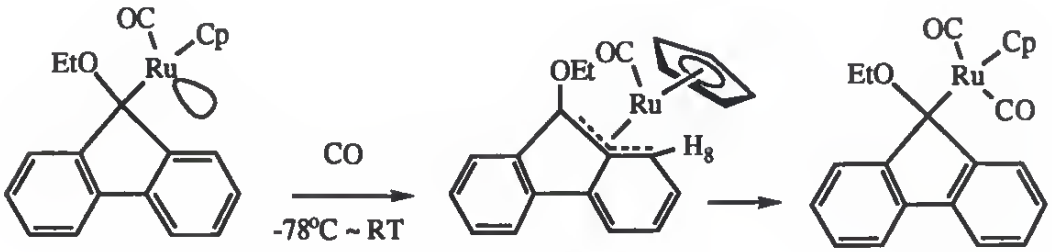

4.06 **4.07** **4.09**

Characterization of the derived η^3–benzyl complex **4.07** and trapping product **4.09** led us to believe that the ruthenaphenanthrene **4.01** had been formed and had undergone migratory insertion rapidly at -50 °C to give these products.

However, the direct observation of **4.01** is desirable. The way to do that is to look for the characteristic low field ^{13}C resonance of the carbene carbon. From our previous experience, we knew that the carbene carbon would be difficult to detect without enrichment by ^{13}C. Therefore, it was decided to enrich the carbene carbon, much as we had enriched earlier studied acyclic carbene complexes **3.01** and **3.09**. The procedure which was used to prepare the enriched ruthenaphenanthrene is presented in Scheme 4-4.

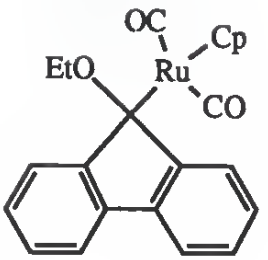

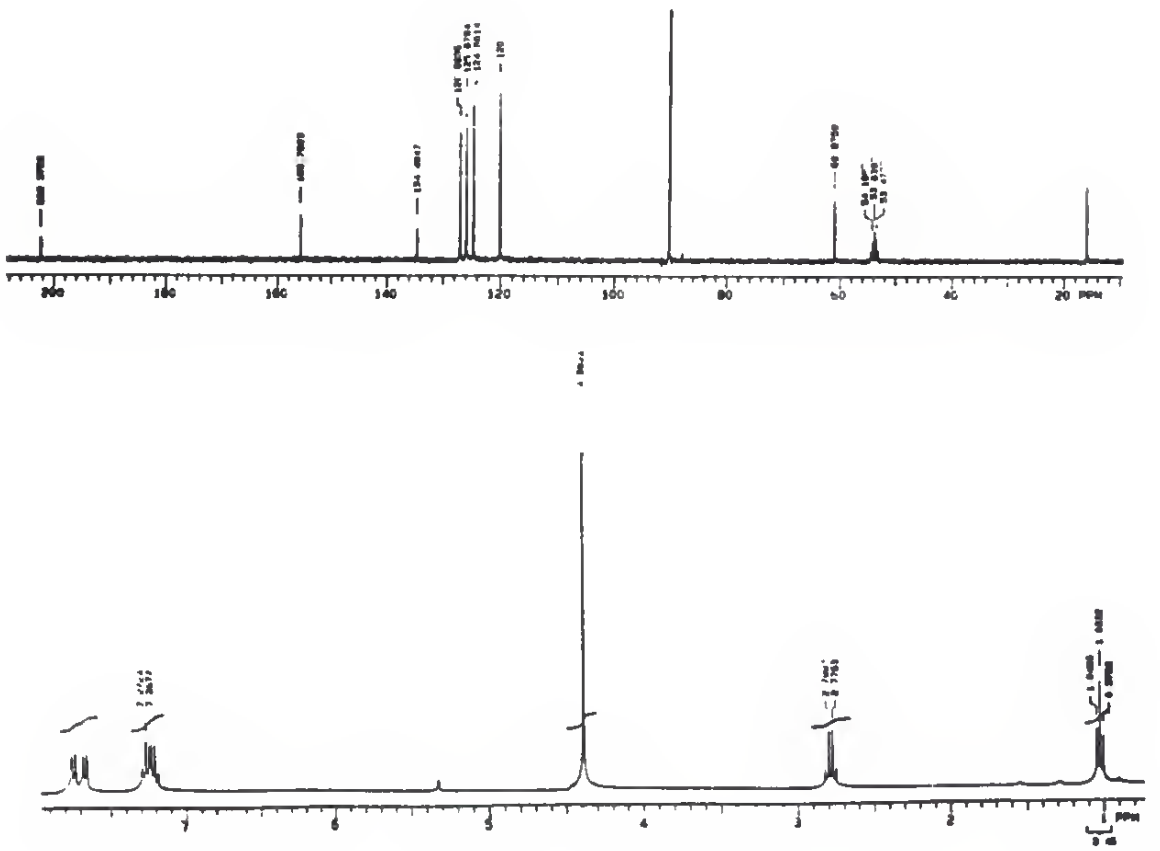

Figure 4-6. ^{1}H and ^{13}C NMR Spectra of **4.09**.

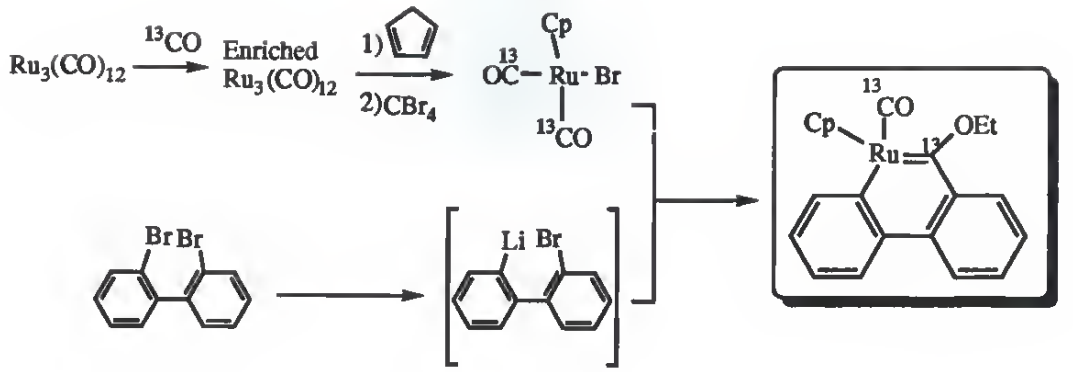

Scheme 4-4

As in the case of the acyclic carbene complex, at -90 °C, multiple resonances in the characteristic carbene carbon region were observed in the ^{13}C NMR spectra when the enriched materials were used (Figure 4-7). These resonances also coalesced upon warming, and upon further warming, the η^3-benzyl complex rearrangement product **4.07** was detected which was consistent with the results from the non-enriched study.

As in the earlier studies of the acyclic carbene complexes **3.01** and **3.09**, we could not be certain whether we were observing the lithium enolate or the ethoxy carbene . To address this question, a control experiment in which no alkylating agent was present was undertaken. From this experiment, it was found that the chemical shifts in the ^{13}C NMR spectrum without alkylating agent were nearly the same as with the alkylating agent at -90 °C. It was additionally found that the lithium enolate **4.05** was stable at temperatures up to 0 °C. Lithium enolate **4.05** could thus not itself be the species to undergo migratory insertion at ca.-50 °C. Therefore, it was concluded that, as in the case of the acyclic ruthium carbene complex, what we were observing in the below -50 °C attempt to synthesize ruthenaphenanthrene **4.01** was instead formation

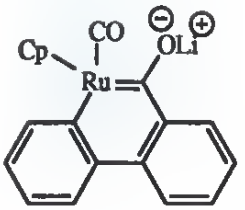

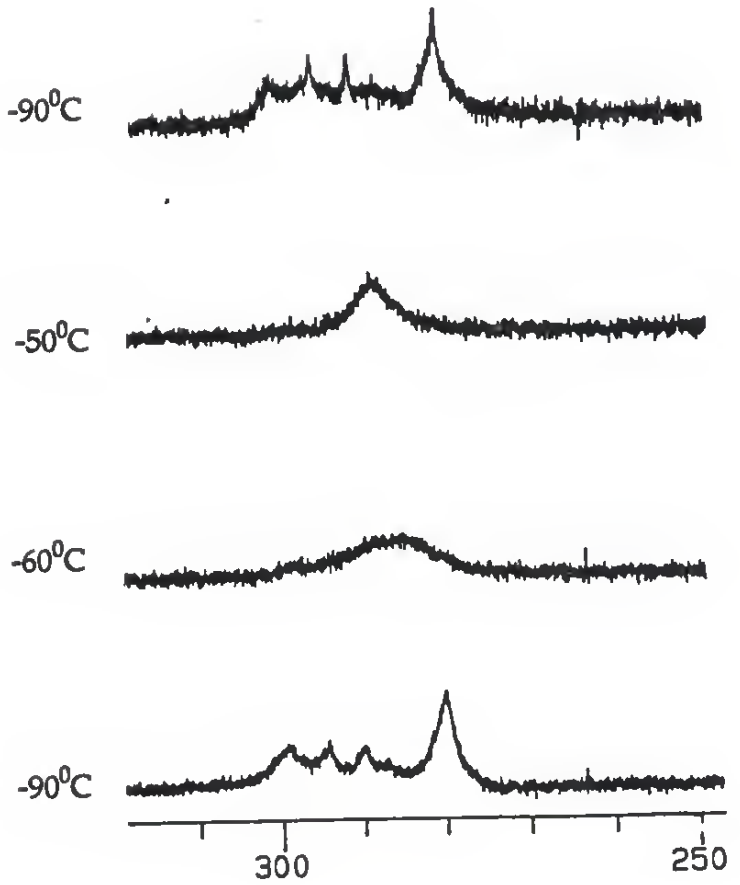

Figure 4-7. ^{13}C NMR Temperature Dependence Study of Mixture of **4.05** + Et_3OBF_4.

of the lithium enolate **4.05**, which when warmed to -50 °C underwent alkylation to afford the desired "aromatic" complex **4.01**.

When reaction mixtures were carefully followed by ^{1}H and ^{13}C NMR spectroscopy with a gradual increase of the temperature, no transient species could be detected (instead only the growth of signals deriving from η^3-benzyl complex **4.07** were seen). It was therefore concluded that even at -50 °C the desired complex **4.01** undergoes migratory insertion reaction to the η^3-benzyl complex **4.07** too fast to be observed.

This result means that there is insufficient aromatic stabilization present in the ruthenaphenanthrene **4.01** to prevent rapid rearrangement at -50 °C. In other words, there was no evidence for the type of aromatic stabilization in **4.01** which we had hoped might sufficiently retard its migratory insertion reaction to permit direct observation of the rethenaphenanthrene.

Since the middle ring of phenanthrene **4.10** itself is not as aromatic as benzene **4.11** (20 kcal/mol vs 36 kcal/mol), it was then decided to incorporate the ruthenium into a non annelated benzenoid system with the idea that, in such a case, there might be enough stabilization to retard the rearrangement to the point that the ruthenabenzene could be detected.

4.10

4.11

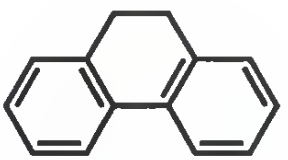

4.12

Resonance energy	92 kcal/mol	36 kcal/mol	72 kcal/mol

Thus, our final goal was focused on the synthesis of a ruthenabenzene. Neil T. Allison* has been interested in metallabenzenes. He reported[30a-c] formation of 1,3-diphenyl-2-methoxyferrocene (**4.13**) *via* an apparent conversion from ferracyclohexatriene or ferrabenzene (**4.14**) several years ago, although **4.14** could not be directly observed.

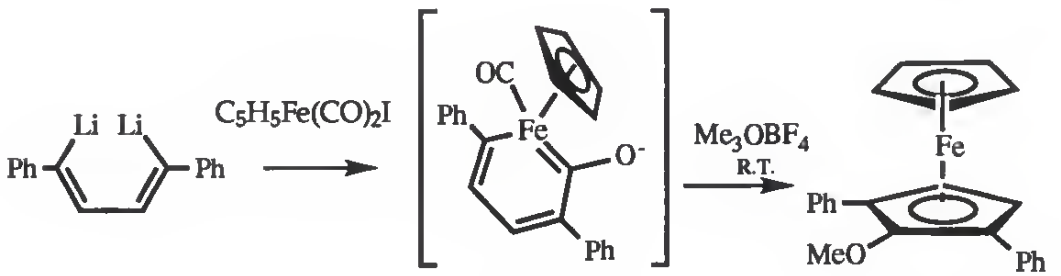

4.14 **4.13**

Dr. Allision provided us with some of his previously synthesized precusor **4.15**, (1Z,3Z)-1,4-dibromo-1,4-diphenyl-1,3-butadiene, and we have thus pursued this project in collaboration with him. The synthesis of ruthenacyclohexatriene or ruthenabenzene **4.16** was carried out as depicted in Scheme 4-4.

---

* A former graduate student of Dr. William Jones who currently is a professor at University of Arkansas.

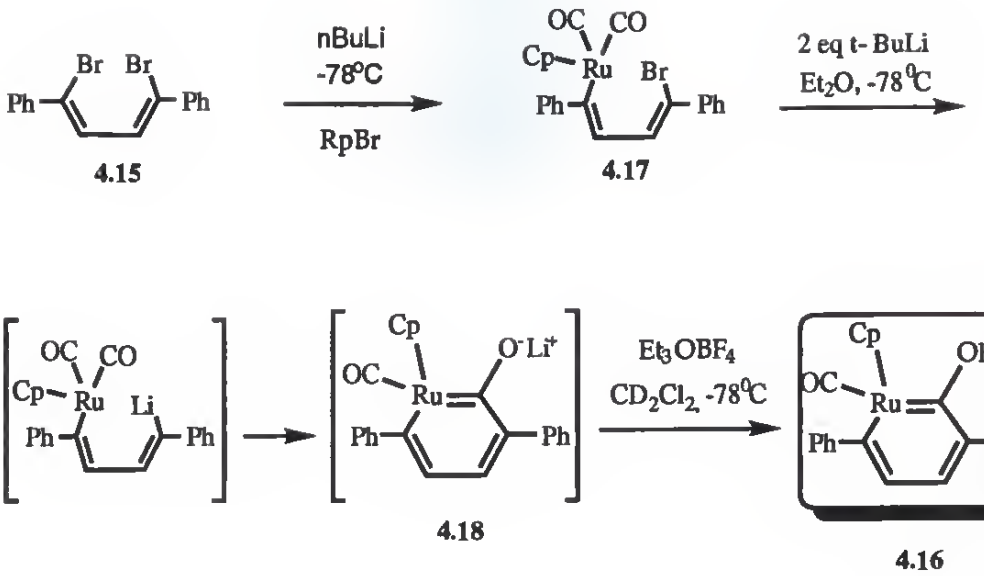

Scheme 4-4

The stable η^1-4-bromo-1,4-diphenylbutadienyl complex of ruthenium **4.17** was prepared in a manner similar to that of complex **4.03** (Scheme 4-2). Addition of two equivalents of t-butyllithium to a cold (dry ice/2-propanol bath) solution of **4.17** in diethyl ether for lithium exchange, followed by cyclization, afforded the reddish residue of ruthenaaromatic lithium enolate **4.18**. Treament of this enolate **4.18** with Et_3OBF_4 in CD_2Cl_2 at -78 °C should lead to the desired product ruthenabenzene **4.16**.

Again, at low temperature, we observed the spectrum of a species which, as it warmed up in the presence of carbon monoxide, gave the same kind of trapping product **4.19** as we obtained from the ruthenaphenanthrene **4.01**.

The isolation and characterization by high resolution mass spectroscopy of the trapping product **4.19** (Figure 4-8) implied that the ruthenabenzene had been formed which rapidly underwent migratory insertion.

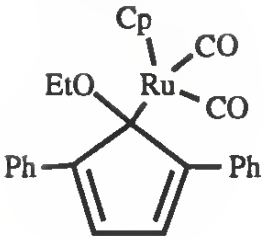

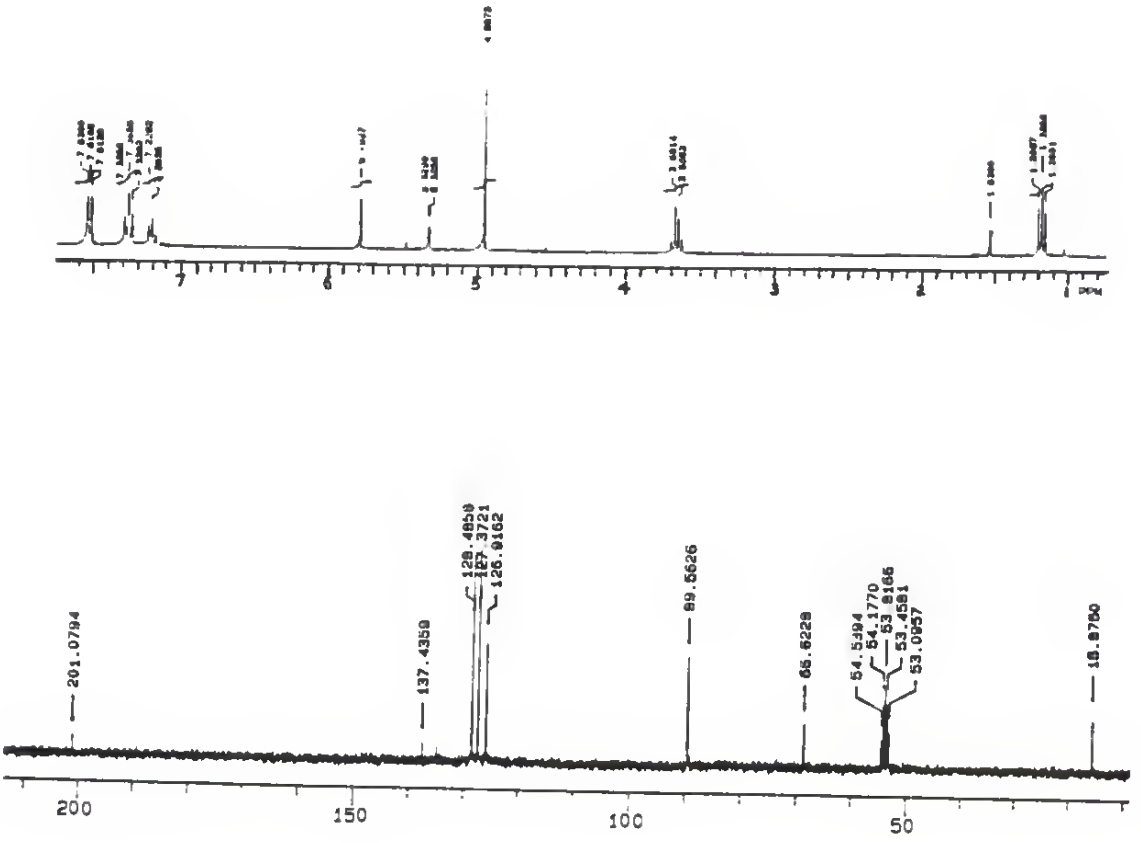

Figure 4-8. ^{13}C and ^{1}H NMR spectra of trapping product **4.19**.

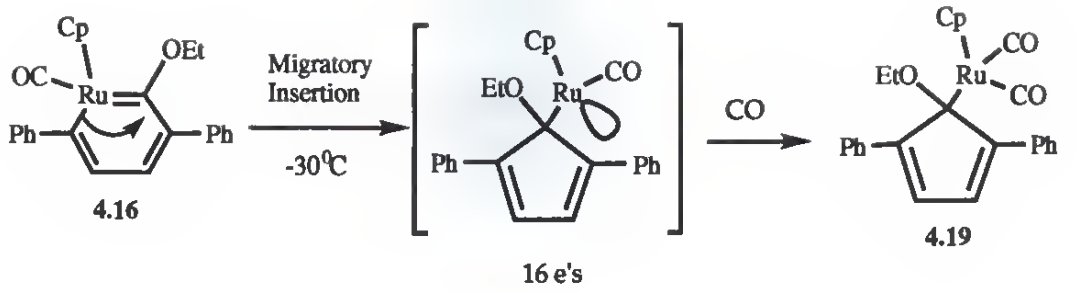

To conclusively demonstrate the presence of the ruthenabenzene, a unique carbene carbon was sought in the ^{13}C NMR spectrum using enriched materials. First of all, a sample containing only the lithium enolate **4.18** was studied by NMR spectroscopy. A broad signal at δ 293.8 ppm was observed at -78 °C in the ^{13}C NMR spectrum which is illustrated in the Figure 4-9. To this sample was added excess alkylating agent (Et_3OBF_4), and the reaction mixture was allowed to react for forty minutes at -78 °C, followed by NMR spectroscopic analysis. At -70 °C, the signal of the unreacted lithium enolate **4.18** was seen to be shifted from δ 293.8 ppm to δ 273.9 ppm and a small sharp new peak at δ 290.8 ppm was observed as illustrated in Figure 4-10, a peak which we believe is due to the desired alkylated ruthenabenzene **4.16**. By carefully monitoring the ^{13}C NMR spectrum as the temperature of the reaction mixture was gradually increased, a series of changes were detected in the 270~300 ppm region as illustrated in Figure 4-11. As the temperature was increased to -50 °C, the signals due to the presumed ruthenabenzene grew at the expense of those of the unreacted lithium enolate. Eventually the peak at 273.9 ppm completely vanished, and there remained only the carbene carbon peak at δ 290.8 ppm due to the ruthenabenzene. Indeed, in the terminal carbonyl (CO) and Cp regions, corresponding new peaks at δ 201.2 ppm and δ 88.86 ppm respectively, were also observed, as illustrated in Figure 4-12.

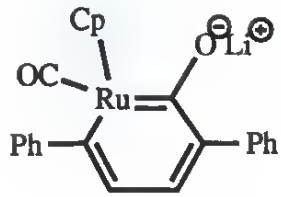

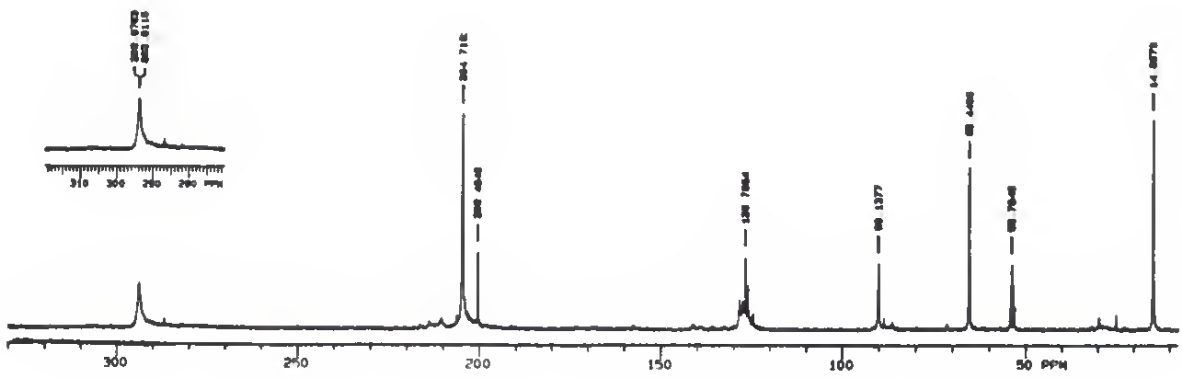

Figure 4-9. ^{13}C NMR sprctrum of Li-enolate **4.18** at -78 °C.

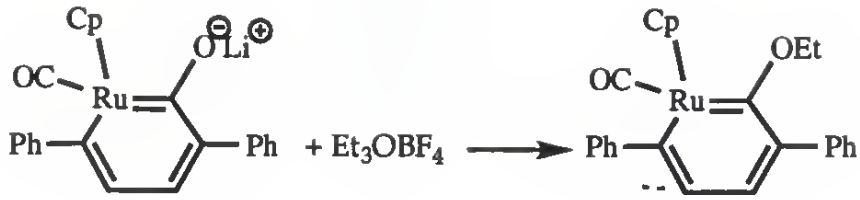

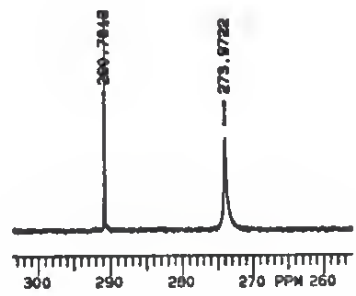

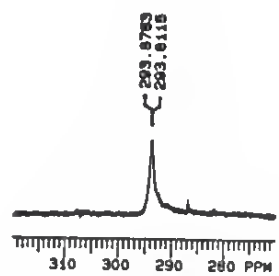

Figure 4-10. ^{13}C NMR spectra of Li-enolate **4.18** (bottom) and alkylated Li-enolate (formation of ruthenabenzene **4.16**) (top) at -70 °C.

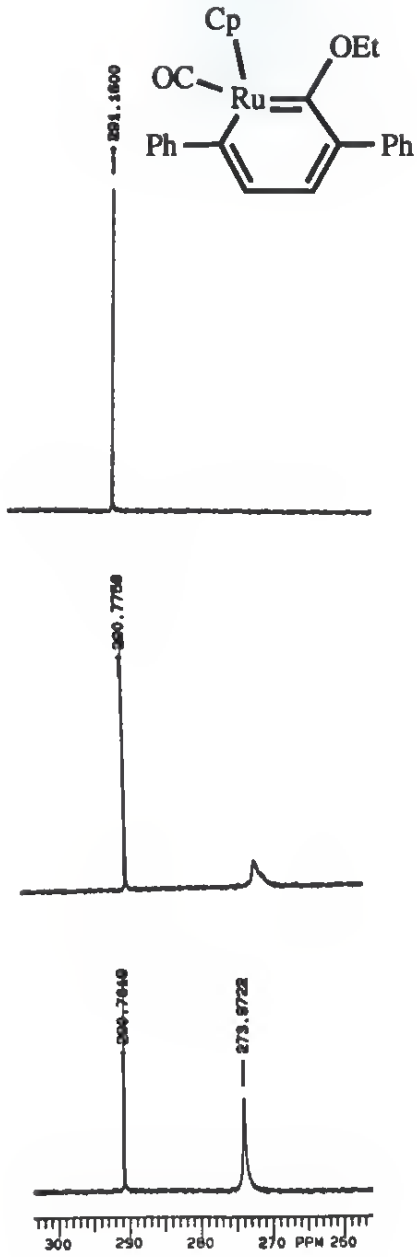

Figure 4-11. ^{13}C NMR spectra of formation of ruthenabenzene **4.16** at -70 °C, -70 °C an hour later, -50 °C, respectively, (From bottom to top) in the Carbene carbon region.

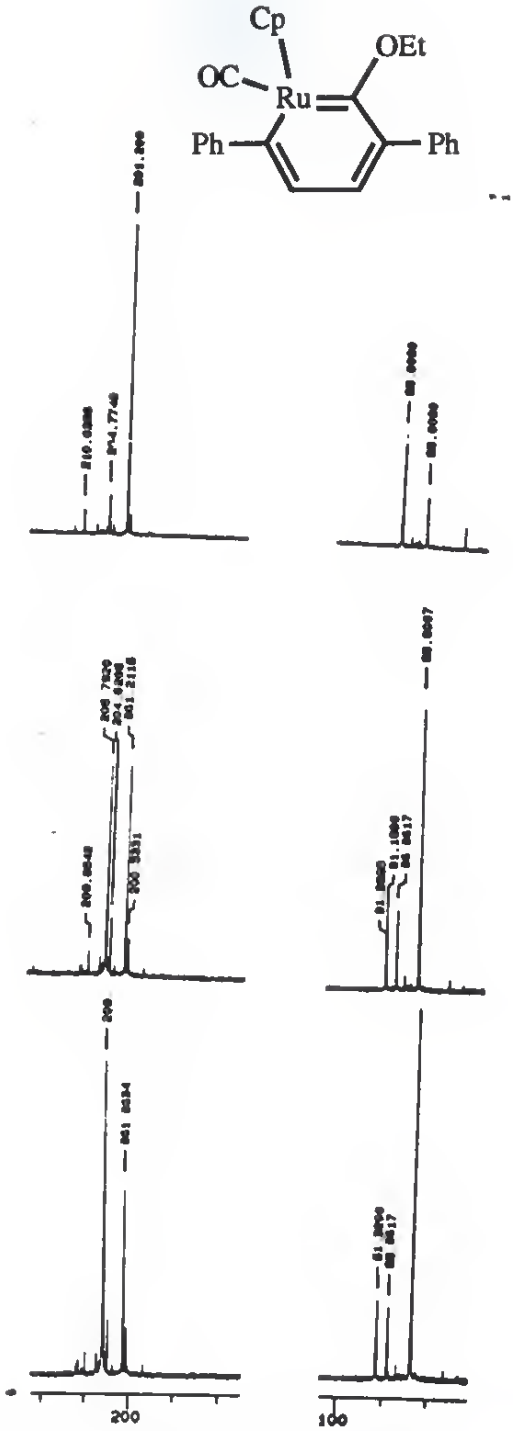

Figure 4-12. ^{13}C NMR spectra of formation of ruthenabenzene **4.16** at -70 °C, -70 °C an hour later, -50 °C, respectively, (From bottom to top) in the CO and Cp regions.

In order to further verify the formation of the ruthenabenzene **4.16**, changes in the ^1H NMR spectrum were also carefully examined as the reaction mixture was gradually warmed from -70 °C to -50 °C. The results, shown in Figure 4-13, revealed a number of changes which were entirely consistent with what was observed in the ^{13}C NMR spectrum. At -70 °C only a broad Cp signal of the lithium enolate **4.18** (in the absence of alkylating agent) at δ 4.95 ppm was observed (spectrum a). After addition of excess alkylating agent to this lithium enolate, a new Cp peak at δ 5.32 ppm (Cp of **4.16**) was detected at -70 °C (spectrum b). At -50 °C the ruthenabenzene **4.16** was seen to be completely formed from its enolate (spectrum e). New multiple peaks around 4.55 ppm ~ 4.75 ppm in the OCH_2 region were also observed.

The ruthenabenzene was stable at -50 °C for at least a half hour. However, it underwent migratory insertion at -30 °C. The rate of decomposition of the ruthenabenzene **4.16** was measured by monitoring the Cp absorption (5.32 ppm) in the ^1H NMR spectrum at -30 °C, as shown in Figure 4-14. [The excess Et_2O (3.52 ppm) peak was used as a reference]

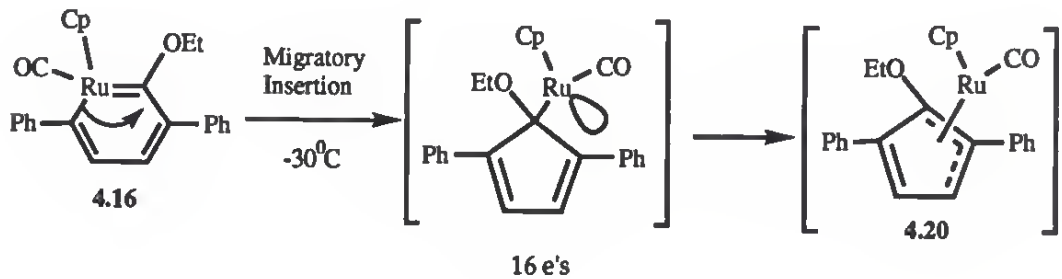

4.16

16 e's

4.20

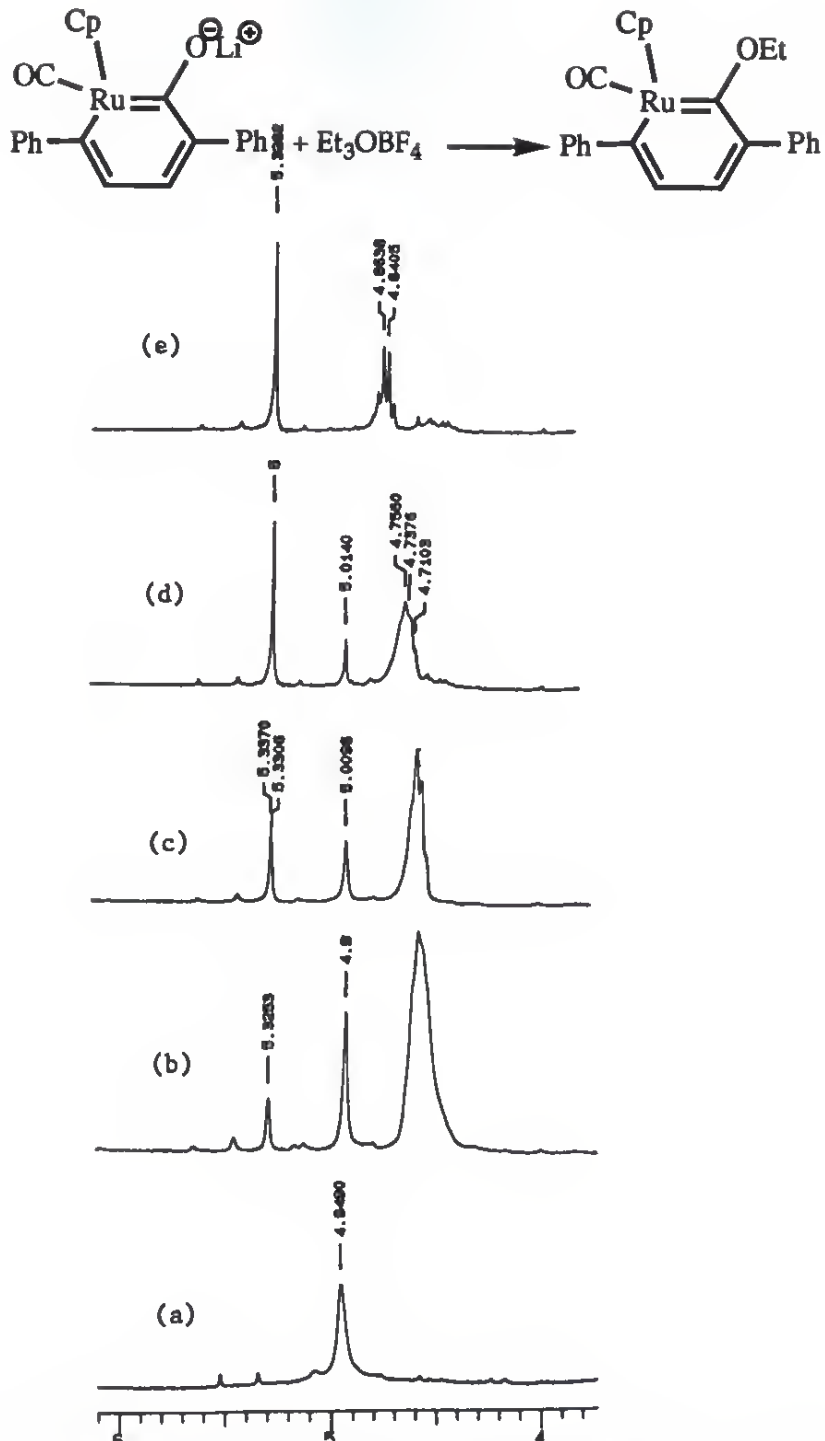

Figure 4-13. (a) ^1H NMR spectrum of Li-enolate **4.18** ; (b) ^1H NMR spectrum of **4.18** upon addition of Et_3OBF_4 (formation of ruthenabenzene **4.16**) at -70 °C; (c) mixture at -70 °C half hour later ; (d) mixture at -70 °C an hour later ; (e) mixture at -50 °C.

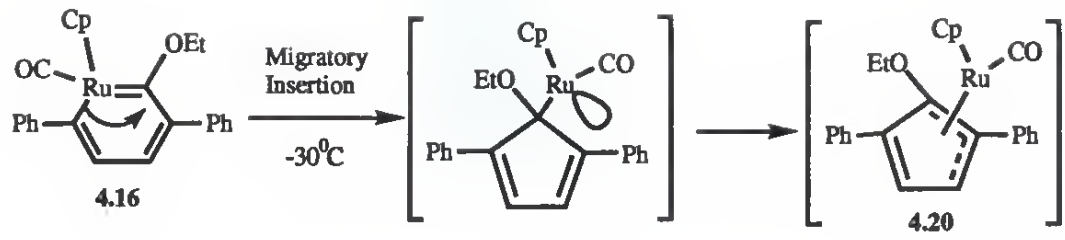

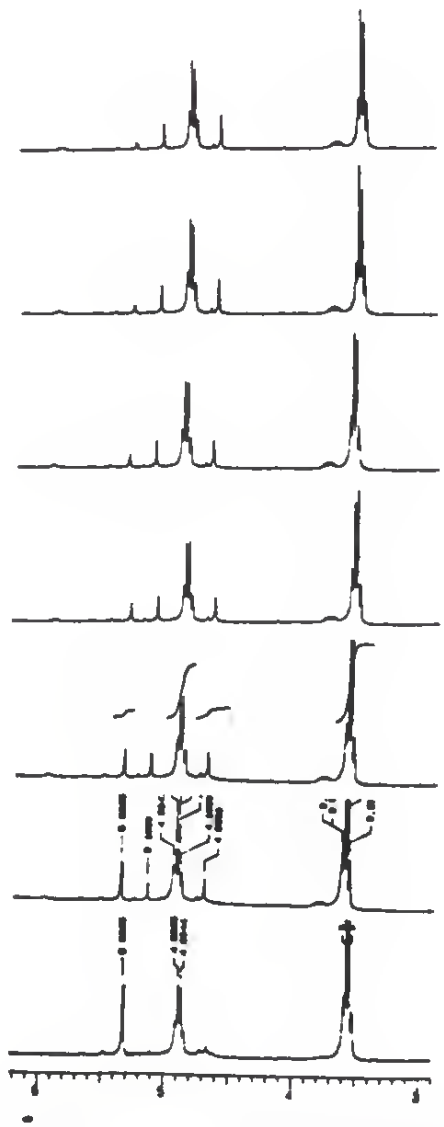

Figure 4-14. ^{1}H NMR spectra of ruthenabenzene **4.16** undergoing migratory insertion at -30 °C. (Loss of Cp peak at 5.322 ppm observed.)

In contrast, to our attempted kinetics in Chapter 2 where we thought we were examining the first-order reaction only later to find that it was a second-order reaction, decomposition of the ruthenabenzene (decrease of the Cp absorption) followed excellent first-order kinetics with a rate constant of approximately $3.7 * 10^{-4} \pm 0.09 * 10^{-4}$ sec^{-1} as illustrated in Figure 4-15.

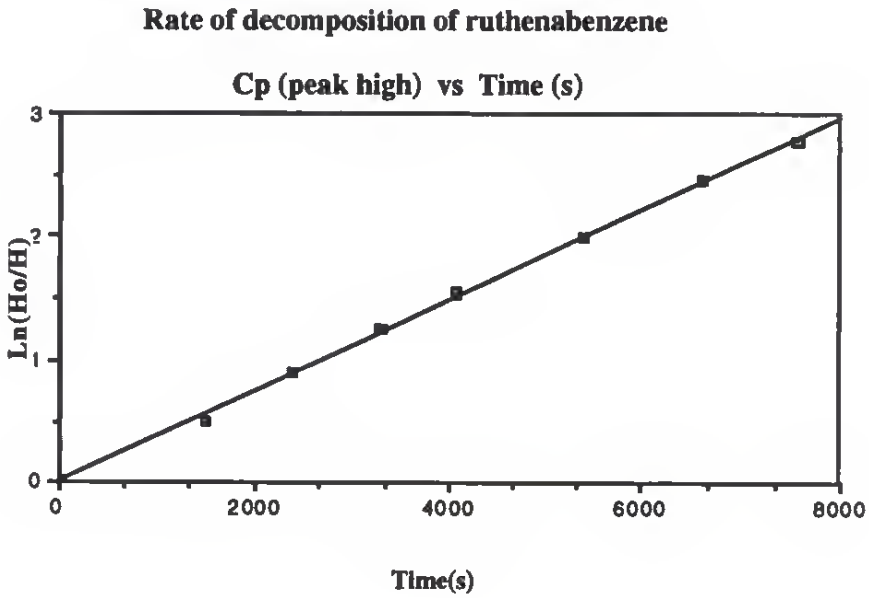

Figure 4-15. A Plot of Ln (Ho/H) VS. Time (sec) for Determination of the Rate of Decomposition of Ruthenabenzene.

This observation of good first-order kinetics also supports the contention that the ruthenabenzene **4.16** was indeed formed and was the species undergoing decomposition.

Peaks from the migratory insertion product **4.23** [δ 200.4 ppm (CO) and 90.2 ppm (Cp) in the ^{13}C NMR spectrum] which resemble those of the η^3-benzyl complex **4.07** were detected. At 0 °C, the η^3-allylic complex **4.20** survived for only a short period of time.

In a final control experiment, it was shown that the lithium enolate was itself stable up to 0 °C. This result further confirmed the formation of ruthenabenzene at -70 °C.

In light of all of these results, we believe that our claim of the intermediacy and detection of the desired ruthenabenzene **4.16** is, in this case, secure.

In conclusion, aromaticity in the ruthenaphenanthrene was not sufficient to slow migratory insertion to the point that the carbene complex could be observed. In contrast, aromaticity in a diphenyl substituted ruthenabenzene appear to be sufficient to permit detection of the ruthenabenzene at -50 °C.

CHAPTER 5
CONCLUSIONS

The purpose of this research has been to study the migratory insertion processes of ruthenium carbene complexes.

A methoxy-stabilized metallaindene complex of ruthenium (**2.04**) was prepared. Reaction of this complex with phenyllithium or *p*-tolylithium followed by treatment with trimethylsilyl triflate afforded the first stable aryl substituted Fischer carbene complexes of ruthenium (**2.03a** and **2.03b**) which do not have a heteroatom stabilizing substitutent on the carbene carbon. In solution, these complexes underwent a novel thermal rearrangement to form ruthenacene derivatives **2.11a** and **2.11b**. A possible mechanism for this rearrangement which involves a ruthenanaphthalene intermediate or carbene insertion into an acyl bond is proposed.

Attempts to isolate and study the kinetics of the migratory insertion of acyclic ruthenium carbene complexes, $CH_3(CO)Ru=C(OR)C_6H_5$ (R = $SiMe_3$ & C_2H_5), were not successful. Neverthless, our study provided some valuable information regarding their reactivity, including the fact that apparently such complexes undergo migratory insertion rapidly at temperatures as low as -78 °C.

Introduction of potential aromaticity into such carbene complexes by synthesis of a ruthenaphenanthrene (**4.01**) was insufficient to slow migratory insertion to the point that the carbene complex could be observed. The rapid rearrangement of **4.01** at -50 °C was observed.

On the other hand, introduction of a greater degree of aromaticity into a ruthenium carbene complex through the synthesis of a diphenyl substituted ruthenabenzene (**4.16**) was sufficient to permit its detection at -50 °C. **4.16** is the first second row, late transition metallabenzene which has been reported.

CHAPTER 6
EXPERIMENTAL

All reactions were carried out under an atmosphere of purified N_2 by using Schlenk tube techniques and a dry box. All solvents were dried by known procedures and distilled under nitrogen prior to use. Trimethylsilylchloride was distilled over proton sponge. PhLi, *o*-bromobenzylbromide, and CD_2Cl_2 were purchased from Aldrich Chemical Company. ^{13}CO and $^{13}CH_3I$ were purchased from ISOTEC INC. $Ru_3(CO)_{12}$ was purchased from Strem Chemical. Proton and carbon NMR spectra were recorded on a Varian VXR-300 (300 MHz) or a Varian Gemini-300 (300 MHz) spectrometer. Chemical shifts were referenced to the residual protons of the deuterated solvents and are reported in ppm downfield of TMS for ^1H and ^{13}C NMR spectra. Mass spectra were run on an AEI MS-30 spectrometer or Finigan MAT 950. Infrared spectra were recorded on a Perkin Elmer 1600 FTIR spectrometer. Photolysis was carried out using a 450-w low pressure Hg-Hanovia lamp in a pyrex well. The alumina used was neutral, activity I, which was deactivated to activity III and degassed on the vacuum line prior to use. The chromatographic separations were accomplished by the flash chromatography method of Still.[44]

The following compounds were prepared as described in the literature, without any modification: Rp_2 or $(CpRu(CO)_2)_2$,[45] $CH_2=C(Ph)(OSiMe_3)$,[36] $CH_2=C(Ph)(OCH_2CH_3)$[34], enriched $Ru_3(^{13}CO)$.[46] 2,2'-dibromobiphenyl,[47] and triethyloxonium tetrafluoborate.[48] The RpMe ($CpRu(CO)_2CH_3$)was prepared as in the literature but with modification.[49]

Preparation of 2-Bromobenzyl Ruthenium complex **2.05**

A solution of 2.2 g (4.95 mmol) of $[CpRu(CO)_2]_2$ in ca. 300 mL of THF was treated with ca. 1.1 g of Na and 11 mL of Hg (as amalgam). The mixture was stirred for 9 h at RT, and then the dark grey solution was transferred into a Schlenk tube. To this solution, cooled to - 78 °C, was added 2.48 g (1 eq, 9.92 mmol) of 2-bromobenzylbromide, and the mixture was stirred over night at RT. The solvent was then removed under vacuum, and the residue dissolved in a small amount of hexane and eluted through an alumina (III) column with hexane, to give a colorless solution. Evaporation of most of the solvent and crystallization at ca. -15 °C, gave 2.56 g of the 2-bromobenzyl ruthenium complex **2.05** (66% yield) as a white crystalline solid. Anal. Calcd for $C_{14}H_{11}O_2BrRu$: C, 42.86; H, 2.81. Found: C, 42.87; H, 2.80. Mp: 52-53 °C. MS (EI, *m/e*): 391.89 (M+1). ^1H NMR (C_6D_6): δ 4.46 (s, 5H, Cp), 3.03 (s, 2H), 6.60 (t, 1H), 6.98 (t, 1H), 7.28 (d, 1H), 7.5 ppm (d, 1H). ^{13}C NMR: δ 210 (CO), 154~121 (phenyl region), 88.39 (Cp), 33.32 ppm. IR (hexane): CO 2025.1 cm^{-1}, 1989 cm^{-1}.

Synthesis of Benzannelated Ruthenium-Carbene Complex **2.04**

To a solution of 0.30 g (0.765 mmol) of **2.05** in 20 mL of THF was added to 0.45 mL (1.2 eq, 2M) of *n*-BuLi at -100 °C, under N_2. The solution was stirred overnight, allowing the temperature to slowly rise to RT. The solution was then cooled to -30 °C, and Me_3OBF_4 was added in small portions until the pH reached 6-7 (about 0.3 g is needed). The orange color of the solution changed to reddish at ca. 0 °C within 30 min and the excess of Me_3OBF_4 was destroyed with 30 mL of degassed water. Then the

mixture was extracted with hexane three times, and the combined extracts evaporated under reduced pressure to dryness. The crude product was chromatographed on alumina (III), with the desired red band eluting very slowly with hexane. After removal of most of the solvent, the product crystallized at -10 °C after several hours to give 110 mg of **2.04** as a red crystalline solid (44% yield). Anal. Calcd for $C_{15}H_{14}O_2Ru$: C, 55.05; H, 4.31. Found: C, 54.87; H, 4.21. Mp = 110-111 °C. HRMS (EI, *m/e*): Calcd for (M^+): 328.003; Found: 328.0028. ^1H NMR ($CDCl_3$): δ 5.23 (s, 5H, Cp), 3.18 (d, J=13.9 Hz, 1H), 3.05 (d, $^2J_{HH}$=13.9 Hz, 1H), 4.51 (s, 3H, OCH_3), 7.0-7.6 ppm (phenyl region). ^{13}C NMR ($CDCl_3$): δ 294.16 (Ru=C), 206.07 (CO), 86.8 (Cp), 67.0 (OCH_3), 10.27 ppm (CH_2).

Synthesis of Phenyl-Substituted Ruthenium Carbene Complex **2.03a**

In a Schlenk tube, 150 mg (0.457 mmol) of **2.04** was dissolved in ca. 30 mL THF and cooled to -78 °C. To this red solution was added 0.38 mL (1.5 eq) phenyllithium, dropwise, which resulted in a gradual change in color to a dark reddish-brown as the solution warmed to -25 °C over a 4 h period. To this solution, cooled by liquid N_2 to -196 °C, was added, *via* vacuum line transfer, ca. 2 equiv of trimethylsilyl triflate ($Me_3SiSO_3CF_3$) which had been distilled over a proton sponge. A dark red color was produced when the temperature was allowed to increase from -196 °C to RT over a period of one hour. Removing the THF under vacuum led to a black-purple residue which was chromatographed on alumina (III), with the black-purple band eluting with hexane. Removal of most of the solvent followed by crystallization at -30 °C led to formation of 110 mg of black crystals of **2.03a** (65% yield). Anal. Calcd for $C_{20}H_{16}ORu$: C, 64.35; H, 4.32. Found: C, 64.29; H, 4.28. Mp: 114-115 °C. MS

(EI, *m/e*): 374 (M+1). ^{1}H NMR (C_6D_6): δ 4.87 (s, 5H, Cp); 3.72 (d, $^2J_{HH}$ = 12.6 Hz, 1H); 6.7-7.4 (phenyl region); 2.58 ppm (d, $^2J_{HH}$ =12.6 Hz, 1H). ^{13}C (C_6D_6): δ 309.53; 209.77; 166.96; 160.29; 158.12; 131.09; 129.14, 128.53; 127.29; 124.46; 122.46; 122.78; 90.32; 15.87 ppm.

Synthesis of *p*-Tolyl-Substituted Ruthenium Carbene Complex **2.03b**

The method used was the same as that described above for the phenyl derivative, **2.03a**, except *p*-tolyllithium was used instead of phenyllithium. Black crystals of **2.03b** were obtained in 58% yield. Anal. Calcd for $C_{21}H_{18}ORu$: C, 65.10; H, 4.65. Found: C, 65.09; H, 4.68. Mp: 95-96 °C. MS (EI,*m/e*): 388 (M+1). ^{1}H NMR (C_6D_6): δ 4.91 (s, 5H, Cp); 3.73 (d, $^2J_{HH}$= 12.6 Hz, 1H); 2.63 (d, $^2J_{HH}$ = 12.6 Hz, 1H); 2.10 (s, 3H, CH_3); 6.8-7.6 ppm (m, 5H, phenyl region). ^{13}C NMR (C_6D_6): δ 309.16 (C=M); 209.9 (CO); 166.84; 160.32; 156.0; 139.56; 131.05; 128.13; 124.40; 122.84 (phenyl region); 90.2 (Cp); 21.4 (CH_2); 15.6 ppm (CH_3). IR (hexane) 1966.7 cm^{-1}.

Thermolysis of **2.03a** -- Preparation of ruthenacene **2.11a**

A black solution of 0.30 g of carbene complex **2.03a** in ca. 0.8 mL C_6D_6 in a sealed NMR tube was heated at 50 °C. The reaction was monitored by ^{1}H and ^{13}C NMR from time to time, and it was seen that **2.11a** was formed slowly as **2.03a** disappeared. After 12 hours, **2.03a** was found to have been quantitatively converted to **2.11a**. The same result can be obtained if the solution of **2.03a** is allowed to sit at room temperature for two days. The solvent was evaporated under vacuum to give 30 mg (100 %) of an

orange solid. Anal. Calcd for $C_{20}H_{16}ORu$: C, 64.35; H, 4.32. Found: C, 64.16; H, 4.31. Mp: 120-135 °C(decomp.). MS (EI, *m/e*): 374 (M^+). ^1H NMR (C_6D_6): δ 5.28 (s, 1H, CH); 4.10 (s, 5H, Cp); 2.90 (br, 1H, OH); 6.75-7.8 ppm (m, 9H, aromatic region). ^{13}C NMR (C_6D_6): δ 135.7; 131.2; 128.7; 127.1; 126.9; 126.1; 123.8; 123.0; 122.9; 90.32; 88.36; 56.7; 31.8 ppm.

Thermolysis of **2.03b**-- Preparation of ruthenacene **2.11b**

The method used was the same as for the preparation of **2.11a**, except the temperature used was 70 °C, and **2.11b** was formed quantitatively. Anal. Calcd for $C_{21}H_{18}ORu$: C, 65.10; H, 4.65. Found: 65.09; H, 4.68. ^1H NMR (C_6D_6): δ 2.20 (s, CH_3); 2.8 (br, OH); 4.15 (s, 5H); 5.33 (s, 1H); 6.75-7.74 ppm (m, 8H, aromatic region). ^{13}C NMR (C_6D_6): δ 136.64-122.84 (aromatic region); 88.40; 86.68; 77.83; 71.78; 56.56; 21.20 ppm.

Thermolysis of Methoxy Ruthenium Carbene Complex **2.04**

A solution of 0.35 g of Ru carbene complex **2.04** in ca. 0.8 mL of C_6D_6 was heated at 80 °C under an N_2 atmosphere in a sealed NMR tube. The mixture was monitored by ^1H NMR and ^{13}C NMR from time to time, and no reaction was observed after 5 days.

Preparation of **2.20**

To a solution of 20 mg (0.54mmol) of **2.03a** in 1 mL of C_6D_6 was added 20 uL of PMe_3 at room temperature. A color change of the solution from dark red to orange occurred immediatedly. The ^1H NMR showed the PMe_3 has added to **2.03a** to form **2.20** completely. The solvent was evaporated to give 23 mg (100%) of an orange solid. ^1H NMR (C_6D_6): 6.6~7.6 (m, 9H), 4.33 (s, 5H), 3.89 (dd, 1H, $^2J_{HH}$=14.8Hz, $^4J_{PH}$=3.8Hz), 2.91 (dd, 1H, $^2J_{HH}$=14.8Hz, $^4J_{PH}$=3.8Hz), 0.9 (br, 9H). This broad peak at 0.9 ppm (PMe_3) appeared as three groups of doublets at -78 °C at 1.55, 0.58 and 0.49 ppm with coupling constants $^2J_{PH}$=9.6 Hz, 11.9 Hz and 9.0Hz respectively. Two groups of doublets were observed at -40 °C at 1.68 and 0.62 ppm with intensity ratio 1:2. The two groups of doublets coalesced at room temperature to give a broad peak. ^{13}C NMR (C_6D_6): 211.95 (d, $^2J_{PC}$=5.5Hz), 162.61, 155.98, 146.99, 130.63, 129.28, 129.20, 127.83, 126.12 (d, J=3.2Hz), 125.8 (br), 123.84, 121.87, 87.26, 4.63. MS (EI, *m/e*) 374 (M^+). Anal. calcd. for $C_{23}H_{25}OPRu$: C, 61.48; H, 5.56. Found: C 61.04; H, 5.58.

Crystallographic Analysis

Data were collected at room temperature on a Siemens R3m/V diffractometer equipped with a graphite monochromator utilizing MoK_α radiation (λ = 0.71073 Å). 50 reflections with $20.0° \leq 2\theta \leq 22.0°$ were used to refine the cell parameters. 4175 and 2741 reflections, for **2.03a** and **2.11b** respectively, were collected using the ω-scan method (1.2° scan range and 3-6° scan speed depending on intensity). Four reflections ($22\bar{3}$, $\bar{1}20$, 023, 202) for **2.03a**, and ($\bar{2}$)21, 023,$2\bar{2}1$, 0,$\bar{1}\bar{3}$) for **2.11b**, were measured every 96 reflections to monitor instrument and

crystal stability (maximum correction on I was < 1 %). Absorption corrections were applied based on measured crystal faces using *SHELXTL plus* (Sheldrick, 1990). Absorption coefficients: **2.03a**, $\mu = 0.97\ mm^{-1}$(min. and max. transmission factors are 0.789 and 0.868, respectively); **2.11b**, $\mu = 0.96\ mm^{-1}$(min. and max. transmission factors are 0.723 and 0.828, respectively).

The structures were solved by the heavy atom method in *SHELXTL plus* [50] from which the positions of the Ru atoms were obtained. The rest of the non-H atoms were obtained from subsequent Difference Fourier maps. The structures were refined in *SHELXTL plus* using full-matrix least squares. All of the non-H atoms were refined with anisotropic thermal parameters. The non-H atoms were treated anisotropically. The H atoms in **2.03a** were located from a Difference Fourier map and were refined without any constraints. In **2.11b**, all of the H atoms were located from a Difference Fourier map and refined freely; except the C16 hydrogen atoms which were calculated in idealized positions and their thermal parameters were fixed at 0.08. 263 and 261 parameters for **2.03a** and **2.11b**, respectively, were refined and $\Sigma\ w\ (\ |Fo| - |F_c|)^2$ was minimized; $w=1/(\sigma|Fo|)^2$, $\sigma(Fo) = 0.5\ kI^{-1/2}\{[\sigma(I)]^2 + (0.02I)^2\}^{1/2}$, I(intensity)= (I peak - $I_{background}$)(scan rate), and $\sigma(I) = (I_{peak} + I_{background})^{1/2}$ (scan rate), k is the correction due to decay and Lp effects, 0.02 is a factor used to down weight intense reflections and to account for instrument instability. $R = 0.0457$ and $wR = 0.061$ for **2.03a**, and $R = 0.0338$ and $wR = 0.0393$ for **2.11b** in the last cycle of refinement. The linear absorption coefficient was calculated from values from the *International Tables for X-ray Crystallography* .[51] Scattering factors for non-hydrogen atoms were taken from Cromer & Mann[52] with anomalous-dispersion corrections from Cromer & Liberman,[53] while those of hydrogen atoms were from Stewart, Davidson & Simpson. [54]

Preparation of $CpRu(CO)_2Me$ (or RpMe) **3.04**

A solution of 1.6 g (3.60 mmol) of $(CpRu(CO)_2)_2$ in 300 mL of THF was treated with ca. 0.80 g Na and 8.0 mL Hg amalgam. The mixture was stirred for 5 hr. The dark grey solution was then transferred into a Schlenk tube. To this solution, cooled to -78 °C, was slowly added excess MeI (1.31 mL) and stirred overnight at RT. The solvent was then removed under vacuum. The resulting residue was extracted with hexane at least three times, and the solution was eluted through an alumina column to give a colorless solution. Evaporation of the solvent gave pure white RpMethyl in 74% yield. The compound was characterized by comparision of IR and NMR spectra with those of the known material [49].

Preparation of ^{13}C enriched $CpRu(CO^*)_2CH_3$ **3.04**

This compound was prepared by the same method as above, except using $^{13}CH_3I$.

Preparation of acyclic ruthenium lithium enolate **3.08**

To a solution of $RpCH_3$ **3.04** (0.10 g, 0.42 mmol) in ca. 10 mL of diethyl ether was slowly added PhLi (1.8M, 0.40 mL, 0.72 mmol) at -78 °C in the special apparatus as shown in chapter 3 page 35. The reaction was allowed to stir for at least 5 h under N_2 followed by warming the mixture to -30 °C. A bright yellow precipitate was formed. The solvent was removed in vacuo at -30 °C over a six hour period, and then the

ruthenium enolate salt **3.08** was treated with 1 mL of CD_2Cl_2 at -78 °C for a half hour. The solution was filtered through a frit covered with a small amount of celite into an NMR tube at -78 °C, and then the NMR tube was sealed at liquid nitrogen temperature. The Ru enolate, **3.08**, was studied by ^1H and ^{13}C NMR spectroscopy at -78 °C. ^1H NMR (CD_2Cl_2, -78 °C): δ 7.26-7.75 (m, 5H, phenyl region); 5.16 and 5.05 (s, 5H, Cp) . ^{13}C NMR (CD_2Cl_2, -78 °C): δ 294.54; 292.23; 291.79 (C=Ru); 215.4, 212.79, 212.03 (CO); 133.2-126.9 (phenyl region); 91.40; 91.34 (Cp); -26.71; -26.77; -28.05 ppm (Ru-CH_3). (Figure 3-6)

Preparation of acyclic ruthenium lithium enolate **3.08** in the presence of 12-crown-4

Lithium enolate **3.08** was prepared exactly the same as above except for the addition of one equivalent of 12-crown-4 (0.063 mL) after the formatiom of **3.08**. ^1H NMR (-90 °C, CD_2Cl_2) δ 7.65~7.056 ppm (m, phenyl region), 4.897 (s, Cp), 0.217 (s, CH_3); ^{13}C NMR (-90 °C, CD_2Cl_2) δ 284.13 (C=Ru), 2.10.82 (CO), 128~123.9 (phenyl region), 89.50 (Cp), -28.09 ppm (CH_3-Ru).

Preparation of acyclic ruthenium lithium enolate **3.08** in the presence of ten pencent THF-d_8

Lithium enolate **3.08** was prepared exactly the same as above except for the addition of 10% deuterated THF. ^1H NMR (-90 °C, CD_2Cl_2) δ 7.60~6.974 ppm (m, phenyl region), 4.859 (s, Cp), 0.1098 (s, CH_3); ^{13}C NMR (-90 °C, CD_2Cl_2) δ

292.12, 282.59 (C=Ru), 2.11.45, 210.35 (CO), 128~121.96 (phenyl region), 90.20, 89.01 (Cp), -28.08 ppm (CH_3-Ru).

Reaction of ruthium lithium-enolate **3.08** with trimethylsilylchloride

The Li-enolate **3.08** was prepared by the same procedure described above, except one equivalent of trimethylsilylchloride (0.05 mL) was added at -78 °C after addition of CD_2Cl_2. Apparently there was no reaction because the key aspects of the observed spectra were much the same as those of the enolate itself: ^1H NMR (CD_2Cl_2, -78 °C): δ 7.26-7.75 (m, 5H, phenyl region); 5.16 and 5.05 (s, 5H, Cp); 0.50 (s, 9H, Me_3Si). ^{13}C NMR (CD_2Cl_2, -70 °C): δ 294.54; 292.23; 291.79 (C=Ru); 215.48, 212.79, 212.04 (CO region); 133.2-126.9 (phenyl region); 91.49, 91.32 (Cp); -1.56 (Me_3Si); -26.71; -26.77; -28.10; -28.05 ppm (M-CH_3). Reaction of **3.08** with trimethylsilylchloride at -40 °C gave **3.09**.

Reaction of ruthenium lithium-enolate **3.08** with trimethylsilyltriflate

The Li-enolate **3.08** was prepared by the same procedure described above except one equivalent of trimethylsilyltriflate (0.077 mL)was added *via* vacuum transfer under liquid nitrogen after addition of the deuterated methylene chloride. The reaction mixture was then warmed to -78 °C for 30 minutes. Apparently the acyclic ruthenium carbene complex **3.09** was not stable and underwent migratory insertion at that temperature. The metal hydride **3.11** were detected at -78 °C.

Reaction of ruthenium Li-enolate **3.08** with Et_3OBF_4

The Li-enolate **3.08** was prepared by the same procedure described above, except one equivalent of triethyloxonium tetrafluoroborate (70 mg) was added at -78 °C. The results were essentially the same as in the case of trimethylsilylchloride. The desired ruthenium carbene complex **3.01** was formed at -40 °C. However, it underwent migratory insertion rapidly.

Reaction of ruthenium Li-enolate **3.08** with Et_3OBF_4 in the presence of 12-crown-4

The Li-enolate **3.08** was prepared by the same procedure described above except 12-crown-4 (0.094 mL, 1.5 eq) was added into the diethyl ether solution after the formation of **3.08** and the mixture was allowed to stir for one hour before removing the solvent. One equivalent of Et_3OBF_4 was then added at -78 °C. The metal hydride was detected at -78 °C.

Conversion of acyclic Ruthium carbene complex **3.01** to **3.05** *via* **3.07**

Migratory insertion product π-complexes **3.07** were formed gradually from the Li-enolate in the presence of triethyloxonium tetrafluoroborate by warming the mixture, prepared as described above, to -40 °C. ^1H NMR (CD_2Cl_2): δ -8.51, -8.62 (s, 1H, Ru-H); 1.20 (t, 3H, CH_3); 2.535, 2.745, 3.155, 3.355 (d, 1H, CH=); 3.40 (q, 2H, OCH_2); 5.04, 5.18 (s, 5H, Cp); 7.25~7.90 (phenyl region). ^{13}C NMR (CD_2CL_2): δ 15.51 (CH_3) ; 19.60, 19.02 (CH_2=); 66.62, 66.35 (OCH_2); 88.25 (Cp); 107.79, 108.96 (C=);

134~126 (phenyl region); 202.79, 203.16 (CO). These two isomers were observed to be stable for a short time at 0 °C, after which they were found to convert to free enol ether **3.05**.

Preparation of ruthenium lithium enolate **3.12**

To a stirred solution of 0.084 g (0.214 mmol) of 2-bromobenzyl ruthenium complex **2.05** in ca.10 mL of diethyl ether was added 2 equivalents of *t*-butylithium (1.7M, 0.25 mL) at -100 °C, followed by warming to room temperature overnight. Evaporation of solvent gave the orange yellow lithium enolate **3.12**. ^{1}H NMR (CD_2Cl_2) δ 3.08 (d, J_{HH}=14.3Hz, 1H), 3.57 (d, J_{HH}=14.3Hz, 1H), 4.99 (s, 5H, Cp), 6.81, 7.22, 7.45 (4H, phenyl region); ^{13}C NMR (CD_2Cl_2) δ 292.57 ppm (C=Ru), 210 (CO), 86.43 (Cp), 9.89 (CH_2), 166.87, 154.92, 130.90, 128.07, 123.45, 117.15 (phenyl region).

Preparation of 2-dicarbonyl-(η^5-cyclopentadienyl)-ruthena-2'-bromo biphenyl **4.03**

To a stirred solution of 1.0 g (3.2 mmol) of 2,2'-dibromobiphenyl in ca. 30 mL tetrahydrofuran at -78 °C was added 1.6 mL (1 eq, 2M) of n-BuLi. The color of the solution changed from colorless to light yellow. The reaction mixture was allowed to warm to -30 °C over a period of 2~3 hours. Addition of this yellow solution to RpBr (0.77 g, 2.6 mmol) in the THF solution at -78 °C *via* a cannula, was followed by warming to room temperature overnight to give a deep reddish color solution. The solvent was removed under reduced pressure, and the crude reaction mixture was eluted through an alumina (III) column using first hexane, and then 30 percent methylene

chloride, monitoring by IR spectroscopy. The desired off-white solid compound was isolated in 36% yield, mp=108~110 °C. Anal. Calcd. for $C_{19}H_{15}O_2RuBr$: C, 50.20; H, 2.86; Found: C, 50.17; H, 2.88. IR (hexane, cm^{-1}) 2028.3; 1972.5; High resolution mass spectrum, calcd for $C_{19}H_{14}O_2RuBr$ (M^{+}) 454.9214, found 454.9264; ^1H NMR (CD_2Cl_2) δ 5.23 (s, 5H, Cp), 7.00 (m, 3H), 7.21 (m, 2H) , 7.36 (t, 1H), 7.63 (d, 2H); ^{13}C NMR (CD_2Cl_2) δ 89.41, 123.14, 125.08, 125.71, 126.99, 128.45, 130.15, 132.71, 133.20, 138.39, 146.64, 149.45, 153.64, 200.33, 201.00.

Preparation of ruthenaphenanthrene Lithium enolate **4.05**

In a specially-designed low-temperature schlenk tube fitted with a stirrer were placed 0.131g (0.288 mmol) of **4.03** and ca. 8 mL of diethyl ether. To this was added two equivalents (0.58 mmol, 0.34mL) of t-BuLi (1.8M in Et_2O) over a period of 5 minutes at -78 °C. The mixture was stirred overnight at this temperature, and a reddish-yellow precipitate was formed. The solvent was evaporated under reduced pressure at ca. -30 °C for several hours, and then the residue was treated with 1 mL of CD_2Cl_2 for an hour. The solution was filtered through a frit into an NMR tube at -78 °C, followed by sealing the NMR tube under liquid N_2. ^1H NMR (-78 °C, CD_2Cl_2) δ 5.04 (br, 5H), 6.70~7.70 (m, phenyl region). ^{13}C NMR (-78 °C, CD_2Cl_2), δ 300.80 (br. Ru=C) , 208.06 (br. CO), 146.0~120.4 (phenyl region), 88.95 (br. Cp).

Reaction of **4.05** with Et_3OBF_4 or Me_3SiCl

The Li-enolate **4.05** was prepared as described above. To this enolate was then added one equivalent of Et_3OBF_4 (0.054 g) or Me_3SiCl (0.02 mL) at -78 °C for 30 min and was transferred into an NMR tube at that temperature. The NMR results were basically the same as those of the **4.05** at -78 °C indicating no reaction. However, **4.01** was fomed at -50 °C and rearranged rapidly to **4.07**.

Conversion of ruthenaphenanthrene **4.01b** to the η^3-π-benzyl complex **4.07b**

The ruthenaphenanthrene **4.01b** underwent migratory insertion at -50 °C to give the η^3-π-benzyl complex **4.07b.** Spectra were obtained at -50 °C: ^{1}H NMR (CD_2Cl_2) δ 7.86 (d, 1H), 7.77 (d, 1H) ,7.71 (t, 1H), 7.63 (d, 1H), 7.44 (t, 1H), 7.31 (m, 2H), 5.48 (d, 1H), 3.79 (s, 5H), -0.257 (s, 9H). ^{13}C NMR (CD_2Cl_2) δ 205.04, 153.66, 138.77,134.75, 130.35, 127.51, 124.12, 123.28, 121.04, 120.53, 117.64, 92.12, 89.05, 84.79, 65.34, -0.149.

Conversion of ruthenaphenanthrene **4.01a** to the η^3-π-benzyl complex **4.07a**

The ruthenaphenanthrene **4.01a** underwent migratory insertion at -50 °C to give the η^3-π–benzyl complex **4.07a.** Spectra were obtained at -50 °C: ^{1}H NMR (CD_2Cl_2) δ 7.89 (d, 1H), 7.80 (d, 1H), 7.65 (m, 2H), 7.44 (t, 1H), 7.31(m, 2H), 5.58 (d, 1H), 3.78 (s, 5H), 3.59 (q, 2H), 3.09 (q, 2H), 0.974 (t, 3H). ^{13}C NMR (CD_2Cl_2) d 205.62,

152.90, 135.09, 134.58, 129.00, 128.09, 124.98, 124.65, 122.14, 121.32, 118.09, 95.92, 90.01, 84.88, 68.99, 67.78, 15.85.

Preparation of the η^3-π–benzyl complex **4.07c**

To a stirred solution of 0.358 g (0.787 mmol) of **4.03** in ca. 30 mL of THF was added 2 eq. (0.93 mL, 1.7M) of t-BuLi at -78 °C. The reaction mixture was stirred overnight at -78 °C and the color of the solution remained clear yellow. Addition of 1.5 eq (0.128 g) of Me_3OBF_4, followed by warming to -20 °C over a period of one hour gave a clear red solution . The solvent was then removed under vacuum at ca. -20 °C . The crude oil product was purified by chromatography with alumina (III) and the mixture of solvents of hexane, diethyl ether and methylene chloride (90:5:5) was used for elution at -20 °C to afford (61.2 mg) of a red oil in 20% yield. IR (hexane, cm^{-1}) 1967.5. Anal.calcd.for $C_{20}H_{16}O_2Ru$: C, 61.70; H, 4.11; found: C, 61.31; H, 4.18. ^1H (CD_2Cl_2) δ 3.15 (s, 3H), 3.76 (s, 5H), 5.58 (d, 1H), 7.29 (m, 2H), 7.42 (t, 1H), 7.62 (m, 2H), 7.78 (d, 1H), 7.86 (d, 1H). ^{13}C (CD_2CL_2) δ 205.63, 155.40, 141.00, 134.48, 133.00, 128.13, 125.08, 124.89, 122.21, 121.40,118.14, 90.10, 84.92, 69.41, 59.81.

Preparation of **4.09**

In a specially-designed low-temperature schlenk tube fitted with a stirrer were placed 0.131 g (0.288 mmol) of **4.03** and ca. 8 mL of diethyl ether. To this was added two equivalents (0.58 mmol, 0.34 mL) of t-BuLi (1.8M in Et_2O) over a period of 5 minutes at -78 °C. The mixture was stirred overnight at this temperature, and a reddish-

yellow precipitate was formed. The solvent was evaporated under reduced pressure at ca. -30 °C for several hours, and then the residue was treated with 1 mL of CD_2Cl_2 for an hour. To this enolate was then added one equivalent of Et_3OBF_4 (0.054 g) at -78 °C. Approximately half of this alkylated reaction mixture was stirred under the one atmosphere of carbon monoxide at -78 °C, which was then allowed to warm up to room temperature overnight. The solvent was removed under reduced pressure. The residue was purified by column chromatagraphy over alumina (III) eluting with hexane. The solvent was removed under vacuum to give a red solid. IR (hexane, cm^{-1}) : 2028.1, 1975. Anal. calcd. for $C_{22}H_{18}O_3Ru$: C, 61.30; H, 4.20. found: C, 61.47; H , 4.35. HRMS (M^+) calcd.432.0293; found , 432.0304. ^1H (CD_2CL_2) δ 1.028 (t, 3H) , 2.790 (q, 2H), 4.395(s, 5H) , 7.248 (m, 4H), 7.699 (d, 2H), 7.745 (d, 2H). ^{13}C (CD_2CL_2) δ 202.37, 155.7, 134.49, 126.99, 125.87, 124.66, 120.06, 90.23, 89.00, 60.97, 16.01.

Synthesis of 1-dicarbonyl (η^5-cyclopentandienyl) rutheno-4-bromo-1,4 diphenylbutadiene **4.17**

An oven dried schlenk tube fitted with a magnetic stirrer and a septum was charged with 1.0g (2.80 mmol) of 1,4-dibromo-1,4-diphenylbutadiene **4.15** and the flask filled with nitrogen. To this solid, was added 30 mL of diethyl ether and the flask was cooled in an ice bath. *n*-Butyllithium (1.4 mL, 2M) was added dropwise over 5 minutes. After stirring for 30 minutes the solution was warmed to room temperature and then cooled in a dry ice bath. Addition of this orange solution to RpBr (0.67 g, 2.2 mmol) in Et_2O at -78 °C *via* a cannula, was followed by slow warming to room temperature overnight. The solvent was removed under vacuum. The crude product was

purified by chromatography with alumina (III) and hexane which was monitored by IR. The colorless solution was concentrated to ca. 20 mL and cooled to ca. -30 °C to afford (0.43 g) of colorless crystalline solids in 37% yield. IR (hexane, CO, cm^{-1}) 2034.6, 1981.8; (enriched CO, 2019.3, 1950.0). Anal. calcd. for $C_{23}H_{18}O_2RuBr$: C, 54.40; H, 3.36. found: C, 54.64; H, 3.36. HRMS calcd. for $C_{23}H_{18}O_2RuBr$ (M^+) 506.9527. found 505.9560. ^1H NMR (CD_2Cl_2) δ 5.28 (s, 5H), 6.92 (s, 2H), 6.98 (t, 3H), 7.14 (m, 3H), 7.26 (t, 2H), 7.50 (d, 2H). ^{13}C NMR (CD_2Cl_2) δ 200.38, 158.76, 156.95, 140.82, 139.75, 134.37, 128.84, 128.42, 127.97, 127.54, 126.90, 125.45, 123.26, 89.19.

Preparation of ruthenabenzene lithium enolate **4.18**

To a colorless solution of **4.17** (100 mg, 0.198 mmol) in ca. 10 mL of diethyl ether was slowly added t-BuLi (1.7M, 0.23 mL, 2 eq) at -78 °C in the special apparatus as shown in chapter 3 page 35. A reddish solution was formed immediately. The reaction was allowed to stir overnight under N_2 followed by warming the mixture to -30 °C. The solvent was removed in vacuo at ca. -30 °C over a six hour period, and then the ruthenium enolate salt **4.18** was treated with 1 mL of CD_2Cl_2 at -78 °C for a half hour. The solution was transferred into an NMR tube using a -78 °C bath, and then the NMR tube was sealed at liquid nitrogen temperature. The Ru enolate, **4.18**, was studied by ^1H and ^{13}C NMR spectroscopy at -78 °C. ^1H NMR (CD_2Cl_2) δ 6.75~7.25 ppm (phenyl region), 4.94 (br. Cp). ^{13}C NMR (CD_2Cl_2) δ 293.84 (br. Ru=C), 204.71(CO), 128.71~124.81 (phenyl region), 90.13 (Cp).

Preparation of ruthenabenzene or ruthenacyclohexatriene **4.16**

To the above lithium enolate **4.18**, excess Et_3OBF_4 was added at -78 °C. The reaction mixture was allowed to react for forty minutes at that temperature, followed by NMR spectroscopic analysis. ^1H NMR (CD_2Cl_2, -50 °C) δ 7.80~7.40 (phenyl region, 12H), 5.32 (s, 5H), 4.56~4.75 (m, 2H), 1.50 (t, 3H). ^{13}C NMR (CD_2Cl_2, -50 °C) δ 291.16 ppm (C=Ru), 201.20 (CO), 152.11~122.86 (phenyl region), 89.01 (Cp), 76.23 (OCH_2), 12.50 (CH_3).

Preparation of trapping product **4.19**

The desired ruthenabenzene **4.16** was prepared as described above. Approximately half of this alkylated reaction mixture was stirred under one atmosphere of carbon monoxide at -78 °C, which was then allowed to warm up to room temperature for several hours. The solvent was removed under reduced pressure. The residue was purified by column chromatography with alumina (III) and hexanes. The solvent was removed under vacuum to give a yellow solid compound. ^1H NMR (CD_2Cl_2) δ 7.62 (d, 4H), 7.36 (t, 4H), 7.20 (t, 2H), 5.79 (s, 2H), 4.95 (s, 5H), 3.67 (q, 2H), 1.18 (t, 3H). ^{13}C NMR (CD_2Cl_2) δ 201.08, 137.43, 135.00, 128.48, 127.37, 125.91, 89.56, 68.62, 15.67 ppm. IR (hexane, cm^{-1}) : 2022.4, 1968.3. HRMS (EI, *m/e*): Calcd for (M^+): 484.0606; Found: 484.0582.

APPENDIX
TABLES OF CRYSTALLOGRAPHIC DATA

Table 2-1. Crystallographic data for ruthenaindene complex **2.03a.**

A. Crystal data (298 K)	**2.03a**
a, Å	9.082(1)
b, Å	10.601(1)
c, Å	16.827(2)
a, deg.	90
b, deg.	92.57(1)
g, deg.	90
V, Å^3	1618.4(3)
d_{calc}, g cm^{-3}(298 K)	1.532
Empirical formula	$C_{20}H_{16}ORu$
Formula wt, g	373.40
Crystal system	Monoclinic
Space group	P $2_1/n$
Z	4
F(000), electrons	752
Crystal size (mm^3)	0.34 x 0.23 x 0.15
B. Data collection (298 K)	
Radiation, l (Å)	Mo-K_a, 0.71073
Mode	w-scan
Scan range	Symmetrically over 1.2∞ about $K_{a1,2}$ maximum
Background	offset 1.0 and -1.0 in w from $K_{a1,2}$ maximum
Scan rate, deg. min.$^{-1}$	3 – 6
2q range, deg.	3 – 55
Range of *h k l*	$0 \leq h \leq 11$ $0 \leq k \leq 13$ $-21 \leq l \leq 21$
Total reflections measured	4175
Unique reflections	3730
Absorption coeff. m (Mo-K_a), cm^{-1}	0.97
Min. & Max. Transmission	0.789, 0.868
C. Structure refinement	
S, Goodness-of-fit	1.96
Reflections used, I > 2s(I)	2851
No. of variables	263
R, wR* (%)	4.57, 6.10
$R_{int.}$ (%)	1.84
Max. shift/esd	0.003

Table 2-1. continued.

min. peak in diff. four. map (e $Å^{-3}$)	-0.59
max. peak in diff. four. map (e $Å^{-3}$)	1.03

* Relevant expressions are as follows, where in the footnote F_o and F_c represent, respectively, the observed and calculated structure-factor amplitudes.

Function minimized was $w(|F_o| - |F_c|)^2$, where $w = (s(F))^{-2}$

$R = Â(||F_o| - |F_c||) / Â|F_o|$

$wR = [Âw(|F_o| - |F_c|)^2 / Â |F_o|^2]^{1/2}$

$S = [Âw(|F_o| - |F_c|)^2 / (m-n)]^{1/2}$

Table 2-2. Bond Lengths (Å) and Angles (°) for the non-H atoms of compound **2.03a**.

1	2	3	1-2	1-2-3
C1	Ru		2.246(7)	
C2	Ru		2.260(7)	
C3	Ru		2.286(7)	
C4	Ru		2.289(6)	
C5	Ru		2.277(7)	
C6	Ru	C19	1.949(5)	79.0(2)
C19	Ru	C20	2.135(6)	84.1(3)
C20	Ru		1.834(6)	
C20	O		1.152(8)	
C2	C1	C5	1.398(14)	107.0(7)
C3	C2	C1	1.401(12)	108.6(8)
C4	C3	C2	1.390(12)	107.2(8)
C5	C4	C3	1.378(12)	109.3(7)
C1	C5	C4	1.413(12)	108.0(7)
C7	C6	C13	1.470(7)	119.8(4)
C13	C6	Ru	1.444(7)	115.9(3)
C8	C7	C12	1.393(8)	118.7(5)
C8	C7	C6		121.2(5)
C12	C7	C6	1.382(8)	120.1(5)
C9	C8	C7	1.398(10)	119.6(6)
C10	C9	C8	1.358(12)	120.8(8)
C11	C10	C9	1.367(12)	120.3(7)
C12	C11	C10	1.395(10)	119.9(7)
C7	C12	C11		120.7(6)
C14	C13	C18	1.411(8)	119.0(5)
C14	C13	C6		127.0(5)
C18	C13	C6	1.404(7)	113.9(5)
C15	C14	C13	1.384(8)	120.4(5)
C16	C15	C14	1.383(10)	119.5(5)
C17	C16	C15	1.379(9)	121.2(6)
C18	C17	C16	1.396(8)	120.0(6)
C19	C18	C13	1.482(8)	114.1(5)
C19	C18	C17		126.3(5)
C13	C18	C17		119.5(5)
Ru	C19	C18		107.5(4)

Table 2-3. Bond Lengths (Å) and Angles (°) of the H atoms of compound **2.03a**.

1	2	3	1-2	1-2-3
H1	C1	C2	0.97(8)	132.(4)
H1	C1	C5		120.(4)
H2	C2	C3	0.89(6)	119.(4)
H2	C2	C1		133.(4)
H3	C3	C4	0.84(8)	129.(5)
H3	C3	C2		123.(5)
H4	C4	C5	0.90(10)	134.(7)
H4	C4	C3		116.(7)
H5	C5	C1	1.01(9)	118.(5)
H5	C5	C4		134.(5)
H8	C8	C9	1.02(4)	122.(2)
H8	C8	C7		118.(2)
H9	C9	C10	0.83(11)	128.(7)
H9	C9	C8		111.(7)
H10	C10	C11	1.09(7)	103.(4)
H10	C10	C9		136.(4)
H11	C11	C12	0.89(6)	118.(4)
H11	C11	C10		122.(4)
H12	C12	C7	0.88(6)	119.(4)
H12	C12	C11		120.(4)
H14	C14	C15	0.93(8)	113.(5)
H14	C14	C13		125.(5)
H15	C15	C16	0.89(5)	123.(3)
H15	C15	C14		118.(3)
H16	C16	C17	0.90(6)	117.(4)
H16	C16	C15		122.(4)
H17	C17	C18	0.84(6)	118.(4)
H17	C17	C16		122.(4)
H19a	C19	H19b	0.82(7)	107.(6)
H19a	C19	Ru		100.(5)
H19a	C19	C18		114.(5)
H19b	C19	Ru	1.03(6)	117.(3)
H19b	C19	C18		111.(3)

Table 2-4. Fractional coordinates and equivalent isotropic[a] thermal parameters ($Å^2$) for the non-H atoms of compound **2.03a**

Atom	x	y	z	U
Ru	0.24506(5)	0.06450(4)	0.10132(2)	0.04017(14)
O	-0.0043(5)	-0.1035(5)	0.1420(3)	0.078(2)
C1	0.3202(11)	0.2295(6)	0.0299(5)	0.075(4)
C2	0.1680(11)	0.2412(6)	0.0369(5)	0.075(3)
C3	0.1396(10)	0.2581(6)	0.1174(5)	0.070(3)
C4	0.2749(9)	0.2586(6)	0.1594(5)	0.063(3)
C5	0.3859(9)	0.2423(6)	0.1072(5)	0.069(2)
C6	0.3835(5)	-0.0568(5)	0.1495(3)	0.039(2)
C7	0.4914(6)	-0.0268(5)	0.2144(3)	0.043(2)
C8	0.6383(7)	-0.0635(7)	0.2111(4)	0.062(2)
C9	0.7391(10)	-0.0287(10)	0.2724(5)	0.084(3)
C10	0.6946(9)	0.0365(8)	0.3365(4)	0.079(3)
C11	0.5498(9)	0.0693(7)	0.3419(4)	0.071(3)
C12	0.4482(8)	0.0390(6)	0.2803(3)	0.052(2)
C13	0.3764(6)	-0.1829(5)	0.1171(3)	0.042(2)
C14	0.4311(6)	-0.2943(5)	0.1535(4)	0.046(2)
C15	0.4042(7)	-0.4105(5)	0.1182(4)	0.057(2)
C16	0.3248(8)	-0.4165(6)	0.0462(4)	0.061(2)
C17	0.2762(7)	-0.3086(6)	0.0075(4)	0.057(2)
C18	0.3046(6)	-0.1906(5)	0.0416(3)	0.044(2)
C19	0.2649(8)	-0.0665(6)	0.0060(3)	0.051(2)
C20	0.0899(7)	-0.0356(5)	0.1276(4)	0.052(2)

[a]For anisotropic atoms, the U value is U_{eq}, calculated as $U_{eq} = 1/3 \sum_i \sum_j U_{ij} a_i^* a_j^* A_{ij}$ where A_{ij} is the dot product of the i^{th} and j^{th} direct space unit cell vectors.

Table 2-5. Crystallographic data for ruthenacene **2.11b**

	2.11b
A. Crystal data (298 K)	
a, Å	8.452(1)
b, Å	12.258(1)
c, Å	15.812(2)
a, deg.	90
b, deg.	90
g, deg.	90
V, Å^3	1638.2(3)
d_{calc}, g cm^{-3}(298 K)	1.571
Empirical formula	$C_{21}H_{18}ORu$
Formula wt, g	387.42
Crystal system	orthorhombic
Space group	$P2_12_12_1$
Z	4
F(000), electrons	784
Crystal size (mm^3)	0.39 x 0.31 x 0.14
B. Data collection (298 K)	
Radiation, l (Å)	Mo-K_a, 0.71073
Mode	w-scan
Scan range	Symmetrically over 1.2∞ about $K_{a1,2}$ maximum
Background	offset 1.0 and -1.0 in w from $K_{a1,2}$ maximum
Scan rate, deg. min.$^{-1}$	3 – 6
2q range, deg.	3 – 60
Range of *h k l*	$0 \leq h \leq 11$ $0 \leq k \leq 17$ $0 \leq l \leq 22$
Total reflections measured	2741
Unique reflections	2716
Absorption coeff. m (Mo-K_a), cm^{-1}	0.96
Min. & Max. Transmission	0.723, 0.828
C. Structure refinement	
S, Goodness-of-fit	1.34
Reflections used, I > 2s(I)	2451
No. of variables	261
R, wR* (%)	3.38, 3.93
$R_{int.}$ (%)	0
Max. shift/esd	0.006

Table 2-5. continued.

min. peak in diff. four. map (e $Å^{-3}$)	-0.38
max. peak in diff. four. map (e $Å^{-3}$)	0.43

* Relevant expressions are as follows, where in the footnote F_o and F_c represent, respectively, the observed and calculated structure-factor amplitudes.

Function minimized was $w(|F_o| - |F_c|)^2$, where $w = (s(F))^{-2}$

$R = \hat{A}(||F_o| - |F_c||) / \hat{A}|F_o|$

$wR = [\hat{A}w(|F_o| - |F_c|)^2 / \hat{A}\,|F_o|^2]^{1/2}$

$S = [\hat{A}w(|F_o| - |F_c|)^2 / (m-n)]^{1/2}$

Table 2-6. Fractional coordinates and equivalent isotropic[a] thermal parameters ($Å^2$) for the non-H atoms of compound **2.11b**.

Atom	x	y	z	U
Ru	0.16129(4)	0.94468(3)	0.80116(2)	0.03033(8)
O1	0.2764(4)	1.1751(3)	0.7221(2)	0.0436(11)
C1	0.2967(5)	1.0981(3)	0.7831(3)	0.0308(11)
C2	0.2255(5)	1.0961(4)	0.8649(3)	0.0345(12)
C3	0.2966(5)	1.0072(4)	0.9100(3)	0.0335(12)
C4	0.2791(7)	0.9689(4)	0.9949(3)	0.045(2)
C5	0.3653(8)	0.8830(5)	1.0211(3)	0.052(2)
C6	0.4729(7)	0.8291(5)	0.9669(3)	0.048(2)
C7	0.4929(6)	0.8606(3)	0.8841(3)	0.0351(12)
C8	0.4036(5)	0.9520(4)	0.8540(3)	0.0293(10)
C9	0.3996(5)	1.0062(3)	0.7725(3)	0.0275(10)
C10	0.4928(5)	0.9794(3)	0.6961(3)	0.0301(10)
C11	0.5732(5)	1.0604(4)	0.6517(3)	0.0369(12)
C12	0.6605(7)	1.0338(4)	0.5795(3)	0.0445(14)
C13	0.6710(6)	0.9279(4)	0.5505(3)	0.0442(14)
C14	0.5913(6)	0.8480(4)	0.5955(3)	0.0429(15)
C15	0.5045(6)	0.8720(4)	0.6669(3)	0.0372(13)
C16	0.7664(10)	0.9003(6)	0.4733(4)	0.069(2)
C17	-0.0033(10)	0.9090(8)	0.7001(4)	0.084(3)
C18	0.0880(10)	0.8135(9)	0.7199(7)	0.094(4)
C19	0.0555(7)	0.7847(5)	0.8064(6)	0.063(2)
C20	-0.0536(6)	0.8613(5)	0.8358(4)	0.052(2)
C21	-0.0883(7)	0.9345(6)	0.7717(5)	0.063(2)

[a]For anisotropic atoms, the U value is U_{eq}, calculated as $U_{eq} = 1/3\ \Sigma_i\Sigma_j\ U_{ij}\ a_i^*\ a_j^*\ A_{ij}$ where A_{ij} is the dot product of the i^{th} and j^{th} direct space unit cell vectors.

Table 2-7. Bond Lengths (Å) and Angles (°) for the non-H atoms of compound **2.11b.**

1	2	3	1-2	1-2-3
C1	Ru		2.220(4)	
C2	Ru		2.181(5)	
C3	Ru		2.204(4)	
C8	Ru		2.214(4)	
C9	Ru		2.198(4)	
C17	Ru		2.163(8)	
C18	Ru		2.150(10)	
C19	Ru		2.157(6)	
C20	Ru		2.155(6)	
C21	Ru		2.164(6)	
C1	O1		1.360(6)	
C2	C1	C9	1.426(7)	110.4(4)
C2	C1	O1		127.0(4)
C9	C1	Ru	1.434(6)	70.2(2)
C9	C1	O1		122.7(4)
Ru	C1	O1		127.9(3)
C3	C2	Ru	1.434(6)	71.8(3)
C3	C2	C1		106.7(4)
Ru	C2	C1		72.6(3)
C4	C3	C8	1.429(7)	119.3(4)
C4	C3	Ru		124.4(3)
C4	C3	C2		132.3(4)
C8	C3	Ru	1.436(6)	71.4(2)
C8	C3	C2		108.3(4)
Ru	C3	C2		70.0(3)
C5	C4	C3	1.346(8)	119.3(5)
C6	C5	C4	1.413(8)	121.9(5)
C7	C6	C5	1.376(7)	121.6(5)
C8	C7	C6	1.432(6)	118.1(4)
C9	C8	Ru	1.449(6)	70.2(2)
C9	C8	C3		108.5(4)
C9	C8	C7		131.7(4)
Ru	C8	C3		70.7(2)
Ru	C8	C7		125.5(3)
C3	C8	C7		119.7(4)
C10	C9	Ru	1.479(6)	125.5(3)
C10	C9	C1		126.4(4)
C10	C9	C8		127.7(4)
Ru	C9	C1		71.9(2)
Ru	C9	C8		71.4(2)
C1	C9	C8		105.7(4)
C11	C10	C15	1.392(6)	118.1(4)
C11	C10	C9		120.9(4)
C15	C10	C9	1.399(6)	121.0(4)
C12	C11	C10	1.398(7)	120.2(5)
C13	C12	C11	1.380(7)	121.7(5)

Table 2-7. continued.

C14	C13	C16	1.386(7)	121.3(5)
C14	C13	C12		117.6(5)
C16	C13	C12	1.502(8)	121.1(5)
C15	C14	C13	1.378(7)	121.9(5)
C10	C15	C14		120.6(4)
C18	C17	C21	1.437(14)	106.7(7)
C18	C17	Ru		70.1(5)
C21	C17	Ru	1.376(10)	71.5(4)
C19	C18	Ru	1.439(14)	70.8(5)
C19	C18	C17		107.7(7)
Ru	C18	C17		71.0(5)
C20	C19	Ru	1.396(9)	71.0(3)
C20	C19	C18		106.1(6)
Ru	C19	C18		70.2(5)
C21	C20	Ru	1.385(10)	71.7(3)
C21	C20	C19		109.4(6)
Ru	C20	C19		71.2(3)
Ru	C21	C17		71.4(4)
Ru	C21	C20		70.9(3)
C17	C21	C20		110.1(6)

Table 2-8. Fractional coordinates and isotropic thermal parameters ($Å^2$) for the H atoms of compound **2.11b**.

Atom	x	y	z	U
H1	0.211(8)	1.221(5)	0.738(4)	0.05(2)
H2	0.149(6)	1.152(4)	0.889(3)	0.029(11)
H4	0.220(6)	1.009(4)	1.027(3)	0.026(12)
H5	0.365(9)	0.855(6)	1.080(5)	0.08(2)
H6	0.539(8)	0.763(5)	0.989(4)	0.05(2)
H7	0.572(5)	0.838(4)	0.841(3)	0.023(11)
H11	0.552(5)	1.134(4)	0.669(3)	0.014(10)
H12	0.714(7)	1.087(5)	0.547(4)	0.05(2)
H14	0.599(9)	0.775(6)	0.579(5)	0.08(2)
H15	0.457(6)	0.818(4)	0.701(3)	0.038(13)
H16a	0.81246	0.96539	0.45023	0.08
H16b	0.69898	0.86708	0.43175	0.08
H16c	0.84891	0.85019	0.48863	0.08
H17	-0.00468	0.94771	0.64737	0.08
H18	0.137(10)	0.786(7)	0.688(5)	0.10(3)
H19	0.103(9)	0.721(6)	0.837(5)	0.09(3)
H20	-0.09803	0.86304	0.89167	0.09(3)
H21	-0.145(9)	0.994(7)	0.774(5)	0.09(3)

Table 2-9. Bond Lengths (Å) and Angles (°) of the H atoms of compound **11b**.

1	2	3	1-2	1-2-3
H1	O1	C1	0.83(6)	110.(4)
H2	C2	C3	1.02(5)	126.(2)
H2	C2	Ru		126.(3)
H2	C2	C1		126.(2)
H4	C4	C5	0.87(5)	125.(3)
H4	C4	C3		115.(3)
H5	C5	C6	1.00(8)	114.(4)
H5	C5	C4		124.(4)
H6	C6	C7	1.04(6)	118.(3)
H6	C6	C5		120.(3)
H7	C7	C8	1.00(5)	110.(3)
H7	C7	C6		131.(3)
H11	C11	C12	0.96(4)	123.(3)
H11	C11	C10		116.(3)
H12	C12	C13	0.95(6)	116.(4)
H12	C12	C11		122.(4)
H14	C14	C15	0.93(7)	118.(5)
H14	C14	C13		120.(5)
H15	C15	C10	0.94(5)	116.(3)
H15	C15	C14		123.(3)
H16a	C16	H16b	0.960(7)	109.5(6)
H16a	C16	H16c		109.5(8)
H16a	C16	C13		109.8(6)
H16b	C16	H16c	0.960(7)	109.5(7)
H16b	C16	C13		109.4(7)
H16c	C16	C13	0.960(8)	109.2(5)
H17	C17	C18	0.960(8)	126.8(8)
H17	C17	C21		126.6(9)
H17	C17	Ru		123.3(7)
H18	C18	C19	0.73(9)	131.(7)
H18	C18	Ru		126.(7)
H18	C18	C17		122.(7)
H19	C19	C20	1.01(8)	129.(4)
H19	C19	Ru		124.(5)
H19	C19	C18		125.(4)
H20	C20	C21	0.960(6)	125.2(6)
H20	C20	Ru		123.6(5)
H20	C20	C19		125.4(6)
H21	C21	Ru	0.87(8)	118.(5)
H21	C21	C17		121.(5)
H21	C21	C20		129.(5)

REFERENCES

1. Light, J. R. C.; Zeiss, H. W. *J. Organomet. Chem.* **1970**, 21,391.

2. Matinez, J. M.: Adams, H.; Bailey, N. A.; Maithis, P. M. J. *Chem. Soc. Chem. Commun.* **1989**, 286.

3. Bleeke, J. R.; Xie, Y. F.; Peng, W. J.; Chiang, M. *J. Am. Chem. soc.* **1989**, 111, 4118.

4. Lisko, J. R.; Jones, W. M. *Organometallics* **1985**, 4, 944.

5. Stenstrom, Y.; Jones, W. M. *Organometallics* **1986**, 5, 178.

6. Stenstrom, Y.; Klauck, G.; Koziol, A.; Palenik, G. J.; Jones, W. M. *Organometallics* **1986**, 5, 2155.

7. Stenstrom, Y.; Koziol, A.; Palenik, G. J.; Jones, W. M. *Organometallics* **1987**, 6, 2079.

8. Conti, N. J.; Jones, W. M. *Organometallics* **1988**, 7, 1666.

9. Conti, N. J.; Crowther, D. J.; Tivakornpannarai, S.; Jones, W. M. *Organometallics* **1990**, 9, 175.

10. Crowther, D.J.; Zheng, Z. Palenik, G. J. Jones, W. M. *Organometallics* **1992**, 11. 622.

11. Tivakornpannarai, S.; Jones, W. M. *Organometallics* **1991**, 10, 1827.

12. Cf. (a) Roper, C. K.; Porter, D. *Chemical Rev.* **1981**, 81, 447. (b) Herrmann, W. A. *Angew. Chem. Int. Ed. Engl.* **1982**, 21, 117.; (c) Henrici-Olive, G. *The Chemistry of the Metal Carbon Bond*. Hartley, F. R.; Patai, S. (Eds), Vol.3, Wiley, New York **1985**, Ch. 9. (d) Roder, K.; Werner, H. *Angew. Chem. Int. Ed. Engl.* **1987**, 26, 686.

13. Carter, E. A.; Goddard, W. A. III *Organometallics* **1988**, 7, 675.

14. Bercaw, J. E; Cf. Parkin, G.; Bunel, E.; Burger, B. J.; Trimmer, M. S.;van Asselt, A. *J. Molec. Cat.* **1987**, 41, 21.

15. Miyashita, A.; Grubbs, R. H. *J. Am. Chem. Soc.* **1978**, 100, 7418.

16. Berke, H.; Hoffmann, R.; *J. Am. Chem. Soc.* **1978**, 100, 7224.

17. Versluis, L.; Tschinke, V.; Ziegler, T.; *J. Am. Chem. Soc.* **1986**, 108, 612.

18. Klemarczyk, P.; Price, T.; Priester, W.; Rosenblum, M.; *J. of Organometallic Chemistry* **1977**, 139, C25-c28.

19. (a) Elliott, G. P.; Roper, W. R.: Waters, J.M. *J. Chem. Soc. Chem. Commun.* **1982**, 811. (b) O'Connor, J. M.; Pu, L.; Rhenigold, A. L. *J. Am. Chem. Soc.* **1987**, 109, 7578. (c) O'Connor, J. M.; Pu, L.; Rhenigold, A. L. *Organometallics* **1988**, 7, 2060. (d) O'Connor, J. M.; Pu, L.; Rhenigold, A. L. *J. Am. Chem. Soc.* **1989**, 111, 4129. (e) Hoover, J. F.; stryker, *J. Am. Chem. Soc.* **1990**, 112, 464. (f) O'Connor, J. M.; Pu, L.; Rhenigold, A. L. *J. Am. Chem. Soc.* **1990**,112, 6232. (g) O'Connor, J. M.; Pu, L.; Woolard, S.; Chadha, R. K. *J. Am. Chem. Soc.* **1990**, 112, 6731. (h) Bleeke, J. R.; Peng, W. J.; Xie, Y. F.; Chiang, M. Y. *Organometallics* **1990**, 9, 1113. (i) Bleeke, J. R.; Xie, Y. F.; Bass, L.; Chiang, M. Y. *J. Am. Chem. Soc.* **1991**, 113, 4703.

20. Trace, R. L.; Sanchez, J.; Yang, J.; Yin, J.; Jones, W. M. *Organometallics* **1992**, 11, 739.

21. Liebman, J. F., "*Strained organic Molecules*" Academic Press, New York, **1978**, 66, 94.

22. Trace, R. L., Jones, W. M., *J. of Organometallic Chemistry*, **1989**, 376, 103.

23. Crowther, D. J.; Tivakornpannarai, S.; Jones, W. M. *Organometallics* **1990**, 9, 739.

24. Jones. W. M. *Unpublished results,* **1993**, p 5.

25. Yang, J.; Yin, J. G.; Abboud, K. A.; Jones, W. M. *Organometallics*, **1994**, 13, 971.

26. Stone, F. G. A.; Robter, W. *Adv. Organomet. Chem.* **1976**, 14, 1.

27. March, J. *Advanced Organic Chemistry*, 4th ed.; Wiley: New York, **1992**; p21.

28. Roder, K.; Werner, H. *Angew. Chem., Int. Ed. Engl.* **1987**, 26, 686.

29. Davey, C. E.; Osborn, V. A.; Winteer, M. J. *In Advances in Metal Carbene Chemistry;* Schuber, U. Ed.; Kluwer: Dordrecht, Boston, London, **1988**; p 159.

30. (a) Ferede, R.; Allison, N. T. *Organometallics* **1983**, 2, 463. (b) Ferede, R.; Hinton, J. F.; Korfmacher, W. A.; Freeman, J. P. Allison, N. T. *Organometallics* **1985**, 4, 614. (c) Mike, C. A.; Ferede, R.; Allison, N. T. *Organometallics* **1988**, 7, 1457. (d) Elliott, G. P.; Roper, W.R.; Waters, J. M. *J. Chem. Soc., Chem. Commun.* **1982**, 811. (e) Bleeke, J. R. *Acc. Chem. Res.* **1991**, 24, 271.

31. Bleeke, J. R.; Bass, L. A.; Xie, Y. F.; Chiang, M. Y. *J. Am. Chem. Soc.* **1992**, 114, 4213.

32. Collman. J. P.; Hegedus, L. S.; Norton. J. R.; Finke, R. G. *Principles and Applications of Organotransition Metal Chemistry,* University Science Books. Mill Valley, California, **1987**, p 379.

33. Casey, C. P.; Scheck, D. M. *J. Am. Chem. Soc.* **1980**, 102, 2723.

34. (a) Arbuzov. *Izv. Akad, Nauk SSSR*, **1963**, 675~83. (b) Hurd, C. D.; Pollack, M. A. *J. Am. Chem. Soc.*, Vol. 60, **1938**, 1905.

35. Periana. R. A.; Bergman. R. G. *J. Am. Chem. Soc.* **1986**, 108, 7332-7346.

36. (a) House, H. O.; Czuba, L. J.; Gall, M.; Olmstead, H. D. *J. of Organic Chemistry,* Vol. 34, No. 8, **1969**. (b) *Organic Syntheses*, Vol. 59, pp 113.

37. Stynes, D. V.; Stynes, H.; James, B. R. *J. Am. Chem. Soc.* **1973**, 4089.

38. Seebach, D. *Angew. Chem. Int. Ed. Engl.* 27, **1988**, 1624~1654.

39. Jackman, L. M.; Lange, B. C. *Tetrahedron,* Vol. 33, **1977**, pp. 2737~2769.

40. Thorn, D. L.; Hoffmann, R. *Nouv. J. de Chimie*. **1979**, 3, 39.

41. Brookhart, M; Buck, R. C.; Danielson, III. E. *J. Am. Chem. Soc.* **1989**, 111, 567~574.

42. Still, W. C.; Kahn, M.; Mitra, A. *J. Org. Chem.* **1978**, 43, 2923.

43. Doherty, N. M.; Knox, A. R. *Inorganic Syntheses*, Vol. 25, pp 180.

44. Darensbourg, D. J.; Gray, R. L.; Pala, M.*Organometallics*, Vol. 3, No. 12, **1984**, 1928.

45. Gilman, H.; Gaj, B. J.; *J. Org. Chem.* 22, 447, **1957.**

46. Corey, E. J.; *Organic Syntheses*, Vol. 46, pp 113.

47. Joseph, M. F.; Page, J. A.; Baird, M. C. *Organometallics*, **1984**, 3, 1749.

48. Sheldrick, G. M. *SHELXTL plus.* Nicolet XRD Corporation, Madison, Wisconsin, USA. **1990.**

49. *International Tables for X-ray Crystallography* **1974**, Vol. IV, p. 55. Birmingham: Kynoch Press. (Present distributor, D. Reidel, Dordrecht.).

50. Cromer, D.T. & Mann, J.B. **1968**, *Acta Cryst.* A24, 321-324.

51. Cromer, D.T. & Liberman, D. **1970**, *J. Chem. Phys.* 53, 1891-1898.

52. Stewart, R.F., Davidson, E.R. & Simpson, W.T. **1965**, *J. Chem. Phys.*, **42**, 3175-3187.

BIOGRAPHICAL SKETCH

Jing Yang was born in September, 1959, in Shanghai, P. R. China. She received her B.S. degree in analytical chemistry from Shanghai University of Technology in August, 1982. She then worked as a research chemist in the Shanghai Institute of Iron and Steel. In the summer of 1985, Jing was invited by Professor Herbert Laitinen to study and work in his lab at the University of Florida as a visiting scholar. One year later, Jing began work as an analytical chemist at ABC Research Company in Gainesville.

In January, 1991, Jing initiated graduate studies in the Department of Chemistry at the University of Florida under the supervision of Professor William M. Jones.

Upon completing her studies, Jing plans to seek new challenges in her life.

I certify that I have read this study and that in my opinion it conforms to acceptable standards of scholarly presentation and is fully adequate, in scope and quality, as a dissertation for the degree of Doctor of Philosophy.

William M. Jones, Chairman
Distinguished Service Professor of Chemistry

I certify that I have read this study and that in my opinion it conforms to acceptable standards of scholarly presentation and is fully adequate, in scope and quality, as a dissertation for the degree of Doctor of Philosophy.

Merle A. Battiste
Professor of Chemistry

I certify that I have read this study and that in my opinion it conforms to acceptable standards of scholarly presentation and is fully adequate, in scope and quality, as a dissertation for the degree of Doctor of Philosophy.

Eric Enholm
Associate Professor of Chemistry

I certify that I have read this study and that in my opinion it conforms to acceptable standards of scholarly presentation and is fully adequate, in scope and quality, as a dissertation for the degree of Doctor of Philosophy.

James M. Boncella
Associate Professor of Chemistry

I certify that I have read this study and that in my opinion it conforms to acceptable standards of scholarly presentation and is fully adequate, in scope and quality, as a dissertation for the degree of Doctor of Philosophy.

James K. Brooks
Professor of Mathematics

This dissertation was submitted to the Graduate Faculty of the Department of Chemistry in the College of Liberal Arts and Sciences and to the Graduate School and was accepted as partial fulfillment of the requirements for the degree of Doctor of Philosophy.

May, 1995

Dean, Graduate School

LD
1780
1995
.Y221

UNIVERSITY OF FLORIDA
3 1262 08554 9557